2017-03-31

Axon Death Pathways Converge on Axed to Promote Axon Disassembly

Thomas C. Burdett
University of Massachusetts Medical School

AXON DEATH PATHWAYS CONVERGE ON AXED TO PROMOTE AXON DISASSEMBLY

A Dissertation Presented
By

Thomas Christopher Burdett

Submitted to the Faculty of the
University of Massachusetts Graduate School of Biomedical Sciences, Worcester
in partial fulfillment of the requirements for the degree of

DOCTOR OF PHILOSOPHY

March 31st, 2017

PhD Program in Biomedical Sciences/Neurobiology

AXON DEATH PATHWAYS CONVERGE ON AXED
TO PROMOTE AXON DISASSEMBLY
A Dissertation Presented
By
Thomas Christopher Burdett

This work was undertaken in the Graduate School of Biomedical Sciences
Program in Neurobiology

The signature of the Thesis Advisor signifies validation of Dissertation content

_____
Marc Freeman, Ph.D., Thesis Advisor

The signatures of the Dissertation Defense Committee signify
completion and approval as to style and content of the Dissertation

_____
Dorothy Schafer, PhD., Member of Committee

_____
Yang Xiang, PhD., Member of Committee

_____
Zuoshang Xu, PhD., Member of Committee

_____
Christopher Gabel, PhD., External Member of Committee

The signature of the Chair of the Committee signifies that the written dissertation meets the requirements of the Dissertation Committee

_____
Patrick Emery, Ph.D., Chair of Committee

The signature of the Dean of the Graduate School of Biomedical Sciences signifies that the student has met all the requirements of the school

_____
Anthony Carruthers, Ph.D.,
Dean of the Graduate School of Biomedical Sciences

PhD Program in Biomedical Sciences/Neurobiology
March 31st, 2017

Acknowledgements

I would first like to thank my wife and family for attempting to understand how cutting off fly wings on a daily basis will someday benefit society. Especially Liz, who moved out to western Massachusetts, put up with long working hours, humored me, and occasionally brought me dinner in lab.

I would also like to thank my advisor and mentor, Marc Freeman, for taking me in and providing support, advice, and an excellent environment to learn flies, good science and the art of courteous yelling at lab meeting.

A big thanks to Freeman lab members past and present as well as fellow graduate students, you should know who you are. Our shared times both in and out of lab are a highlight of my graduate career.

Lastly, I want to thank members of the Freeman Lab, especially Lukas Neukomm, my TRAC, and everyone in the Neurobiology department for their fly stocks, critical feedback, guidance, and support of my projects in lab.

Abstract

Axons use a conserved program to actively drive their own destruction after injury. Axon degeneration is present in many neurological disorders and an axon death program could be a major pharmaceutical target to preserve neuronal function. This intrinsic signaling cascade activates pro-degenerative dSarm/Sarm1, rapidly depletes axonal stores of NAD+, and terminates in cytoskeletal breakdown. Conversely, loss of dSarm/Sarm1, maintenance of NAD+ levels or its biosynthetic enzyme Nmnat, result in long-term morphological perseveration of severed axons. Exactly how dSarm/Sarm1 and loss of NAD+ execute axon death remains poorly defined.

We sought to uncover novel regulators of axon death and maintenance by performing a deficiency screen and a forward genetic mutagenesis screen in axotomized Drosophila wing sensory neurons. We identified a BTB domain protein enriched in neurons, we named Axundead (Axed), which is specifically required for axon death. Severed axons harboring loss of function mutations in *axed*, similar to *dSarm* mutants, remain preserved for 50 days post axotomy. Spontaneous neurodegeneration induced by activated dSarm or dNmnat depletion are both suppressed in *axed* mutants, but not in *dSarm* mutant alleles. Additionally, severed *axed* mutant axons also expressing activated *dSarm* or lacking *Nmnat* are preserved. These results indicate that dSarm acts upstream of dNmnat loss, and both events precede essential Axed function and axon destruction. Thus, the axon death pathway converges on Axed function.

TABLE OF CONTENTS

List of Figures

List of Tables

List of Abbreviations

- ARM - armadillo/HEAT domain
- AD - axon death
- ADP - adenosine diphosphate
- ATP - adenosine triphosphate
- BACK - BTB and carboxyterminal kelch
- BTB - bric-à-brac, tramtrack and broad complex
- BTBD - BTB/POZ domain-containing protein
- Ca^{2+} - calcium ion/s
- Calp - calpain
- CaMKII - calcium/calmodulin-dependent protein kinase II
- CNS - central nervous system
- Cul - cullin
- Df – deficiency/deletion
- DLK - dual leucine kinase
- dpa - day post axotomy
- dpe - day post eclosion
- DRG - dorsal root ganglia
- DUB - deubiquinating eznyme
- EMS - ethyl methane sulfonate
- ey - eyeless
- Fsn/Fbxo - F-box portein
- FLP - flippase
- FRT - flippase recognition target
- GEF - guanine exchange factor
- GFP - green fluorescent protein
- GOI - gene of interest
- Hiw - highwire
- HSF-1 - heat shock transcription factor 1
- hpa - hours post axotomy
- JNK - c-Jun NH_2-terminal kinase
- MAPK(K)(K) - mitogen-activated protein kinase (kinase) (kinase)
- MARCM - mosaic analysis with a repressible cell marker
- MB - mushroom body
- MEKK = mitogen-activated protein Kinase/ERK kinase kinase
- MLK - Mixed Lineage Kinase
- MKK - Mitogen-activated protein kinase kinase
- PPM-2 - Protein-Phosphatase-Methyltransferase-1
- NaAD - nicotinate adenine dinucleotide

- NAD+ - nicotinamide adenine dinucleotide
- NAMPT - nicotinamide phosphoribosyltransferase
- NaMN - nicotinate mononucleotide
- NF-L/M/H – neurofilament light/medium/heavy chain
- NGF – nerve growth factor
- Nmnat - nicotinamide/nicotinic acid mononucleotide adenylyltransferase
- NMN - nicotinamide mononucleotide
- NR - nicotinamide riboside
- NRK - nicotinamide riboside kinase
- ORN - olfactory receptor neuron
- PAM - protein associated with myc
- PHR - PAM Hiw RPM-1
- PNS - peripheral nervous system
- RAE-1 - Ribonucleic-Acid-Export-1
- RBX-1 - RING-box protein
- RCC1 - Regulator-of-Chromosome-Condensation-1
- RING - really interesting new gene
- RNAi - ribonucleic acid intereference
- ROS - reactive oxygen species
- RPM-1- regulator of presynaptic morphology
- SAM - sterile alpha motif
- Sarm - sterile alpha and Armadillo motif
- SCF - Skp/Cul/F-box
- SCG - superior-cervical-ganglion-10
- SIAH-1 - seven in absentia homolog 1
- smGdP – spaghetti monster GFP
- TIR - Toll/Interleukin-1 receptor homology domain
- TOP1 - topoisomerase I
- TRIM5δ - tripartite motif family 5 alpha splice variant
- UAS - upstream activating sequence
- Ube4B - ubiquitin conjugation factor E4B
- UBP2 - yeast ubiquitin protease 2
- UBE2D2 - Ubiquitin Conjugating Enzyme E2 D2
- UPS - ubiquitin-proteasome system
- UTR - untranslated region
- Wld^{s} - Wallerian degeneration slow
- Wnd - wallenda
- WT - wild type

List of Third Party Copyrighted Material

Drosophila illustrations (male, female, & wing) were produced by Lukas Neukomm and used in Figure 1.1. Published in manuscript below, no permissions required:
Neukomm, L.J., Burdett, T.C., Gonzalez, M.A., Züchner, S., and Freeman, M.R. (2014). Rapid in vivo forward genetic approach for identifying axon death genes in Drosophila. Proc Natl Acad Sci USA *111*, 9965–9970.

Preface

All of the work presented here was performed by myself in close collaboration with Lukas Neukomm PhD in the laboratory of Marc Freeman. Specific attribution for experiments, figures, and writing are given in the preface of each chapter. *Drosophila* images in the introduction are modified from Neukomm et al., *PNAS* 2014. Members of the Freeman lab, the Neurobiology Department, the UMass community, and others shared fly stocks, and gave critical feedback and advice on the work presented in this thesis.

I isolated the genetic mutations and identified the causative genes, through lethality mapping and genetic rescue experiments, responsible for two unique phenotypes: 1) a partial blockade of axon degeneration (*gene-of-interest-#1*^{345x}); 2) a progressive dying-back of axons with extreme membrane dysregulation (*gene-of-interest-#2*^{596x} & *gene-of-interest-#2*^{1013x}), however, due to my own time constraints and focus on probing *axed* mechanism, other graduate students are working to complete and publish these projects. As such, data I obtained beyond basic phenotypes will not be presented in this thesis.

CHAPTER I: Introduction

Introduction 1-1: Neuronal Architecture & the Nervous System

Neurons evolved a unique cellular morphology to receive, interpret, and respond to cellular stimuli, via a dendritic arbor, a cell soma/body, and a long axon, respectively. In order to connect disparate locations in an organism, bursts of electrochemical impulses, generated and propagated by membrane depolarization, transmit information down the length of an axon to synaptic terminals. Synaptic linkages between neurons form nervous systems ranging in complexity from the very simple neural nets in radially symmetric organisms to mammalian central nervous systems with trillions of connections.

Axons form the bulk of the neuronal volume and vary widely in length, width, and branching complexity. For example, the axon-like process of primary sensory afferents in the blue whale can be as long as ~25-30 meters in length (Smith, 2009), while a similar neuron in humans extends a ~1m long process along the spinal cord from the dermal layer of the largest toe to the brain. Axons also differ widely in caliber depending on the information they are required to transmit in the form of electrical spikes, the number of which influence an axon's energy consumption (Perge et al., 2012). Maintaining a functional axon is energetically demanding and requires coordination of a vast economy of organelles such as mitochondria to provide cellular energy in the form of adenosine triphosphate (ATP), an axoplasmic reticulum to store calcium ions (Ca^{2+}) among other functions, an intracellular filament system to define membrane cytoskeletal structure and serve as transport rails for vesicles with attached or enclosed proteins and messenger/transfer ribonucleic acids (RNA) from the cell body to the axon, a cellular

garbage clearing ubiquitin-proteasome system (UPS) and a lysosomal network. Axons do not exist in a vacuum however, and are supported by several types of glial cells that enwrap single axons or bundles of axon in nerves. Glial cells support axons by accepting waste, transferring energy-rich glycolytic substrates such as pyruvate or lactate in exosomes or microvesicles, and speeding information transmission by providing a layer of electrical insulation in the form of myelin (Davis et al., 2014; Frühbeis et al., 2013; Fünfschilling et al., 2012). Even with the aid of supporting glial cells, disease and trauma can lead to catastrophic breakdown of the axon, such as in trauma brain injury or neurodegenerative ailments such as multiple sclerosis or Parkinson's disease (Adalbert and Coleman, 2013; Burke and O'Malley, 2013; Dikranian et al., 2008).

Introduction 1-2: Wallerian Degeneration

Complete transection of axons is a devastating injury that leads to axon destruction. Degeneration of axons after transection was first described in 1850 by Augustus Waller. He observed three distinct phases of destruction after severing hypoglossal nerve fibers in frog tongues (Waller, 1850). In the first phase, now termed the 'latency period', no morphological changes are observable in the nerve for up to four days post axotomy. In the second phase, lasting from approximately five to ten days, severed nerves undergo an explosive granular fragmentation which Waller described as "disorganized, fusiform masses at intervals" and regression of surrounding glia membranes (Waller, 1850). Finally, fragments are cleared by twelve to fifteen days, likely by neighboring macrophages. Today, these three phases of degeneration have been

observed in many neuronal subtypes across a range of organisms from *Drosophila* to humans, both *in vivo* and *in vitro*, albeit on faster time scales than frogs, usually less than 24 hours (MacDonald et al., 2006; Schlaepfer and Bunge, 1973).

In addition to his observations, Waller presciently hypothesized that simple transection caused "certain organic and physical changes in the tubular fibre" that may also be intimately related to diseases of the nervous system (Waller, 1850). We now have evidence that axon degeneration often precedes, and possibly induces, the death of neuronal cell bodies across a range of neurodegenerative diseases and traumas (Alobuia et al., 2013; Conforti et al., 2014). Thus, we might attenuate overall neuron loss and halt disease progression by promoting axon survival or inhibiting axon death. However, in order to therapeutically target axons we must understand those organic and physical changes in the axon that contribute to their demise. To do this the field has developed a variety of model systems, described below, to genetically and biochemically probe how axons degenerate after a simple transection in a process now called Wallerian degeneration.

Wallerian degeneration was first thought to result from a gradual consumption and subsequent loss of "essential metabolic factors" no longer supplied by the cell body and early models of axon degeneration followed the breakdown of excised rat nerve segments *ex vivo* (Joseph, 1973; Vial, 1958). These descriptive experiments observed the disruption of axoplasmic reticulum, swelling of mitochondria, and the disintegration of microtubules and neurofilaments using electron microscopy (Vial, 1958). Additionally, it was discovered that rising axoplasmic [Ca^{2+}] was necessary and sufficient for axon

degeneration: transected axons remained intact when nerves were incubated in Ca^{2+}-free media or with L-type calcium channel blockers and accelerated with the addition of Ca^{2+} ionophore, A23187 (George et al., 1995; Schlaepfer, 1974, 1977; Schlaepfer and Hasler, 1979). This was the first clue that an intrinsic activation of pro-degenerative molecules, namely calcium-sensitive proteases, were required for axon death (Schlaepfer and Hasler, 1979). Additionally, severed axon segments degenerate at a glacial pace in some invertebrate cell types such as crayfish medial giant axons, where anucleate axons remain intact for 5-9 months (Ballinger and Bittner, 1980), and even in vertebrates: goldfish spinal cord Mauthner axons, ~160 days (Murray and Edwards, 1982), frog optic axons, ~30-60 days (Lázár, 1980; Matsumoto and Scalia, 1981), and garfish olfactory axons, ~19 days (Cancalon, 1982). One such microscopic wasp even survives in its adult form with a nervous system comprised of primarily anucleated neuronal processes (Polilov, 2012). Other evidence from emerging apoptosis and cell death fields suggested that some degeneration was strictly controlled by intrinsic cellular processes. Thus, axons might contain their own signaling cascade to destroy themselves, which is altered or not present in some organisms or cell types.

Shifting the field from a passive to active degeneration model required more striking evidence provided by C57/BL/6/Ola mutant mouse strain. In this mouse, severed sciatic nerve axons remained morphologically intact for weeks and able to conduct action potentials up to 16 days post injury, in striking contrast to wild type axons that degenerated and failed to conduct action potentials by 2-3 days (Lunn et al., 1989). This mouse strain was renamed Wallerian Degeneration Slow or Wld^S and harbored

spontaneous tandem triplication which fused *nmnat1* and *ube4b.* This fusion resulted in the overexpression of a novel fusion protein consisting of *nmnat1* plus18 amino acids of its 5'UTR and 70 amino acids of the N-terminus of *ube4b* (nmnat = nicotinamide/nicotinic acid mononucleotide; ube4b = Ubiquitin conjugation factor E4B; UTR = untranslated region) (Mack et al., 2001). Axonal protection afforded by Wld^S was not limited to mice, it also strongly preserved severed axons when expressed in models of axotomy in *Drosophila* and zebrafish (MacDonald et al., 2006; O'Donnell et al., 2013). Cross species axonal protection suggested that Wld^S may be impinging on a conserved axon death program activated post injury, however the mechanism of inhibition remained an open question. In order to determine which Wld^S domains were required for axon preservation, *in vivo* and *in vitro* model systems recapitulating axon degeneration were developed in *Drosophila* and mouse. Each system also provided a platform to uncover novel endogenous molecules required for injury-induced axon death using either a candidate approach or unbiased forward screening. Before proceeding to proposed mechanisms of axon death, it is necessary to describe the main model systems used to disentangle the pathway, with a focus on the *Drosophila* wing model of axon death, as it was used to acquire the majority of data presented in this thesis.

Introduction 1-3: Model Systems to Study Axon Degeneration

The transection of mouse sciatic nerve and observation of degeneration either *in vivo* or *ex vivo* was an early model of injury-induced axon death used to discover and describe Wld^s. Sciatic nerve transection provides platform with properties replicated by

later model systems in the following ways: 1) axons undergo stereotyped Wallerian degeneration, 2) the injury is non-lethal, so axon integrity can be assessed over time and 3) the site of assessment is distant from the site of injury and avoids artifacts induced by mechanical stress involved with the surgery or perturbation of surrounding glial/epithelial cells. The *in vivo* environment might also provide signals required for axon degeneration from the surrounding tissues or extracellular milieu which would be especially relevant for future therapeutics. Optic nerve crush can also model injury-induced axon death (Knöferle et al., 2010). Additionally, several other mouse *in vivo* models display prominent axon dysfunction, but involve more complex etiologies than Wallerian degeneration: traumatic brain injury paradigms, vincristine or taxol induced peripheral neuropathy, progressive motor neuropathy mouse model, and some other neurodegenerative disease models (Bommel et al., 2002; Geisler et al., 2016; Henninger et al., 2016; Wang et al., 2002; Yang et al., 2015).

Several different neuronal types can be successfully cultured *in vivo* that extend processes long enough to be transected and analyzed after injury. Both PNS and CNS neurons undergo Wallerian degeneration after injury in culture and are typically derived from sensory/motor neurons within the DRG or cortical neurons from the superior cervical ganglia, respectively (PNS = peripheral nervous system; CNS = central nervous system, DRG = dorsal root ganglia) (Buckmaster et al., 1995; Osterloh et al., 2012). PNS neuron processes can even be induced to grow directionally towards supplied nerve growth factor (NGF) (Campenot, 1977). Removal of this NGF leads to a caspase dependent axon retraction and neuronal cell death independent from injury-induced

degeneration (Cusack et al., 2013; Finn et al., 2000; Simon et al., 2012). Campenot chambers utilize directional axonal growth into isolated compartments, enabling axon or cell body specific experimental interventions, as well as the collection of pure, axon only material for biochemical analysis (Campenot, 1977). Proteins packaged inside viral-like particles introduced directly into severed axons in such systems has become the gold standard to definitely demonstrate protein function within the axon after injury and define a time post injury in which a protein is required (Sasaki and Milbrandt, 2010). *In vitro* models also allow for high throughput screening of inhibitors or enhancers of axon death by either genetic approaches, like RNAi knockdown, or using large drug/small molecule libraries. A few criticisms of *in vitro* culture systems is that they lack extracellular signals present *in vivo* and neonatal derived cultures may remain in a permanent developmental state with altered gene expression profiles (Zhu and Oxford, 2011).

Drosophila in vivo models of axon death allow for rapid genetic screening and pathway dissection, using extensive genetic tools developed by a rich history of fly geneticists. The co-opting binary systems from yeast, particularly the transcriptional activator, GAL4, and upstream activator sequence, UAS, enables expression of unique proteins under UAS control, restricted to the subset of cells expressing GAL4 (Brand and Perrimon, 1993). For example, Wallerian degeneration was first demonstrated in *Drosophila* by using an olfactory receptor neuron (ORN) specific GAL4 to drive expression of UAS controlled membrane tagged green fluorescent protein (GFP) and severing axons by removing cell bodies housed in the antenna (MacDonald et al., 2006). Axons underwent prototypical axon degeneration characterized by a short lag phase and

followed by complete granular fragmentation by 24 hours post axotomy (hpa) and full clearance of axonal debris by 3 days post axotomy (dpa) (MacDonald et al., 2006). As previously noted, overexpressing Wld^S, also using UAS, remarkably preserved axons for the lifetime of the fly (MacDonald et al., 2006). The ORN model of axon degeneration allows for long term observation of sensory axons within the adult fly brain and visualization of proteins by antibody staining or genetically encoded fluorescent tags, but requires time consuming adult brain dissection and mounting. *Drosophila* larvae also provide a platform for assessing axon death by crush injury or laser ablation of ventral abdominal nerves containing axons from both sensory and motor neurons (Xiong et al., 2010). Larval injury models allow for live imaging of axon bundles and observation of stereotyped neuromuscular junction structure proximal to injury site, but analysis is limited to 2-3 dpa since larvae begin to pupate. (Avery et al., 2012; Xiong and Collins, 2012; Xiong et al., 2012). This system was used to identify *highwire* (*hiw),* an E3 ligase required for axon death.

Recently, mechanosensory neurons in *Drosophila* wing have emerged as an efficient model of axon death, easily visualized through the thin cuticle of the wing without dissection (Figure 1.1) (Fang et al., 2012; Neukomm et al., 2014). In this model, cell bodies receive input from dendritic contacts with sensory bristle shafts and transmit sensory information down axons, within the L1 vein, into the thoracic ganglia. By cutting the wing, a subset of axons with cell bodies distal to the injury site undergo Wallerian degeneration within 12-24 hours. Injured axons proximal to the cut site can be visualized live or fixed at any time within the lifetime of the fly, as long as wings are kept free of

damage, by expressing GFP with variety of neuronal GAL4 drivers. Importantly, the injury caused by a crush or transection of axon bundle is non-lethal and takes place far from the point of axon assessment, avoiding complications induced by damaged glia near the transection site (Neukomm et al., 2014). Since a random subset of labeled neurons are axotomized when removing the distal half of the wing, neurons proximal to the cut site are used as uninjured controls and are noted in figures as cell bodies. Thus, within an injured wing, severed axons undergo granular fragmentation within 12-24 hours, while uninjured axons remain intact within the same axon bundle (Figure 1.1).

Each of the *Drosophila* model systems is amenable to screening using both mutagenesis and a variety of genetic tools such as RNAi knockdown, transposon disruption, and UAS overexpression (St Johnston, 2002). However, the tools noted above sometimes induce homozygous lethal alternations to the genome, thus limiting screening to non-lethal homozygous or heterozygous animals. To overcome this limitation, mosaic analysis with a repressible cell marker (MARCM) can be used to generate clones, homozygous for somatic lethal mutations and labeled with a fluorescent marker such as GFP (Figure 1.1) (Lee and Luo, 2001). This system requires the use of flippase (FLP) recombinase, under the control of specific promoters, to drive recombination between short flippase recognition target (FRT) sites located near the centromere of each *Drosophila* chromosomal arm, excluding the 4^{th} and Y.

In the case of the wing, differential expression strengths randomly inserted *asense* driven FLPs can induce a graded number of neuronal clones. Using FLPs that induce few clones produces an added benefit of enabling single axon resolution within the L1 wing

vein. This resolution allows the integrity of each individual severed axon to be assessed, rather than attempting to assess the status ~40+ neurons labeled using OK371-GAL4 or dpr-GAL4 (Figure 1.1) (Neukomm et al., 2014). This system was used to generate mutant clones in both ORN and wing models of axotomy, and it was required to identify homozygous lethal *Drosophila* Sterile alpha/ARMadillo/toll-interleukin receptor homology protein (dsarm) loss of function alleles that suppress axon death (Osterloh et al., 2012). Unique mutations were then identified using a combination of traditional genetic mapping and whole genome sequencing with next generation sequencing (NGS) technology (Gonzalez et al., 2012).

Introduction 1-4: Nmnat is an Axon Survival Factor

A series elegant experiments were undertaken in several labs to tease apart the axon protective determinants of the Wld^S molecule. Briefly, domains of Wld^s were overexpressed in a number of combinations and each was assessed for efficiency of axon protection post injury. Also included in these studies were each of the three mammalian Nmnat genes, which have distinct neuronal localization patterns: Nmnat1 in the nucleus, Nmnat2 in the cytoplasm/axoplasm and attached to Golgi derived vesicles, and Nmnat3 to mitochondria. To summarize evidence from experiments in a variety of model systems, the efficiency axon preservation from Wld^s was dependent on enzymatically active, stabilized Nmnat1 localized within the axoplasm (Araki et al., 2004; Avery et al., 2009; Babetto et al., 2010; Milde et al., 2013; Sasaki and Milbrandt, 2010). The Wld^s N16 linker interaction with valosin-containing protein (VCP) results in the usually nuclear

Nmnat1, to be re-localized to the axoplasm and axonal mitochondria. Consistent with this finding, each Nmnat protein can suppress axon death if stably re-localized to the axoplasm (Avery et al., 2009; Conforti et al., 2009; Laser et al., 2006; Wilbrey et al., 2008). Axon death can even be suppressed when Nmnat protein is delivered directly to severed axons within viral-like particles (Sasaki and Milbrandt, 2010). This experiment convincingly ruled out any contribution to axon death by Nmnat-induced alterations of gene expression within the nucleus.

If artificial Nmnat overexpression suppressed axon death so strongly, the field hypothesized that levels of an endogenous Nmnat may be tightly correlated to axon death and genes required for Nmnat turnover might be required for degeneration. In mammals, Nmnat2 was the most attractive candidate for the role of axon survival factor due to its endogenous localization to axoplasm. Subsequent analysis confirmed this hypothesis as Nmnat2 depletion caused axon death that could not be rescued by overexpression of Nmnat1 or Nmnat3 (Gilley and Coleman, 2010). Additionally, Nmnat2 or the sole *Drosophila* Nmnat is required for axon development and survival both *in vivo* and *in vitro* (Fang et al., 2012; Hicks et al., 2012; Zhai et al., 2006). Since Nmnat2 has a short half-life within the axonal compartment and requires constant replenishment by fast axonal transport on Golgi derived vesicles from the cell soma, it would follow that disruptions to trafficking induced by axon transection or damage to cytoskeletal rails would lead to a rapid fall in Nmnat2 levels and degeneration (Milde et al., 2013). As predicted, both mammalian Nmnat2 and *Drosophila* Nmnat levels drop after axonal injury and, conversely, disrupting turnover by inhibiting palmitoylation induced

membrane localization enhances Nmnat2 protective ability (Milde et al., 2013; Walker et al., 2017; Xiong et al., 2012; Yang et al., 2015). Palmitoylation at cysteine residues 164/165 governs membrane localization, enhances ubiquitination and thus increases targeting to the proteasome (Milde and Coleman, 2014; Milde et al., 2013). Conversely overexpressing Nmnat2 without these sites decreases turnover and enhances axon protection after injury (Milde et al., 2013). Consistent with these results, axon death is also suppressed modestly with broad proteasome inhibitors *in vitro*, such as MG132, and strongly suppressed when yeast de-ubiquitinating (DUB) ubiquitin-specific protease 2 (UBP2) is overexpressed *in vivo* (Baker et al., 1992; Xiong et al., 2012; Zhai et al., 2003). What proteins were responsible for rapid Nmnat2 turnover?

The E3 ligase, Highwire (hiw)/Phr1, in an atypical SCF complex with SkpA/Skp1a and dFsn/Fbxo45, governs the ubiquitination and turnover of Nmnat, possibly coordinating this action at membranes (Phr1 = Protein-Associated-with-Myc[PAM]/Highwire/Regulator-of-Presynaptic-Morphology[RPM1]; Skp = S-phase kinase associated protein; dFsn/Fbxo = F-box protein; SCF = Skp/Cullin/F-box) (Babetto et al., 2013; Brace et al., 2014; Xiong et al., 2012; Yamagishi and Tessier-Lavigne, 2016). Although the atypical SCF complex has only been described in mammalian cell culture systems, loss of function alleles of *hiw* strongly inhibit axon degeneration in *Drosophila* and extend protection for the lifetime of the fly (Neukomm et al., 2014; Xiong et al., 2012). Also, mutations in the really-interesting-new-gene (RING) domain lead to dominant protection of axons, indicating the ubiquitin ligase activity by the RING domain is functionally required for Nmnat turnover (Neukomm et al., 2014; Xiong et al.,

2012). Knocking down Phr1/Skp1a/Fbxo45 also potently suppresses axon death in mammalian models, however it is unclear whether individual components offer different levels for protection because experiments recorded axon integrity only up to 24 hours (Yamagishi and Tessier-Lavigne, 2016). Removing the components in this complex cannot suppress death induced by Nmnat knockdown in mammals or *Drosophila*, suggesting a role for Hiw upstream of Nmnat loss in an axon death pathway (Xiong et al., 2012; Yamagishi and Tessier-Lavigne, 2016). Taken together, the existing data argue that Hiw/Phr1 regulates fast turnover of Nmnat/Nmnat2.

Interestingly, proteasome inhibition does not increase basal Nmnat levels to the same degree as *hiw* nulls or UBP2 overexpression, suggesting a regulation is more complex than proteasomal turnover (Xiong et al., 2012). Also, MG132 at high concentrations inhibits non-proteasomal proteases like calpains, while more specific proteasome inhibitors, such as lactacystin or epoxomicin, have variable axon protective affects in cultured PNS vs CNS neurons, suggesting that proteasome blockade is not universally protective after axon injury and thus, not essential to the axon death pathway (Meng et al., 1999; Yang et al., 2013).

Hiw is a large multi-domain protein with an N-terminal RCC1-like GEF domain, two PAM-homology-related (PHR) domains, and a RAE-1 binding domain (RBD) capable of multiple cellular processes in addition to its role as a ubiquitin ligase (RCC1 = Regulator-of-Chromosome-Condensation-1; GEF = guanine exchange factor; RAE-1 = Ribonucleic-Acid-Export-1)(Grill et al., 2016). These domains control synaptic morphology, axon guidance, growth cone termination, and possibly other functions that

seem to be separable from Nmnat regulation with one exclusion, the regulation of MAPKKK, Wnd/Dlk levels by ubiquitination and activity through PHR-PPM-2 phosphatase interactions (MAPKKK = mitogen-activated protein kinase kinase kinase; Wnd/Dlk = wallenda/dual-leucine-kinase; PPM-2 = Protein-Phosphatase-Methyltransferase-1) (Baker et al., 2014; Collins et al., 2006; Klinedinst et al., 2013; Shin and DiAntonio, 2011; Wang et al., 2013; Wu et al., 2007; Yan et al., 2009). Loss of function alleles of *wnd/Dlk* modestly suppress axon degeneration and downstream MAP kinase signaling cascade components, MLK2/MEKK4, MKK4/MKK7, and JNK1-3 knock-down and loss of function alleles display variable protection of severed axons (MLK = Mixed Lineage Kinase ;MEKK = mitogen-activated protein Kinase/ERK kinase kinase; MKK = mitogen activated protein kinase ; JNK = c-Jun NH_2-terminal kinase) (Yang et al., 2015). The protective abilities from restricting MAPK function likely derives from increased basal levels of Nmnat2, however several MAPK are phosphorylated within minutes to hours post injury and may play a more complex role in downstream degeneration (Walker et al., 2017; Yang et al., 2015). Further complicating this additional layer of Nmnat2 regulation, JNK also negatively regulates the axon protective microtubule stabilizing SCG10, phosphorylates, although no SCG10 homologs have been described in *Drosophila* (SCG = superior-cervical-ganglion-10) (Morii et al., 2006; Shin et al., 2012a; Walker et al., 2017).

Introduction 1-5: Axon Survival and Maintenance of NAD+

While increasing Nmnat levels has been clearly demonstrated to be axon protective, how exactly does Nmnat provide axon protection? Nmnats can play multiple roles, both acting as molecular chaperones and as the key biosynthetic enzyme required to produce NAD+ directly from its precursor NMN, or indirectly from NaMN to NaAD then NAD synthetase conversion to NAD+ (NAD+ = nicotinamide adenine dinucleotide; NMN = nicotinamide mononucleotide; NaMN = nicotinate mononucleotide; NaAD = nicotinate adenine dinucleotide) (Schweiger et al., 2001; Zang et al., 2013; Zhai et al., 2006). Several experiments with Wld^{s} and Nmnats determined that enzymatic NAD+ activity is absolutely required for suppression of axon death (Araki et al., 2004; Avery et al., 2009; Milde et al., 2013; Sasaki et al., 2006; Wang et al., 2005). Furthermore, NAD+ is rapidly depleted by approximately four hours post injury and depleting NAD+ using a dimerizable tankyrase-poly-ADP-ribose domain leads to axon death (Araki et al., 2004; Gerdts et al., 2015). In contrast, addition of exogenous NAD+, increasing NMN through co-application of NR and conversion enzyme NRK1/2, or upregulating Nam conversion to NMN by increasing NAMPT activity can modestly delay axon death after injury (NR = nicotinamide riboside; NRK = nicotinamide riboside kinase; Nam = ; NAMPT = nicotinamide phosphoribosyltransferase)(Araki et al., 2004; Ratajczak et al., 2016; Wang et al., 2005).

It is not surprising axons require NAD+, as it is used in variety of cellular process as a co-factor, precursor to other molecules, or in redox reactions, the most important of which is accepting or donating H+ protons in energy production. NAD+ is required for

both glycolysis in the cytoplasm and several energy production steps in mitochondria including pyruvate oxidation to acetyl coenzyme A and ATP generation by oxidative phosphorylation (Rongvaux et al., 2003). Since ATP seems to fall coincident NAD+ levels, the field gravitated toward a model of axon death where injury halted new Nmnat2 supply, leading to NAD+ depletion and ATP production failure. Without NAD+/ATP, Ca^{2+} ATPase pumps cease and mitochondria depolarize leading to mitochondrial permeability transition pore (mPTP) opening (Barrientos et al., 2011; Stein and Imai, 2012). Both causing a rise of intracellular [Ca^{2+}] to high enough levels to activate cytoskeletal destroying calpain proteases (Ma et al., 2013; Yang et al., 2013).

Seemingly in conflict to this hypothesis however, was data showing that overall NAD+ levels had little predictive correlation with axon death (Sasaki et al., 2016). For example, NMN deamidase alone or expressed with NMN synthetase + NR protected aculeated axon fragments, but had lower and higher basal NAD+ levels relative to wild type, respectively (Sasaki et al., 2016). Axons with these manipulations also had similar changes in basal levels of NMN, arguing against an alternative theory that NMN levels are a degenerative trigger (Loreto et al., 2015; Sasaki et al., 2016; Di Stefano et al., 2015). While overall levels of NAD+ and metabolites failed to explain axon protection, the ability of a specific intervention to suppress a 2-3 fold increase in NAD+ consumption rate post injury strongly predicted the degree of axon preservation (Sasaki et al., 2016). Thus rapid NAD+ consumption likely drives degeneration by inducing local energy deficits leading to the obvious question of what consumed NAD+ post injury. A candidate approach ruled out requirements of PARP domain proteins or sirtuins for axon

death, but it took unbiased forward genetic screens in the Freeman lab and Millbrandt labs to uncover a possible candidate for NAD+ depletion in the pro-degenerative dsarm/Sarm1 (Avery et al., 2009; Gerdts et al., 2013, 2015; Osterloh et al., 2012; Wang et al., 2005).

Introduction 1-6: Pro-degenerative dSarm/Sarm1

dsarm is required for axon death and was discovered in a mutagenesis screen using the *Drosophila* ORN model of axotomy (Osterloh et al., 2012). Multiple loss of function alleles strongly suppress axon death for the lifetime of the fly, similar to the phenotypes observed with Wlds and loss of function *hiw* alleles (Neukomm et al., 2014; Osterloh et al., 2012). The mammalian knockouts the homolog of *dsarm*, *Sarm1*, also displayed strong suppression of axon death both *in vitro* and *in vivo* in all neuronal subtypes assayed (Gerdts et al., 2013; Osterloh et al., 2012). Dsarm/Sarm1 is expressed in neurons and required cell autonomously within axons after injury for axon death to proceed, however plays no role in degeneration induced by NGF withdrawal (Gerdts et al., 2013; Osterloh et al., 2012).

Dsarm/Sarm1 protein consists of several conserved domains, even present in *C. elegans* homolog, TIR-1: 1) an N-terminal 27aa mitochondrial localization domain (N27), 2) an N-terminal/HEAT/armadillo (ARM) domain, 3) dual, centrally located sterile alpha motif (SAM) domains, and 4) a C-terminal toll/interleukin-1 receptor homology domain (TIR) (Chuang and Bargmann, 2005; Gerdts et al., 2013; Osterloh et al., 2012; Summers et al., 2016). Functional analysis of the domains revealed that Sarm

required both SAM and TIR domains to induce axon death and removal of the N-terminal domain/ARM domain led to a constitutively active form of Sarm that induced spontaneous cell death in multiple cell types and organisms (Freeman Lab - Unpublished Data, Gerdts et al., 2013; Panneerselvam et al., 2013; Summers et al., 2016). The N27 mitochondrial localization domain is dispensable for axon death (Gerdts et al., 2013). Homotypic interaction between SAM domains results in multimerization between Sarm1 molecules and TIR dimerization is sufficient to induce a degenerative response, although an exact mechanism remains controversial (Gerdts et al., 2013, 2015; Summers et al., 2016).

In immunity, TIR domains typically signal downstream by homo/hetero-dimerizing with toll-like receptor (TLR) proteins at the plasma membrane and serve as scaffolding for a variety of kinase signaling cascades including MAPKs (Banerjee and Gerondakis, 2007; O'Neill and Bowie, 2007). Sarm1 TIR domain is capable of these interactions and works as a repressor in innate immunity, yet this function is separable from axon death function as other TIR domains proteins, TLRs, or TLR-adaptor proteins show no defects in axon death when removed or inhibited (Carlsson et al., 2016; Lin et al., 2014a; Liu et al., 2014). Sarm1 and TIR-1 TIR domains have also been demonstrated to control neuronal identity and morphology through MAPK signaling, particularly MKK4 and JNK, ultimately regulating cytoskeletal dynamics through transcriptional responses (Chang et al., 2011; Chen et al., 2011; Chuang and Bargmann, 2005). Knocking down MAPKs however, cannot prevent degeneration induced by artificial dimerization of Sarm1 TIR domains, suggesting that MAPKs do not play roles

downstream of Sarm1 in degeneration (Walker et al., 2017). Since all of the gain-of-function or constitutively active forms of dSarm/Sarm1, including dimerized TIR domains, induce rapid consumption of NAD+, it has been proposed that TIR dimers directly and actively destroy NAD+ using Sarm-specific amino acids, which are not present in related TIR domains, between the TIR BB and DD loop structures (Gerdts et al., 2015; Summers et al., 2016). Though strongly correlated, direct TIR consumption of NAD+ has not been demonstrated and it remains possible that TIR domains work with other protein partners to destroy NAD+. Degenerative processes directly downstream of Sarm1 remain poorly defined.

Sarm1 is likely activated by the removal of physical N-terminal/ARM domain inhibition of the TIR domain, however the mechanism governing de-repression remains unknown. In *C. elegans*, TIR-1 is dis-inhibited by upstream Ca^{2+} activation of calcium/calmodulin-dependent protein kinase II (CamKII), likely through kinase activity, although this has not been demonstrated (Chuang and Bargmann, 2005). Calcium is an attractive upstream activator of Sarm1, as two distinct calcium waves occur after injury and calcium is necessary and sufficient for axon death, although recent evidence argues against this hypothesis (Loreto et al., 2015; Vargas et al., 2015). Several kinases, maybe those MAPKs phosphorylated early post injury, might also mimic CaMKII activity and phosphorylate either the ARM or TIR domain to disrupt inhibitory interaction, although no evidence currently supports this hypothesis (Yang et al., 2015).

Conversely, several lines of evidence suggest a role for Nmnat2 upstream of Sarm1, where injury-induced loss of Nmnat2 leads directly to Sarm1 disinhibition. First,

Nmnat2 -/- are embryonic lethal and can be fully rescued by also knocking out Sarm1 (Gilley et al., 2015; Hicks et al., 2012). Also, Sarm -/- protects axons after injury, despite a precipitous fall in Nmnat2 levels, arguing Sarm1 activity is required downstream of Nmnat2 loss (Gilley et al., 2015; Yang et al., 2013). Finally, cytoplasmic Nmnat1 or NMN deamidase prevent NAD+ consumption, presumably by blocking Sarm1 activity, while NAMPT and NRK+NR do not prevent consumption, but supplement enough NAD+ to counteract downstream Sarm1-mediated NAD+ destruction (Sasaki et al., 2016). Since direct interaction between Nmnat2 and Sarm1 has not been demonstrated, it remains possible that a variety of post-translational modifications such as protease cleavage, ubiquitin addition, or ADP ribosylation or removal of a specific chaperone, possibly Nmnat, are responsible for removal of ARM repression. Whatever the stimulus, the ARM domain seems to act as general, yet caspase-independent, degenerative sensor since Sarm1 is required for cell death downstream of mitochondrial dysfunction, viral infection, oxygen/glucose deprivation, reactive oxygen species, and excitotoxic stress (Hou et al., 2013; Massoll et al., 2013; Mukherjee et al., 2013; Panneerselvam et al., 2013; Summers et al., 2014).

Introduction 1-7: Therapeutic Prevention of Axon Death

While complete transection is one of the more severe insults axons can experience, a vast array of traumatic insults and chronic maladies can lead to axon dysfunction followed by neuronal death (Coleman and Perry, 2002; Dikranian et al., 2008). Even without neuronal death, focal axonal swellings can cause cognitive and

functional deficits by disrupting protein transport (Millecamps and Julien, 2013). Therapeutics targeting components within axon death pathway could prevent degeneration long enough for cytoskeletal repair, thus inhibiting axonal 'dying-back' and subsequent neuronal loss. Due to the complex etiologies of neurodegenerative disease, targeting axon death is not a panacea, however therapeutics could be especially beneficial in diseases with prominent axon dysfunction and testing models of disease in Wld^{s} or Sarm1 -/- background provides good indication of potential therapeutic success.

Traumatic brain injury and spinal cord injury without transection are examples of insults that result in diffuse and focal axonal dysfunction, respectively, where downstream degenerative processes are alleviated by either removing Sarm1 or overexpressing Wld^{s} (Gillingwater et al., 2006; Henninger et al., 2016; Yin et al., 2016; Zhang et al., 1996). Long axons are particularly affected due to the shear forces encountered in these injuries and axonal damage leads to a destructive feedback loop where axonal debris drive secondary inflammatory responses from macrophages, microglia, and astrocytes in mouse injury models (Gyoneva and Ransohoff, 2015; Lin and Wen, 2013).

Axonal dysfunction is also prominent in both acquired and hereditary neuropathies. Acquired peripheral neuropathies occur in ~50% of patients with diabetes and in 38% of cancer patients treated with existing chemotherapeutics (Kerckhove et al., 2017; Stino and Smith, 2017). Both Sarm -/- and Wld^{s} mice have shown resistance to axon dysfunction and dying back neuropathies after exposure to chemotherapeutic agents such as vincristine and taxol as well as hereditary disorders such as Charcot-Marie-Tooth

disease (Berbusse et al., 2016; Geisler et al., 2016; Meyer zu Horste et al., 2011; Wang et al., 2002).

The above are only a few examples of disease states that could benefit from drugs targeting axon death and still others may benefit from inhibiting axon degeneration in combination with existing therapies. Intriguingly, therapeutics designed to prevent NAD+ consumption or enhance NAD+ levels may also provide alleviation of age related decline of NAD+ in neurons and muscle tissue (Chung et al., 2016; Srivastava, 2016).

Introduction 1-8: Thesis Overview

This thesis describes a screen of 40,319 unique chromosomal arms in the *Drosophila* wing model of axotomy to identify a novel BTB domain containing gene required for axon degeneration, *axundead* (*axed*). Chapters 2, 3, and 4 present the rational, the results, and brief discussion of experiments undertaken. In Chapter 2, I describe the genetic schemes used to screen, isolate, and identify two mutations in *axed* as well as other mutants essential for both axon death and maintenance. Chapter 3 demonstrates Axed requirement downstream of dSarm pro-degenerative signaling and death induced by reduction or ablation of Nmnat. Chapter 4 attempts to determine which conserved domains of Axed are required for axon death function, as well as which cellular processes Axed might utilize to destroy axons. Finally, Chapter 5 is a discussion of how our experimental data fits with existing hypotheses in the axon death field and specific future experiments that could address outstanding questions. Finally, I briefly address how to therapeutically target axon death proteins in neurodegenerative diseases.

To adequately proceed requires a brief review of BTB containing proteins and their roles in diverse cellular processes.

Introduction 1-9: BTB Domain Containing Proteins

The bric-a-brac tramtrack broad (BTB) domain has a wide variety of roles in a complex tree of evolutionarily diverged proteins that function as transcriptional repressors (Melnick et al., 2000), cytoskeletal regulators (Bomont et al., 2000), ion channels (Kreusch et al., 1998), and adaptors for ubiquitin E3 ligase complexes (Canning et al., 2013). To accomplish these functions, the versatile BTB fold can homo-tetramerize (Kreusch et al., 1998), homodimerize (Melnick et al., 2000; Soltysik-Espanola et al., 1999), or heterodimerize with other BTB domain containing proteins (Errington et al., 2012) as well as interact with non-BTB structures such as ATP (T'Jampens et al., 2002). BTB family of proteins have well described roles aiding cullin-RING-ligase (CRL) complexes to covalently attach ubiquitin to specific substrates for designation to the proteasome or mono-ubiquitin modification that can alter the substrate function or subcellular localization (Canning et al., 2013; Pintard et al., 2004). Two BTB domains unify the complex into an efficient ubiquitinating dimer by enhancing concentration and substrate availability (Errington et al., 2012; Zhuang et al., 2009). To tune CRL complex activity, recent evidence suggests alternate BTB-domain containing proteins can be incorporated in the complex by heterodimerization (Errington et al.,

2012). This type of modularity could act as a ‘molecular rheostat’ and possibly shift the complex between long chain polyubiquitination and monoubiquitylation (Errington et al., 2012). Interestingly, the BTB domain only Skp family, plays noted roles in axon degeneration and pruning, with Skp1a/SkpA aiding a Phr1-Fbxo45 complex in the regulation of basal levels of Nmnat2/dNmnat (Brace et al., 2014; Yamagishi and Tessier-Lavigne, 2016).

Drosophila CG8398 is located on chromosome 3L and has a conserved BTB and BACK domain, though notably, no Kelch domains or DNA binding domains. *CG8398* is expressed in neurons according to FlyAtlas Anatomical Expression dataset and enriched in the testis (Chintapalli et al., 2007). In *C. elegans*, CG8398 homolog BTBD2 contributes to non-apoptotic linker cell death in complex with CUL-3, RBX-1, and SIAH-1 plus UBE2D2 downstream of a pathway similar to a proposed model of axon degeneration: active dsarm/TIR-1 signaling via a MAPK cascade then through a non-canonical function of HSF-1(RBX-1 = RING-box protein; SIAH-1 = seven in absentia homolog 1; UBE2D2 = Ubiquitin Conjugating Enzyme E2 D2; HSF-1 = heat shock transcription factor 1) (Kinet et al., 2016). What that CRL complex tags with ubiquitin for proteasomal degradation remains unknown.

CG8398 closest related protein in mammals is BTBD2 with 39% amino acid identity homology (short isoform of CG8398), followed by closely related proteins BTBD3, BTBD6, and BTBD1. These four proteins have a BTB domain and a BACK domain in which the C-terminal kelch repeats have been replaced by a PHR domain, curiously similar to domains in *Drosophila* Hiw. Homology between CG8398 and

BTBD2 is strongly determined by the BACK domain. BTBD2 and BTBD1 share 80% amino acid identity and interact with topoisomerase I (TOP1) in the nucleus and also with tripartite motif family 5 alpha splice variant (TRIM5δ) in punctate cytoplasmic bodies in HeLa cells (Xu et al., 2002, 2003). Complexed together, BTBD1/BTBD2/TRIM5/TOP1 may serve as a first line of defense against retroviral infections such as HIV-1 (Khurana et al., 2010). Interestingly, loss of function mutations in a related TRIM E3 ligase, TRIM2, cause early onset axonal neuropathy by failing to recycle NF-L via the UPS (Ylikallio et al., 2013).

Figures

Figure 1.1: An F1 mutagenesis screen for regulators of axon death in the *Drosophila* wing

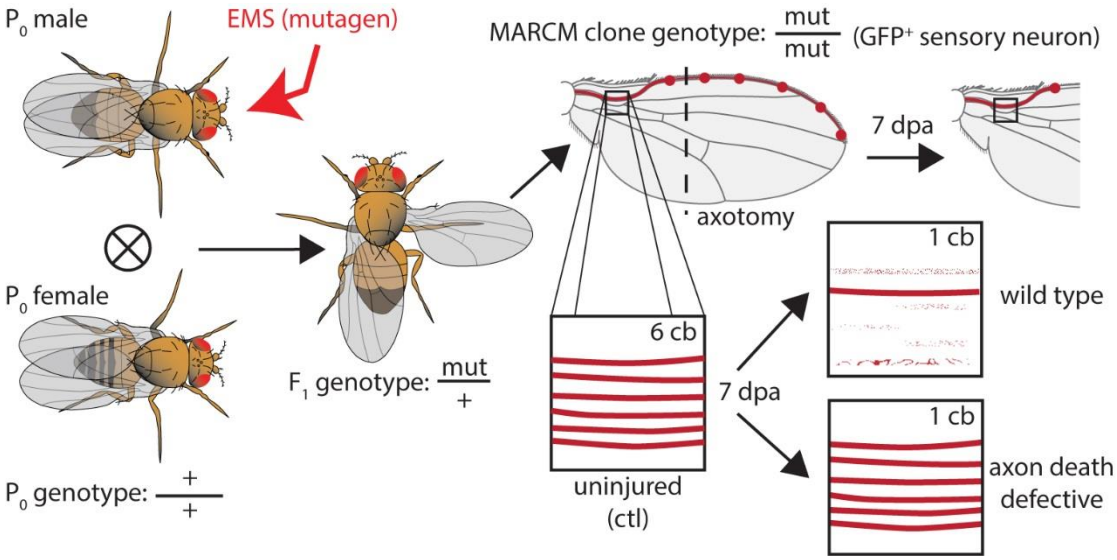

Figure 1.1:
P0 males were fed mutagen (ethyl methanesulfonate, EMS), and crossed to virgin females. Both males and females carried genetic elements to induce MARCM clones. The resulting F1 males were heterozygous (mut/+) and mosaic for EMS-induced mutations. Sensory neuron MARCM clones were GFP+-labeled and homozygous (mut/mut) mutant. One wing was injured and used to screen for axon death defective phenotypes at 7 days post axotomy (dpa). Wild type axons degenerate and are cleared by 7dpa, while severed axons persist in axon death mutants. Genotypes are listed in Materials & Methods in Chapter II.

CHAPTER II: Deficiency and Mutagenesis Screening for Regulators of Axon Death

This work was conducted in the laboratory of Marc Freeman. Lukas Neukomm built many of the *Drosophila* lines required for the screen as described in the 2014 *PNAS* article (Neukomm et al., 2014). I performed the *Drosophila* screen described, along with Lukas Neukomm, Jonathan Farley, and Elizabeth Allen. I performed all of the described Drosophila work in close collaboration with Lukas Neukomm who performed the following: 1) isolated and characterized $axed^{2094}$ 2) cloned $axed^{long}$ and $axed^{short}$ 3) tested 3L deficiency and mimic lines. Tim Rooney tested a subset of deficiency lines listed in the ORNs, which I repeated in the wing. Drosophila mutations were sequenced in the laboratory of Stephan Zuchner. As described in the thesis preface, *gene-of-interest-#1*^{345x}, *gene-of-interest-#2*^{596x}, *gene-of-interest-#2*^{1013x} are introduced, however a full characterization of function is currently being performed by Jon Farley and others.

The following publication is in preparation as follows:
Axon death pathways converge on Axed to promote functional and structural axon disassembly. Lukas J. Neukomm* & Thomas C. Burdett*, Jaeda Coutinho-Budd, Andrew M. Seeds, Stefanie Hampel, Jack Wong, Yonca Karadeniz, Jeannette M. Osterloh, Amy E. Sheehan, and Marc R. Freeman
(* denotes co-first authorship)

Abstract

This chapter describes the work undertaken to identify novel candidate genes required for axon degeneration and maintenance. Two different unbiased forward genetic screens were utilized. In the first, numerous genes within molecularly defined deletions that removed large sections of the *Drosophila* genome were screened, while in the second screen, a mutagen was used induce random mutations across the genome. In both strategies, mutant phenotypes derived from cell autonomous malfunctions, as only neuronal clones homozygous for deletions or mutations were observed. Causative mutations for each candidate were determined by a combination of next generation sequencing, Sanger sequencing, and classic genetic techniques such as complementation testing, deficiency mapping and rescue by adding back functional genes. Initial phenotypic analysis is presented, describing the lack of axon degeneration in $axed^{0011}$ & $axed^{2094}$. Additionally, I describe two other distinct genes with notable axon death and maintenance phenotypes.

Chapter II: Results & Discussion

Results 2-1: Deficiency screening for axon death genes in Drosophila wing neurons clones.

To identify novel genes required for axon death we first screened a set of molecularly defined deletions with FRT sites in axotomized *Drosophila* wing sensory clones after injury. We generated deletion homozygous GFP+ clones as described previously and (detailed genotypes in Material & Methods) allowed flies to age for 5 days before injury to ensure clearance pre-clone induction protein. Since, the majority of axonal debris from severed axons are cleared by ~5 dpa in wild type, we decided to screen for severed mutant axons that remained preserved at 5-7dpa.

Deficiencies tested comprised of 38.7% of the 1st chromosome, 24.2% of the 2nd chromosome (30.1% of the left arm and 18.7% of the right arm), and 14.5% of the whole *Drosophila* genome. I uncovered a single deficiency with an axon death defective phenotype, Df(1)ED7289 that uncovers *hiw* (Figure 2.1, Table 2.1) Several deficiencies resulted visible clones only in wing sensory neurons, but not ORNs (Df(2L)Exel6001 & Df(2L)Exel6036) and some deficiencies where no clones were generated (Df(2L)Exel6012, Df(2L)Exel7043, & Df(2L)Exel7059).

Results 2-2: Mutagenesis screening for axon death and maintenance genes in Drosophila wing neurons clones.

To identify novel genes required for axon death and maintenance, we performed an unbiased forward genetic mutagenesis screen in glutamatergic sensory neuron MARCM

clones in the adult *Drosophila* wing (Figure 1.1) (Neukomm et al., 2014). We introduced random mutations by ethyl methanesulfonate (EMS) screened extensively on the 1st, 2nd, and 3rd chromosomes. Since this was a clonal screen, we were unable to analyze Chromosome 4 and the male Y chromosome because they lack FRT sites. We were also unable to screen any mutations as homozygous if the affected genes were located between the FRT site and telomere. To effectively saturate the genome, we screened 40,319 mutant flies on the 1st, 2nd, and 3rd chromosome.

On the 1st chromosome we performed an F_2 screen, while on autosomes we were able to perform a more rapid F_1 screen. In the F_2 screen, P_0 males were mutagenized with EMS and bred to virgin females with balancers twice to generate a mutant F_2 stock. Mutant F_2 flies were crossed to flies harboring the required genetic elements to generate homozygous mutant GFP+ neuronal clones in the wing (detailed genotypes in Materials & Methods). In the F_1 screen, P_0 males were mutagenized with EMS and bred to virgin females to produce F_1 offspring males heterozygous for randomly introduced mutations and homozygous for the same mutations in GFP^+-labeled sensory neuron clones (Figure 1.1) (detailed genotypes in Materials & Methods). As described previously, we then transected axons by mechanically severing the wing and assessed axon death in the L1 vein at 7 days post axotomy (Figure 1.1) (Neukomm et al., 2014).

We screened 2,045 mutants on the 1st chromosome, 15959 on the 2nd left arm, 7286 on 2nd right arm, 7646 on the 3rd left arm, and 7383 on the 3rd right arm and identified one mutant on the X chromosome where a subset of severed axons were preserved at 7 dpa, *345x* (Figure 2.2), two mutants on the X chromosome in which uninjured axons

progressively degenerate, *596x* & *1013x* (Figure 2.3), and two mutants on chromosome arm 3L with severed axons that remained morphologically preserved at 7 dpa, *3L.0011* & *3L.2094* (Figure 2.4).

I also isolated several axon death defective mutant alleles of *highwire*: hiw^{157x} encoding an early nonsense mutation (K1312*), hiw^{587x} encoding nonsense mutation in the middle of the gene (W3641*), and hiw^{275x} encoding a dominant nonsense mutation in the RING domain. Characterization of these can be found in the following publication: Neukomm, L.J., Burdett, T.C., Gonzalez, M.A., Züchner, S., and Freeman, M.R. (2014). Rapid in vivo forward genetic approach for identifying axon death genes in Drosophila. Proc Natl Acad Sci USA *111*, 9965–9970.

Results 2-3: Isolation & identification of alleles defective for axon death & axon maintenance on the 1st chromosome

We recovered a single mutant stock, *345x*, harboring both intact and degenerating severed axons at 7 dpa (Figure 2.2-A). To quantify axon death in this assay and others, we scored uninjured control axons extending from cell bodies proximal to the wing cut site (cb, indicated in the upper right corner of each example), extra axons that were severed but axon death defective (severed intact), as well as uncleared axonal fragments (debris). An initial characterization of the axon death phenotype revealed a delay in degeneration with ~20% & ~12% of severed axons remaining intact at 7 & 14 dpa, respectively, compared to no intact remaining anucleated axons after 1 day in wild type (Figure 2.2-B). The stock was embryonic lethal and lethality was linked to the axon death

defective mutation even after five rounds of outcrossing to a wild type genome. Duplications uncovering *hiw* failed to rescue lethality and no mutations within *hiw* locus were observed (data not presented in this thesis). Subsequent duplication mapping, PCR confirmation of mutations, and rescue experiments revealed a single causative mutation within the splice site of the 1st and 2nd exons of *gene-of-interest #1,* (*GOI#1*), a transcription factor (data not presented in this thesis).

I also isolated two distinct mutants on the 1st chromosome with wild type axon death, but severely altered axon morphology in uninjured neurons characterized by large protrusions of the plasma membrane in both axons and dendrites (Figure 2.3-A). Each mutant was homozygous lethal and lethality was linked to the membrane blebbing phenotype after several rounds of outcrossing to a wild type genome. Sequencing revealed one stock, *596x,* with a single missense mutation and mutant stock *1013x* with two missense mutations within the accessory or catalytic domains of *gene-of-interest #2* (*GOI#2*). Additional loss of function alleles and RNAi knockdown of *GOI#2* recapitulated membrane dysfunction (data not in this thesis). Initial characterization of *GOI #2^{596x}* revealed progressive membrane swelling over time culminating in axonal breaks and dying back from distal axonal portions to proximal, while mitochondria within axon fragments and blebs are condensed rather than elongated, matching observations in transected axons (Figure 2.3-B).

Results 2-4: Isolation & identification of novel axon death defective mutations in *axed*.

We isolated two individual mutants with defective axons death on the 3rd left chromosomal arm that were both homozygous lethal at the larval L1 stage. After several

rounds of outcrossing to a wild type chromosome, lethality was consistently linked to axon degeneration suppression. Mutations *3L.0011* & *3L.2094* failed to produce trans-heterozygous offspring (Table 2.2), forming a single complementation group suggesting a single affected gene, which we named *axundead* or *axed.*

Severed axons in $axed^{0011}$ and $axed^{2094}$ mutants exhibited robust morphological preservation equivalent to that observed in dsarm mutants at 7 dpa (Figure 2.4-A/B) (Neukomm et al., 2014). Axon preservation was quantified as above. To precisely assess axon preservation, we compared the number of neuronal cell bodies removed to the number of intact severed axons remaining and found that 99.3% and 100% of severed $axed^{0011}$ and $axed^{2094}$ mutant axons, respectively, remained morphologically intact at 7 dpa (Figure 2.4-C).

Next, we asked if Axed is required for axon death broadly in the nervous system. We assessed axon death cholinergic olfactory receptor neurons (ORNs) using a previously established antennal ablation assay (MacDonald et al., 2006). In wild type, unilateral antennal ablation destroys ORN cell bodies and induces fragmentation of ipsilateral axons that is cleared from the CNS in ~ 7 days, while contralateral axons serve as uninjured controls. In contrast to wild type, mutant axons lacking axed remain preserved at both 7 and 50 dpa (Figure 2.4-D), far beyond the mean lifespan of the fly. Thus, *axed* is essential for axon death, and *axed* mutations preserve axonal morphological integrity to a similar extent as mutations in *dsarm* or *hiw* (Osterloh et al., 2012; Xiong et al., 2012).

To identify the causative gene, we mapped the lethality of *axed*^{0011} and *axed*^{2094} using molecularly defined deficiencies (Dfs) (Figure 2.5-A) and assayed those Dfs that failed to complement lethality for defects in axon death in homozygous Df MARCM clones (Figure 2.5-B). Both axed alleles failed to complement a large Df *ZN47*, and within that region, one smaller Df, *BSC411* (uncovering ~100 genes), while all other partially overlapping deficiencies were able complement the lethality of both axed alleles. Within the non-overlapping region of *ED211* and *BSC411* were 7 candidate genes that could be responsible for *axed* phenotype. We used all available mutations in these genes to complement the lethality of both *axed* alleles and found only a single Minos transposon insertion within *CG8398* (*Mi{MIC}13270* or *CG8398*^{MI13270}) (Figure 2.5-C) (Table 2.2). Consistent with our mapping strategy, MARCM clones of *BSC411* or *Mi{MIC}13270* (hereof *axed*^{MI13270}) were also defective in axon death (Figure 2.5-B/D).

While NGS failed to detect mutations in *CG8398*, focused Sanger sequencing revealed a 16bp deletion in exon 3 in *axed*^{0011} resulting in loss of function. However, we were not able to identify a molecular lesion within the open reading frame of CG8398 in *axed*^{2094}, suggesting it might be a regulatory mutation (Table 2.3). To support our findings that CG8398 is required for axon death, we also created de novo *axed* alleles using two distinct methods, CRISPR/Cas9 and imprecise transposon excision (Metaxakis et al., 2005; Sebo et al., 2014) (Materials & Methods). CRISPR/Cas9 mutants harboring deletions in exon 2 (*axed*^{CrisprA}, *axed*^{CrisprB} & *axed*^{CrisprC}; containing 194bp, and two distinct 14bp deletions, respectively), and Minos imprecise excision-based alleles (*axed*^{ExMI07}, *axed*^{ExMI65} & *axed*^{ExMI96}), all failed to complement the lethality of our original

axed mutagenesis alleles, and they were also defective in axon death (Table 2.3). We therefore conclude that *CG8398* encodes the *axed* gene.

The *CG8398* locus (hereafter *axed*) encodes two predicted isoforms ($axed^{long}$ and $axed^{short}$, respectively) (Figure 2.5-C). We generated transgenic flies harboring isoform specific cDNA rescue constructs containing endogenous 5' and 3' UTRs under the control of the Gal4/UAS binary expression system (*UAS-*$axed^{long}$ and *UAS-*$axed^{short}$, respectively). Expression of either $axed^{long}$ or $axed^{short}$ was sufficient to rescue the axon death phenotype in all axed alleles tested (Figure 2.5-D).

Chapter II: Materials and Methods

Mutagenesis Screen:
Males were starved for 12 hours before consuming mutagen, 25 mM ethyl methane sulphonate (EMS) in 1% sucrose, for 12 hours. Before breeding, males recovered in fresh vials for 12 hours.

Wing injury & antennal ablation assays:
Both assays are described previously (Neukomm et al., 2014). Wing: Wings were cut with MicroPoint Scissors (EMS, VANNAS Scissors; angled on side, delicate, 5-mm cutting edge, # 72933–04) and mounted in Halocarbon Oil 27 on a microscopy slide and covered with a coverslip, and immediately used for microscopy. Antennae: Antennae were ablated using high precision and ultra-fine tweezers (EMS, 78520-5). Adult brain dissections were performed as described(Wu and Luo, 2006).

Immunohistochemistry & Confocal microscopy:
Slides with *Drosophila* wings, mounted in Halocarbon Oil 27 (Neukomm et al., 2014), and brains, stained with anti-GFP mounted in Vectashield anti-fade reagent, were imaged on a Zeiss spinning disc confocal microscope (Intelligent Imaging Innovations, Denver, CO).

Drosophila sequencing
Next-generation sequencing technology (Gonzalez et al., 2012) was used to produce 74bp reads and align reads of each mutant to the *Drosophila melanogaster* reference genome. Backcrossing to a wild type genome was used to remove random background mutations and 'clean up' stocks before sending for sequencing or re-sequencing. PCR and Sanger sequencing of used to confirm NGS results and uncover novel genetic changes overlooked by NGS in specific difficult to read areas.

Cloning:
The cDNA of *axed*^{long} & *axed*^{short} was cloned from clone AY075255 (Berkeley Drosophila Genome Project, http://www.fruitfly.org/). Gibson Assembly was used to clone long and short cDNAs into *pUAST* (Brand and Perrimon, 1993). pUAST was linearized (*EcoRI* & *XbaI*), and PCR products containing endogenous 5' and 3' UTRs as well as coding sequences were inserted using the following primers:
pLN287: p(5x)UAST-axed^{long}*,w*$^{+}$
5'primer:CTCTGAATAGGGAATTGGGAATTCgttttgccatcaactggcaggtattttc
3'primer:CCACAGAAGTAAGGTTCCTTCACAAAGATCCTCTAGAcataagcgctaatattcgtttaatgc

pLN288: *p(5x)UAST-axed^{short},w^{+}*
5'primer:GAGAACTCTGAATAGGGAATTGGGAATTCccaaattccctctggtgggcgccc
3'primer:CCACAGAAGTAAGGTTCCTTCACAAAGATCCTCTAGAcataagcgctaatattcgtttaatgc
Plasmids were sequenced & injected (Bestgene).

Drosophila Stocks and Genotypes in Display Items:
Flies were raised and maintained on standard Drosophila media at 25°C unless otherwise noted. Most stocks listed below were obtained from the Bloomington *Drosophila* Stock Center (NIH P40OD018537)

Deficiency lines:
Chromosomal deficiencies (Cook et al., 2010, 2012; Parks et al., 2004; Thibault et al., 2004). Deficiency stocks recombined with FRTs generously provided by Chris Doe, PhD.

X chromosome:
w, y, sn^{1} & *5xUAS-mCD8::GFP,* and most stocks listed below were obtained from the Bloomington *Drosophila* Stock Center (NIH P40OD018537); *elav-Gal4* (Lin and Goodman, 1994), *ey-FLP^{2}* (Newsome et al., 2000), *hs-FLP^{12}* (Chou and Perrimon, 1996), *hiw$^{\Delta N}$* (Wu et al., 2005), *FRT19A$^{(ry+,hs\text{-}neo)}$* (Xu and Rubin, 1993), *axed cDNA* rescue (including endogenous 5' & 3' UTR, $P_{element}$): *5xUAS-axed$^{long\ \#6}$* (Lukas Neukomm)

Chromosome 2:
5xUAS-mCD8::GFP, *OR22a-Gal4* (Dobritsa et al., 2003), *OK371-Gal4* (Mahr and Aberle, 2006), *FRT40A$^{(ry+,hs\text{-}neo)}$* (Xu and Rubin, 1993), *FRTG13$^{(hs\text{-}w+)}$ (FRT42B)* (Chou and Perrimon, 1996), *ase-FLP^{2a}* & *ase-FLP^{2e}* (Neukomm et al., 2014), *axed cDNA* rescue (including endogenous 5' & 3' UTR, $P_{element}$): *5xUAS-axed$^{long\ \#4}$*, *5xUAS-axed$^{short\ \#2}$* (Lukas Neukomm)

Chromosome 3:
*5xUAS-mCD8::*GFP, *ey-FLP^{6}* (Newsome et al., 2000), *FRT2A$^{(hs\text{-}w+)}$ (FRT79D)* (Chou and Perrimon, 1996), *FR82B$^{(ry+,hs\text{-}neo)}$* (Xu and Rubin, 1993), *axed* alleles (See Table 2.3), *dMCU^{22}*, *dMCU^{46}*, *Jv^{1}* (Shapira et al., 2011), *ndl^{7}* (Anderson and Nüsslein-Volhard, 1984), *ndl^{rm5}* (LeMosy and Hashimoto, 2000), *Zpg ^{LA00675},cg8368^{LA00675}*(Bellen et al., 2004) *Zpg^{z2532} & ^{z2533}* (Tazuke et al., 2002).

Chapter II: Figures & Tables

Figure 2.1: Chromosomal coverage of deficiency lines tested for deficits in axon death.

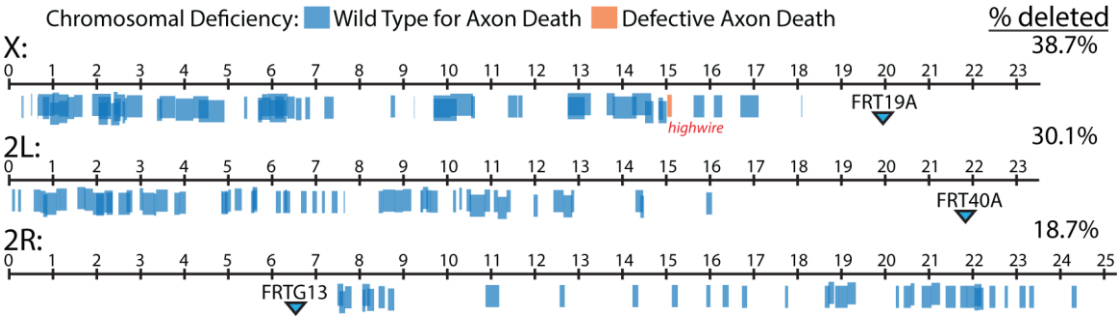

Figure 2.1:
A collection a chromosomal deficiencies screened for axon death defective phenotypes at 5-7 dpa. Deletions with wild type axon degeneration are noted in blue, while a single deletion defective for axon death, Df(1)ED7289 which removes *hiw*, is noted in orange. Shading indicates deletion overlap.

Figure 2.2: Incomplete axon death after injury in *gene-of-interest-#1*^{345x}

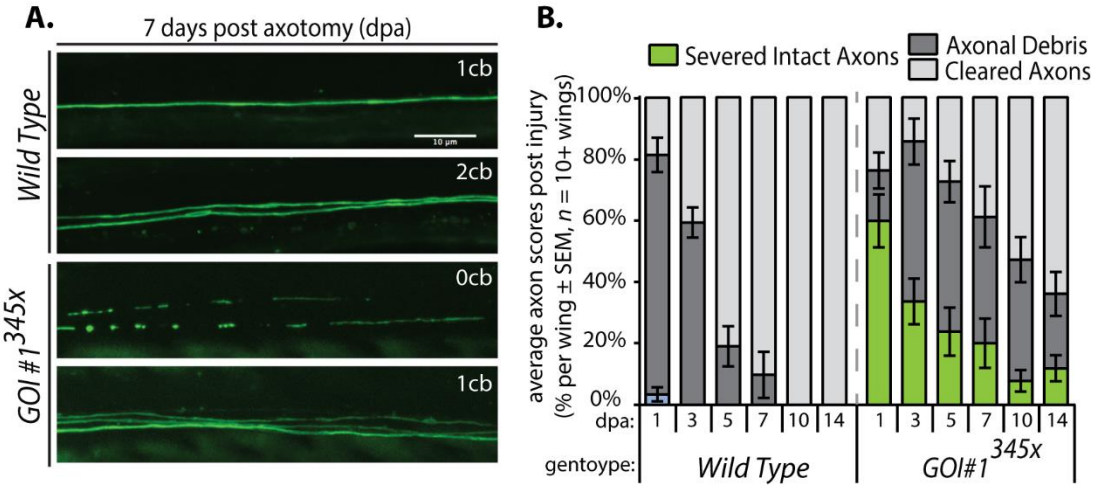

Figure 2.2:

A. A subset of severed axons in *gene-of-interest-#1*^{345x} fail to degenerate. Uninjured axons are noted as cell bodies (cb) proximal to injury site in the upper right hand corner. Scale bar, 10um.

B. Quantification of severed wild type and axed mutant axon phenotype between 1 to14 dpa. (Average percent per wing of severed intact axons, green; fragmented, dark gray; cleared by glia – no axon present; light gray). (n = 10+ wings).

Figure 2.3: Progressive axon die-back in *gene-of-interest-#2*

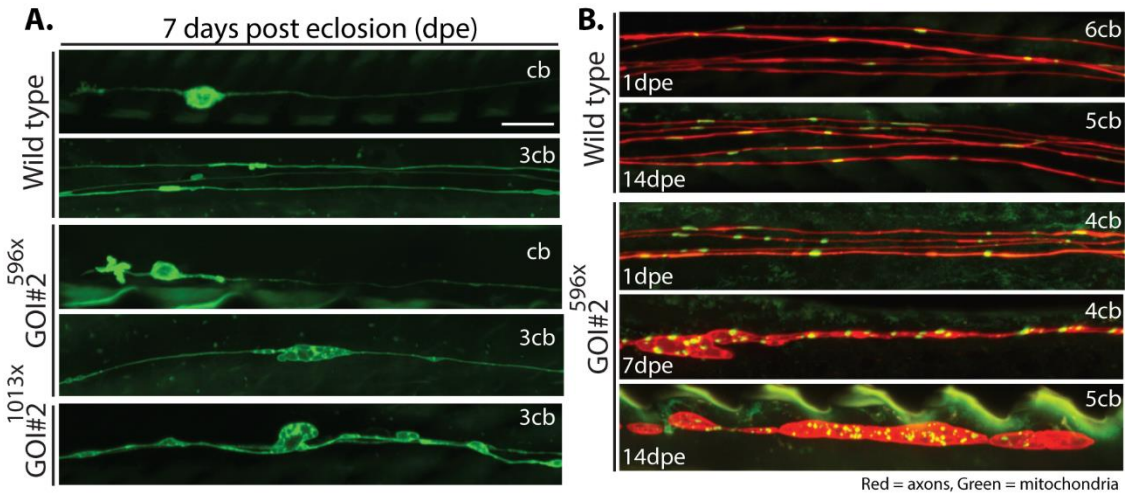

Figure 2.3:

A. Uninjured axons in two mutant alleles of *gene-of-interest-#2* exhibit membrane deformations and axon death at 7 days post eclosion (dpe). Representative images of dendrites & cell bodies (cb) in the distal wing and their axons (number of axons of expected axons is noted as number of cell bodies (#cb) in the distal wing). Axons project left to right from distal wing to synapse in thoracic ganglion.

B. Membrane deformations and axon degeneration increase over time in *gene-of-interest-#2*^{596x} mutant axons. Axons are labeled in tdTomato (red), while mitochondria are labeled with GFP (green). Representative axons in the L1 vein near base of wing, top three images, and in distal wing, bottom.

A & B. Scale bar, 5µm.

Figure 2.4: *Axundead* (*axed*) is required for injury-induced axon degeneration

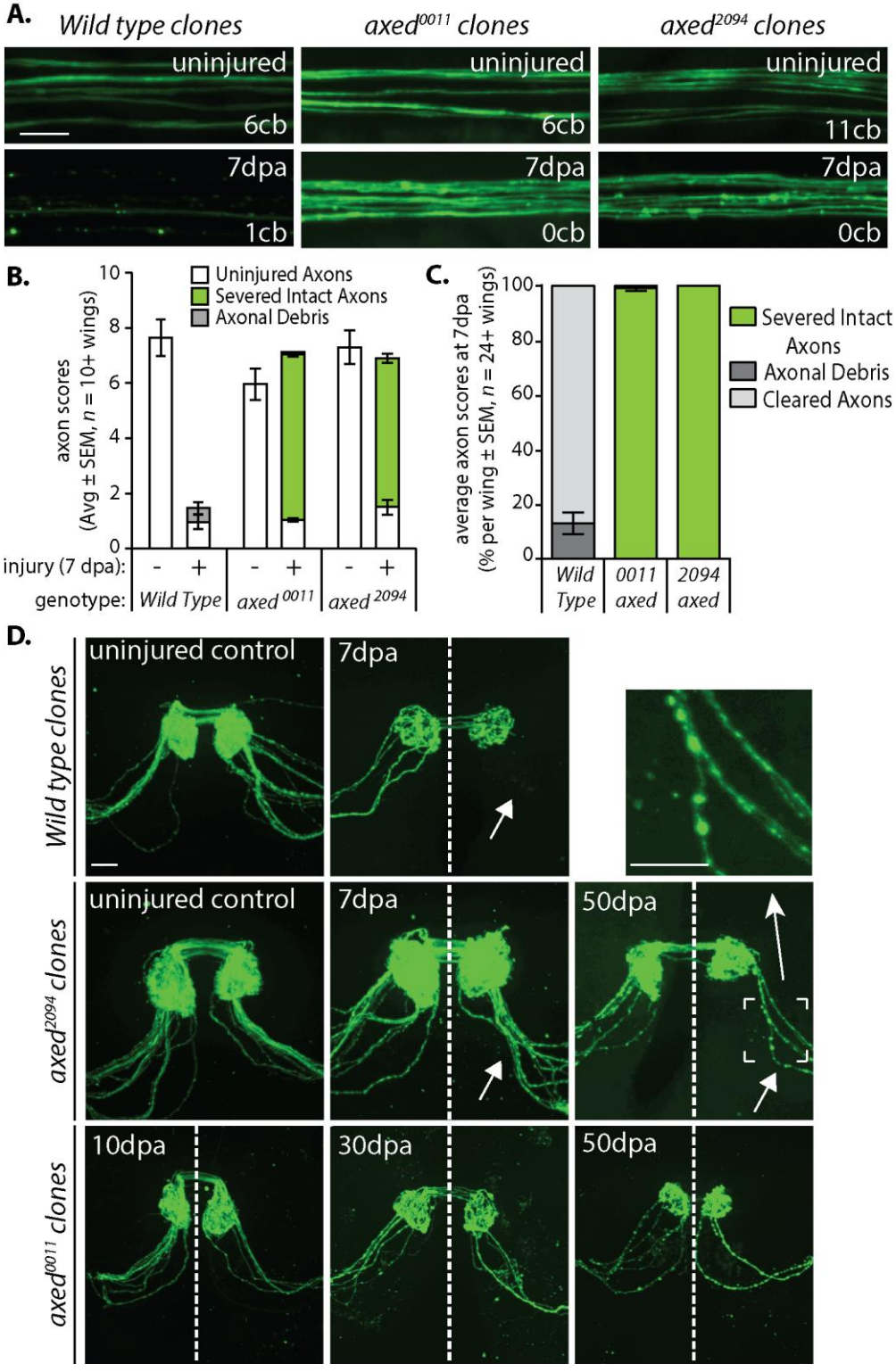

Figure 2.4:
A. Mutant alleles *axed*^{0011} & *axed*^{2094} block axon death in sensory neurons in the wing. Examples uninjured and injured (7 days post axotomy (7 dpa)) axons, respectively. In injured wings, cell bodies (cb) proximal to cut site and their axons remain intact and uninjured, the number is indicated in the lower right corner of each example (scale bar, 5 μm).
B. Axon death quantification in the wing. Uninjured control axons (not severed from cell bodies in uninjured or injured wings), severed intact axons, and axonal debris (white, green and light gray, respectively). Data are shown as average scores (n = 10+ wings).
C. Quantification of severed wild type and axed mutant axon phenotype at 7 dpa (Average percent per wing of severed intact axons, green; fragmented, dark gray; cleared by glia – no axon present; light gray). (n = 24+ wings).
D. Severed axed mutant axons remain intact for the lifespan of *Drosophila*. Unilateral antennal ablation severs axons from cell bodies in wild type, *axed*^{2094} & *axed*^{0011} olfactory receptor neuron (ORN) clones. Axon preservation was scored at indicated time points. A magnified representative image of severed *axed*^{2094} mutant axons at 50 dpa is shown in the upper right corner (scale bar, 10 μm).

Figure 2.5: *Axed*^{0011} and *axed*^{2094} are alleles of the *Drosophila* gene *CG8398*.

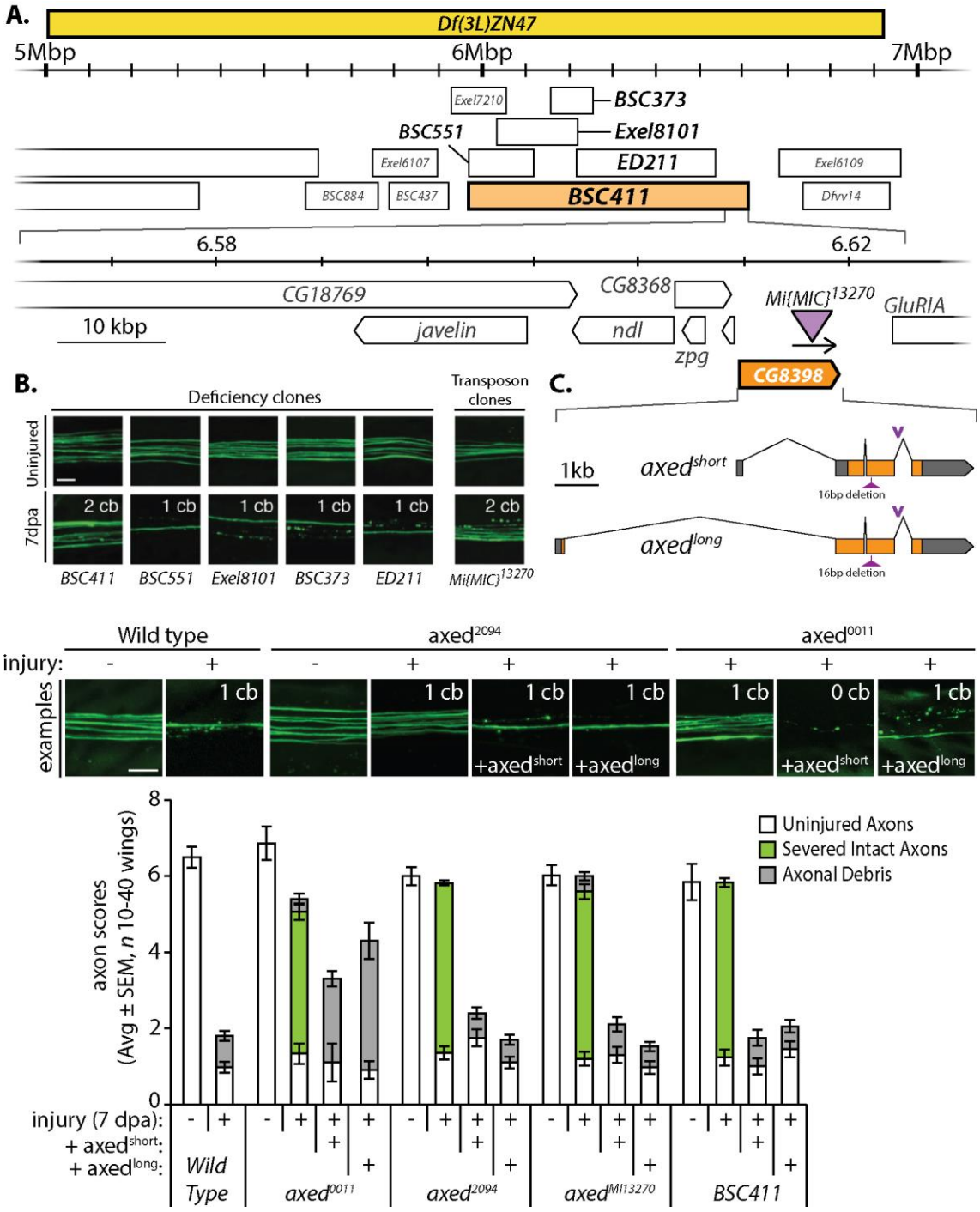

Figure 2.5:

A. The lethality of *axed* maps to *CG8398*. Schematic illustration of the left arm of chromosome 3 uncovered by deficiency *ZN47* (yellow orange bar) with sequence coordinates noted. The lethality of $axed^{2094}$ & $axed^{0011}$ was mapped to *ZN47* and within the smaller deficiency *BSC411* (light orange bar), whereas other deficiencies were viable over both *axed* mutant alleles. While mutant alleles of neighboring genes (names in light gray) complemented the lethality of the mutant *axed* alleles, the Minos transposon *MI13270* ($Mi\{MIC\}^{13270}$) within the annotated gene *CG8398* failed to complement (see Table 2-2).

B. Loss of *CG8398* phenocopies *axed.* Severed axons of clones harboring either *BSC411* or $Mi\{MIC\}^{13270}$ ($axed^{MI13270}$) remain preserved at 7 dpa (scale bar, 5 μm).

b)

C. *CG8398* (*axed*) encodes two predicted transcripts, short and long (UTR and coding region; gray and green, respectively). *MI13270* insertion in the intron between the last two coding exons is noted (v, purple). A 16bp deletion in the 3rd exon of the long isoform and 2nd exon of the short isoform responsible for disruption in $axed^{0011}$ is noted (purple wedge).

D. Clonal expression of either long or short isoform of *axed* ($axed^{long}$ or $axed^{short}$, respectively) rescues the axon death defective phenotype of $axed^{0011}$, $axed^{2094}$, $axed^{MI13270}$, and the deficiency *BSC411* (scale bar, 5 μm). Shown are averages (n = 10-40 wings each).

Table 2.1: List of deficiency lines tested for deficits in axon death

Deficiency	Stock #	Location	Wing Injury:	ORN Ablation:
Chromosome X (1)				
Df(1)Exel6221	7699	X:470743..523667	WT	ND
Df(1)ED6396	9052	X:493529..523630	WT	ND
Df(1)G1	34050	X:644873..654238	WT	ND
Df(1)ED6443	9053	X:656023..1026707	WT	ND
Df(1)Exel6223	7700	X:769982..909250	WT	ND
Df(1)ED404	8030	X:934942..1135445	WT	ND
Df(1)Exel6225	7702	X:986063..1134927	WT	ND
Df(1)Exel6226	7703	X:1134227..1322377	WT	ND
Df(1)ED6521	9281	X:1135273..1353976	WT	ND
Df(1)Exel6227	7704	X:1322377..1478819	WT	ND
Df(1)Exel8196	7769	X:1478819..1669248	WT	ND
Df(1)ED6565	9299	X:1894112..2317631	WT	ND
Df(1)ED409	8950	X:2042227..2317631	WT	ND
Df(1)ED6574	9054	X:2184630..2387766	WT	ND
Df(1)ED11354	9345	X:2325942..2517801	WT	ND
Df(1)Exel6230	7705	X:2387572..2545663	WT	ND
Df(1)Exel6231	7706	X:2387754..2469301	WT	ND
Df(1)ED411	8031	X:2469859..2642686	WT	ND
Df(1)ED6579	9518	X:2589210..2642686	WT	ND
Df(1)ED6584	9348	X:2636213..2685435	WT	ND
Df(1)ED6630	8948	X:2685540..3036910	WT	ND
Df(1)Exel6233	7707	X:3372961..3485687	WT	ND
Df(1)ED6712	9169	X:3432535..3789615	WT	ND
Df(1)ED6716	24145	X:3799196..4204584	WT	ND
Df(1)ED6720	9055	X:4204351..4544753	WT	ND
Df(1)ED6727	8956	X:4325174..4911061	WT	ND
Df(1)Exel6290	7753	X:5364532..5428543	WT	ND
Df(1)Exel6235	7709	X:5516611..5593966	WT	ND
Df(1)ED6802	8949	X:5679980..5965880	WT	ND
Df(1)Exel6236	7710	X:5679987..5770561	WT	ND
Df(1)Exel6237	7711	X:5770561..5892790	WT	ND
Df(1)ED418	8032	X:5901689..6279401	WT	ND
Df(1)ED6829	8947	X:5901976..6353095	WT	ND
Df(1)Exel6238	7712	X:6068994..6268593	WT	ND
Df(1)Exel6239	7713	X:6344333..6516952	WT	ND
Df(1)Exel6240	7714	X:6543963..6669857	WT	ND
Df(1)ED6878	9625	X:6759293..6862948	WT	ND

Df(1)ED6906	8955	X:7195084..7405806	WT	ND
Df(1)Exel6241	7715	X:8709821..8806576	WT	ND
Df(1)Exel9049	7770	X:9247113..9252165	WT	ND
Df(1)ED6989	9056	X:9686653..10070473	WT	ND
Df(1)ED6991	9216	X:9686653..10211524	WT	ND
Df(1)ED7005	9153	X:10071922..10585431	WT	ND
Df(1)ED7010	9057	X:10546870..10629307	WT	ND
Df(1)ED7067	9154	X:11390038..11600997	WT	ND
Df(1)Exel6242	7716	X:11622385..11715783	WT	ND
Df(1)ED7170	8898	X:12752602..13277326	WT	ND
Df(1)ED7165	9058	X:12752602..13138948	WT	ND
Df(1)ED7217	8952	X:13642083..13822321	WT	ND
Df(1)ED7225	24146	X:13784406..14322206	WT	ND
Df(1)ED7229	9352	X:14222234..14653944	WT	ND
Df(1)ED7261	9218	X:14653809..14839412	WT	ND
Df(1)Exel6248	7719	X:14825993..14923667	WT	ND
Df(1)ED7265	9414	X:14826069..15007907	WT	ND
Df(1)ED7289	29732	X:15024777..15125750	AD Suppressed	ND
Df(1)ED7344	9220	X:15626447..15868141	WT	ND
Df(1)ED7355	8899	X:16091487..16278417	WT	ND
Df(1)ED7374	8954	X:16695187..17107632	WT	ND
Df(1)ED13478	29733	X:18085406..18102011	WT	ND
Chromosome 2 (Left)				
Df(2L)Exel6001	7488	2L:67166..129261	WT	no clones
Df(2L)Exel7002		2L:203089..264275	WT	no clones
Df(2L)Exel8003	7774	2L:559139..715085	WT	ND
Df(2L)Exel7005	7775	2L:777148..868373	WT	ND
Df(2L)Exel6003	7490	2L:826173..1074079	WT	no clones
Df(2L)Exel6004	7491	2L:1074079..1158137	WT	no clones
Df(2L)Exel7006	7776	2L:1158197..1311170	WT	no clones
Df(2L)Exel6005	7492	2L:1555098..1737249	WT	no clones
Df(2L)Exel7007	7778	2L:1716977..1909976	ND	no clones
Df(2L)Exel6006	8000	2L:1911627..2175599	WT	no clones
Df(2L)Exel7008	7780	2L:1989057..2152458	WT	no clones
Df(2L)Exel6007	7493	2L:2175607..2362917	WT	no clones
Df(2L)Exel7010	7782	2L:2221020..2362808	ND	WT
Df(2L)Exel6008	7494	2L:2494660..2755377	WT	no clones
Df(2L)Exel6277	7744	2L:2677694..2808100	WT	no clones
Df(2L)Exel7014	7784	2L:2979654..3056809	WT	no clones
Df(2L)Exel7015	7785	2L:3046635..3310250	WT	no clones

Df(2L)Exel8008	7786	2L:3302636..3354856	ND	WT
Df(2L)Exel7016	7787	2L:3354818..3473493	WT	no clones
Df(2L)Exel6009	7495	2L:3771368..3888977	WT	no clones
Df(2L)Exel8010		2L:3887981..4031325	WT	ND
Df(2L)Exel9062	7792	2L:4846961..4887766	WT	ND
Df(2L)Exel8012	7793	2L:4846961..4977638	WT	no clones
Df(2L)Exel7021	7795	2L:4915628..4979299	WT	no clones
Df(2L)Exel8013	7796	2L:4975605..5000943	WT	ND
Df(2L)Exel7022	7794	2L:5000837..5058522	ND	WT
Df(2L)Exel6011	7497	2L:5147258..5305646	WT	WT
Df(2L)Exel6012	7498	2L:5305646..5555049	no clones	no clones
Df(2L)Exel7023	7797	2L:5524375..5594234	WT	no clones
Df(2L)Exel6256	7724	2L:5555049..5658629	ND	WT
Df(2L)Exel8016	7798	2L:5555049..5659285	ND	WT
Df(2L)Exel6015	7501	2L:6088361..6200227	WT	no clones
Df(2L)Exel6016	7502	2L:6253010..6411492	ND	WT
Df(2L)Exel9038	7800	2L:6292895..6338855	ND	WT
Df(2L)Exel7027	7801	2L:6664818..6786906	WT	no clones
Df(2L)Exel7029	7802	2L:6922143..7022660	ND	WT
Df(2L)Exel8019	7803	2L:7140259..7202317	ND	WT
Df(2L)Exel7031	7804	2L:7364976..7495492	WT	ND
Df(2L)Exel9031	7805	2L:7637689..7660390	ND	WT
Df(2L)Exel7038	7809	2L:8438123..8528528	WT	no clones
Df(2L)Exel7039	7810	2L:8529124..8801960	WT	no clones
Df(2L)Exel7040	7811	2L:8797995..8984993	ND	WT
Df(2L)Exel6021	7505	2L:8989308..9176164	WT	no clones
Df(2L)Exel8022	7813	2L:9388129..9448660	WT	ND
Df(2L)Exel9064	7814	2L:9415663..9431473	ND	WT
Df(2L)Exel6022	7506	2L:9447643..9560489	WT	no clones
Df(2L)Exel7042	7812	2L:9522946..9622987	ND	WT
Df(2L)Exel6024	7507	2L:9613611..9782218	WT	ND
Df(2L)Exel6025	7508	2L:9782218..9897536	no clones	ND
Df(2L)Exel7043	7816	2L:9860016..9940209	no clones	no clones
Df(2L)Exel9032	7818	2L:10134181..10198945	ND	WT
Df(2L)Exel7046	7819	2L:10276871..10333704	ND	WT
Df(2L)Exel7048	7999	2L:10443323..10544859	ND	WT
Df(2L)Exel8026	7820	2L:10516675..10861982	WT	ND
Df(2L)Exel7049	7821	2L:10853446..10975285	WT	ND
Df(2L)Exel6027	7510	2L:11067029..11155825	ND	no clones
Df(2L)Exel6028	7511	2L:11155825..11358603	WT	no clones

Df(2L)Exel6029	7512	2L:11358603..11445762	ND	WT
Df(2L)Exel6031	7514	2L:11971081..12066847	WT	ND
Df(2L)Exel6033	7516	2L:12423459..12655793	WT	ND
Df(2L)Exel6034	7517	2L:12655793..12854729	WT	no clones
Df(2L)Exel8028	7822	2L:12832803..12896409	WT	ND
Df(2L)Exel7059	7826	2L:13800829..13878188	no clones	no clones
Df(2L)Exel6035	7518	2L:14300969..14470247	WT	ND
Df(2L)Exel6036	7519	2L:14409711..14490657	WT	no clones
Df(2L)Exel6038	7521	2L:15912343..16042754	WT	WT
Chromosome 2 (Right)				
Df(2R)Exel6052	7534	2R:7493197..7623083	WT	ND
Df(2R)Exel6053	7535	2R:7533553..7665795	WT	ND
Df(2R)Exel6054	7536	2R:7665795..7812472	WT	ND
Df(2R)Exel6056	7538	2R:8061165..8232456	WT	ND
Df(2R)Exel7094		2R:8061165..8131743	WT	ND
Df(2R)Exel6057	7539	2R:8174651..8327431	WT	ND
Df(2R)Exel7096		2R:8433672..8572773	WT	ND
Df(2R)Exel7098	7864	2R:8649482..8733630	WT	ND
Df(2R)Exel6059	7541	2R:10874385..11185938	WT	ND
Df(2R)Exel7121	7869	2R:12570687..12679753	WT	ND
Df(2R)Exel7130	7875	2R:14073080..14212783	WT	ND
Df(2R)Exel7131	7876	2R:14230665..14360425	WT	ND
Df(2R)Exel7135	7879	2R:15129956..15262942	WT	ND
Df(2R)Exel7137		2R:15575885..15859248	no clones	ND
Df(2R)Exel7138	7883	2R:15918423..16007733	WT	ND
Df(2R)Exel7142	7886	2R:16289254..16425289	WT	ND
Df(2R)Exel7145	7887	2R:16731494..16846621	WT	ND
Df(2R)Exel7150	7891	2R:17716262..17782032	WT	ND
Df(2R)Exel7157	7894	2R:18621522..18730771	WT	ND
Df(2R)Exel7158	7895	2R:18705526..18829728	WT	ND
Df(2R)Exel6067	7549	2R:18858042..18947279	WT	ND
Df(2R)Exel6068	7550	2R:18947286..19141949	WT	ND
Df(2R)Exel6069	7551	2R:19141949..19325623	WT	ND
Df(2R)Exel7162	7896	2R:20245186..20313635	WT	ND
Df(2R)Exel7163		2R:20423944..20582746	WT	ND
Df(2R)Exel7164	7898	2R:20582171..20666850	WT	ND
Df(2R)Exel6071	7553	2R:20836033..21056798	WT	ND
Df(2R)Exel6072	7554	2R:21056798..21250845	WT	ND
Df(2R)Exel6076	7556	2R:21379527..21607081	WT	ND
Df(2R)Exel6077	7557	2R:21713968..21872028	WT	ND

Df(2R)Exel7169	7900	2R:21862233..22039630	WT	ND
Df(2R)Exel6078	7558	2R:22039540..22197643	WT	ND
Df(2R)Exel7170	7901	2R:22039641..22135929	WT	ND
Df(2R)Exel7171	7902	2R:22136002..22243250	WT	ND
Df(2R)Exel7173	7903	2R:22380451..22514138	WT	ND
Df(2R)Exel6079	7559	2R:22729367..22798322	WT	ND
Df(2R)Exel7177	7906	2R:23068684..23203998	WT	ND
Df(2R)Exel7178		2R:23291485..23395914	WT	ND
Df(2R)Exel6082	7561	2R:24257897..24369777	WT	ND

Table 2.1:
MARCM clones for each deficiency line were generated and injured at ~5 days post eclosion. Severed axonal integrity was assessed in the L1 wing vein at 5-7days post axotomy. At least 10 flies were tested for each deficiency.
WT = wild type axon death; AD suppressed = axon degeneration is suppressed or defective; no clones = no clones were visible in the wing or olfactory glomeruli; ND = no data.

Table 2.2: *Axed* complementation test for lethality

Trans-het.	Detailed description	Lethal or Viable
axed^{0011}/ *axed*^{2094}	-	Lethal
axed^{2094}/ *Df(3L)ZN47*	Deficiency uncovering genomic *axed*	Lethal
axed^{2094} OR *0011*/ *Df(3L)BSC411*	Deficiency uncovering genomic *axed*	Lethal
axed^{2094}/ *Df(3L)****	***Deficiencies noted in Figure 2-5(A) + large deficiencies not uncovering genomic *axed*.	Viable
axed^{2094} OR *0011*/ *axed*^{MI13270}	Minos transposon *Mi{MIC}CG8398*^{MI13270}	Lethal
axed^{2094} OR *0011*/ *dMCU*^{46} OR *22*	CRISPR/Cas9 generated alleles of *CG18769*	Viable*
axed^{2094} OR *0011*/ *Jv*^{1}	Hypomorphic allele of *javelin*	Viable*
axed^{2094} OR *0011*/ *ndl*^{7} OR *rm5*	EMS mutagenesis (*ndl*^{7}) LOF allele (*ndl*^{rm5})	Viable*
axed^{2094} OR *0011*/ *Zpg+cg8368-LA00675*	CRISPR/Cas9, 194bp deletion, exon 2	Viable*
axed^{2094} OR *0011*/ *Zpg z2532,z2533*	CRISPR/Cas9, 14bp deletion, exon 2	Viable*

Table 2.2:
Axed mutant alleles fail to complement lethality of each other and deficiencies uncovering *CG8398*, but are viable as trans-heterozygotes over other deficiencies and genes. If viable, a (*) indicates that trans-heterozygous animals axons degenerated normally after injury.

Table 2-3: Novel axed alleles generated

Axed allele	Detailed description	Axon death phenotype
axed^{0011}	EMS mutagenesis, 16bp deletion exon 3	yes
axed^{2094}	EMS mutagenesis	yes
BSC411	Deficiency uncovering genomic *axed*	yes
axed^{MI13270}	Minos transposon *Mi{MIC}CG8398*^{MI13270}	yes
axed^{Ex05}	Precise Minos excision	no
axed^{Ex07}	Imprecise Minos excision	yes
axed^{Ex65}	Imprecise Minos excision	yes
axed^{Ex96}	Imprecise Minos excision	yes
axed^{CrisprA}	CRISPR/Cas9, 194bp deletion, exon 2	yes$^{\#}$
axed^{CrisprB}	CRISPR/Cas9, 14bp deletion, exon 2	yes$^{\#}$
axed^{CrisprC}	CRISPR/Cas9, 14bp deletion, exon 2	yes$^{\#}$

Table 2-3:
Summary of all *axed* alleles used and their axon death phenotypes. If known, the molecular nature of each lesion is indicated. $^{\#}$, partial axon death phenotype.

Table 2.4: Genotypes for figures/experiments:

Abbreviations: *Y: Y* chromosome, *w: w^{1118}* or *w^{-}*, *OK371: OK371-Gal4*, *mCD8::GFP: 5xUAS-mCD8::GFP, OR22a: OR22a-Gal4*

Figure 2-1:
X: *Deficiency,FRT19A/tubGal80,hsFLP,FRT19A ; OK371,mCD8::GFP,aseFLP^{2a}/+ ; mCD8::GFP,aseFLP^{3b}/+*
2L: *elav-Gal4,mCD8::GFP/+ ; Deficiency,FRT40A/tubGal80,FT40A ; mCD8::GFP,aseFLP^{3a}/+*
2R: *elav-Gal4,mCD8::GFP/+ ; FRTG13,Deficiency/FRTG13,tubGal80 ; mCD8::GFP,aseFLP^{3b}/+*
Mutagenesis Screen:
X: *mut*,FRT19A/tubGal80,hsFLP,FRT19A ; OK371,mCD8::GFP,aseFLP^{2a}/+ ; mCD8::GFP,aseFLP^{3b}/+*
2L: *elav-Gal4,mCD8::GFP/+ ; mut*,FRT40A/tubGal80,FT40A ; mCD8::GFP,aseFLP^{3a}/+*
2R: *elav-Gal4,mCD8::GFP/+ ; FRTG13,mut*/FRTG13,tubGal80 ; mCD8::GFP,aseFLP^{3b}/+*
3L: *w/Y ; OK371,mCD8::GFP,aseFLP^{2e}/+ ; mut*,FRT2A/tub-Gal80,FRT2A*
3R: *w/Y ; OK371,mCD8::GFP,aseFLP^{2a}/+ ; FRT82B,mut*/FRT82B,tub-Gal80*
Figure 2-2:
A-B. *wild type:* *FRT19A/tubGal80,hsFLP,FRT19A ; OK371,mCD8::GFP,aseFLP^{2a}/+ ; mCD8::GFP,aseFLP^{3b}/+*
A-B. *gene of interest #1^{345x}:* *GOI#1^{345x},FRT19A/tubGal80,hsFLP,FRT19A ; OK371,mCD8::GFP,aseFLP^{2a}/+ ; mCD8::GFP,aseFLP^{3b}/+*
Figure 2-3:
A. *wild type:* *FRT19A/tubGal80,hsFLP,FRT19A ; OK371,mCD8::GFP,aseFLP^{2a}/+ ; mCD8::GFP,aseFLP^{3b}/+*
A. *gene of interest #2^{596x}:* *GOI#2^{596x},FRT19A/tubGal80,hsFLP,FRT19A ; OK371,mCD8::GFP,aseFLP^{2a}/+ ; mCD8::GFP,aseFLP^{3b}/+*
A. *gene of interest #2^{1013x}:* *GOI#2^{1013x},FRT19A/tubGal80,hsFLP,FRT19A ; OK371,mCD8::GFP,aseFLP^{2a}/+ ; mCD8::GFP,aseFLP^{3b}/+*
B. *wild type:* *FRT19A/tubGal80,hsFLP,FRT19A ; OK371,10XUAS-IVS-myr::tdTomato,5xUAS-mito-HA-GFP.AP/+ ; 10XUAS-IVS-myr::tdTomato,aseFLP^{3b}/+*
B. *gene of interest #2^{596x}:* *GOI#2^{596x},FRT19A/tubGal80,hsFLP,FRT19A ; OK371,10XUAS-IVS-myr::tdTomato,5xUAS-mito-HA-GFP.AP/+ ; 10XUAS-IVS-myr::tdTomato,aseFLP3b/+*
Figure 2-4:
A-C. *wild type:* *w/Y ; OK371,mCD8::GFP,aseFLP^{2e}/OK371,mCD8::GFP ; FRT2A/tub-Gal80,FRT2A*
A-C. *axed^{2094}:* *w/Y ; OK371,mCD8::GFP,aseFLP^{2e}/OK371,mCD8::GFP ; axed^{2094},FRT2A/tub-Gal80,FRT2A*
A-C. *axed^{0011}:* *w/Y ; OK371,mCD8::GFP,aseFLP^{2e}/OK371,mCD8::GFP ; axed^{0011},FRT2A/tub-Gal80,FRT2A*
D. *wild type:* *w,eyFLP^{2}/Y ; OR22a,mCD8::GFP/+ ; FRT2A/tub-Gal80,FRT2A*
D. *axed^{2094}:* *w,eyFLP^{2}/Y ; OR22a,mCD8::GFP/+ ; axed^{2094},FRT2A/tub-Gal80,FRT2A*
D. *axed^{0011}:* *w,eyFLP^{2}/Y ; OR22a,mCD8::GFP/+ ; axed^{0011},FRT2A/tub-Gal80,FRT2A*
Figure 2-5:
A. Complementation groups for lethality: *w/Y ; +/+ ; Deficiency OR Mi{MIC}^{13270}OR lethal alleles of neighboring genes / axed^{2094} OR axed^{0011},FRT2A*
B. *BSC411:* *w/Y ; OK371,mCD8::GFP,aseFLP^{2e}/+ ; BSC411,FRT2A/tub-Gal80,FRT2A*
B. *BSC551:* *w/Y ; OK371,mCD8::GFP,aseFLP^{2e}/+ ; BSC551,FRT2A/tub-Gal80,FRT2A*
B. *Exel8101:* *w/Y ; OK371,mCD8::GFP,aseFLP^{2e}/+ ; Exel8101,FRT2A/tub-Gal80,FRT2A*
B. *BSC373:* *w/Y ; OK371,mCD8::GFP,aseFLP^{2e}/+ ; BSC373:,FRT2A/tub-Gal80,FRT2A*
B. *ED211:* *w/Y ; OK371,mCD8::GFP,aseFLP^{2e}/+ ; ED211,FRT2A/tub-Gal80,FRT2A*
B. *Mi{MIC}^{13270}:* *w/Y ; OK371,mCD8::GFP,aseFLP^{2e}/+ ; Mi{MIC}^{13270},FRT2A/tub-Gal80,FRT2A*
C. -
- *wild type:* *w/Y ; OK371,mCD8::GFP,aseFLP^{2e}/+ ; FRT2A/tub-Gal80,FRT2A*
- *axed^{2094}:* *w/Y ; OK371,mCD8::GFP,aseFLP^{2e}/+ ; axed^{2094},FRT2A/tub-Gal80,FRT2A*
- *axed^{2094} + axed^{long}:* *w/Y ; OK371,mCD8::GFP,aseFLP^{2e}/5xUAS-axed$^{long\ \#4}$; axed^{2094},FRT2A/tub-Gal80,FRT2A*
- *axed^{2094} + axed^{short}:* *w/Y ; OK371,mCD8::GFP,aseFLP^{2e}/5xUAS-axed$^{short\ \#2}$; axed^{2094},FRT2A/tub-Gal80,FRT2A*
- *axed^{0011} & axed^{MI13270} & BSC411:* as above
Table 2-2:
Complementation groups for lethality: as noted in Figure 2-5.A

Axon death in viable transheterozygotes: *w/Y ; OK371,mCD8::GFP ; lethal alleles of neighboring genes / axed^{2094} OR axed^{0011},FRT2A*
Table 2-3:
w/Y ; OK371,mCD8::GFP,aseFLP^{2e}/+ ; axed^{alleles},FRT2A/tub-Gal80,FRT2A

CHAPTER III: Axon Death Pathways Converge on Axed to Promote Axon Disassembly.

This work was conducted in the laboratory of Marc Freeman. I conducted all of the described Drosophila work in close collaboration with the following people who performed the following: Lukas Neukomm: 1) generated *axed*$^{EGFP::FLAG}$; 2) tested *axed* allele suppression of hid; 3) tested *bsk* mutant alleles. Jaeda Coutinho-Budd dissected and imaged *axed*$^{EGFP::FLAG}$ and *UAS-axed::smGdP-cMyc* larval and adult brains; Yonca Karadeniz tested axed alleles in mushroom body pruning; Amy Sheehan cloned *5xUAS-axed::smGdP-cMyc*; Jeannette Osterloh initially characterized *dsarm* deletion constructs used. They were generated by Amy Sheehan, re-tested by myself, Lukas Neukomm, & Jon Farley in the wing.

The following publication is in preparation as follows:

Axon death pathways converge on Axed to promote functional and structural axon disassembly

Lukas J. Neukomm* & Thomas C. Burdett*, Jaeda Coutinho-Budd, Andrew M. Seeds, Stefanie Hampel, Jack Wong, Yonca Karadeniz, Jeannette M. Osterloh, Amy E. Sheehan, and Marc R. Freeman

Abstract

In the previous chapter I described the identification of Axed a novel, essential component for injury induced axon death. In this chapter I present our attempts to definitively position Axed degenerative function within that pathway. To do this we first demonstrate that endogenous, fluorescently tagged Axed is expressed in neurons and within the axonal compartment. Next, we show that Axed function is specific to axon death and is independent from other axon destroying pruning programs as well as broad apoptotic cell death. Finally, we define a position for Axed in the axon death pathway. We find that Axed is required for whole cell degeneration induced by constitutively active dSarm and induced by Nmnat knock-down or knock-out. Additionally, we find Hiw to be upstream of Axed. We do not find a role for MAPKs in several degenerative contexts and thus are unable to determine any relationship to Axed. Taken together our results suggest a role for Axed downstream of both dSarm pro-degenerative signaling and death resulting from declining Nmnat after injury.

Chapter III: Results & Discussion

Results 3-1: Axed is expressed in neurons & within the axonal compartment

While our data in neuronal clones strongly suggested a cell autonomous role for Axed, we sought to visualize endogenous Axed in neurons and define its subcellular localization. While attempts to generate Axed antibodies failed, we generated endogenously EGFP::FLAG tagged Axed (*axed*$^{EGFP::FLAG}$) by Recombination Mediated Cassette Exchange (RMCE) (Venken et al., 2011) with the *axed*^{MI13270} Minos transposon inserted in the intron of the last two coding exons (Figure 2.5-C). If *axed* protein was produced with this transposon present, it would be truncated removing the C-terminal region (Figure 3.1-A), however it is likely the mRNA transcript in these flies is subject to nonsense mediated decay. In contrast to *axed*^{MI13270}, *axed*$^{EGFP::FLAG}$ animals are homozygous viable and exhibit normal axon death after axotomy, indicating that Axed$^{EGFP::FLAG}$ is functional. Western blots revealed two different Axed$^{EGFP::FLAG}$ proteins in heads of *axed*$^{EGFP::FLAG}$ flies (Figure 3.1-B), which correspond to Axed^{long} and Axed^{short}. These findings confirmed that both protein isoforms are expressed in adult brains.

We took advantage of *axed*$^{EGFP::FLAG}$ animals to assess if Axed was expressed in neurons and where it localized. First, we explored the expression pattern of Axed, and found that it was enriched in the neuropil of the larval ventral nerve cord (Figure 3.1-C, top) and adult brain (Figure 3.1-F). The neuropil consists mainly of axons and dendrites (neurites), synapses and astrocytic processes, while the cortex houses neuronal cell bodies and cortex glia (Coutinho-Budd and Freeman, 2013). We stained for a variety of

markers in third instar larval Axed$^{EGFP::FLAG}$ brains, and found that Axed is in close proximity to synapses (nc82) (Figure 3.1-C), whereas markers for astrocytic processes (GAT) did not indicate a prominent expression of Axed (Figure 3.1-C). Axed also expressed at lower relative levels in surrounding cortex. To differentiate between neuronal cell bodies and cortex glial processes, we stained for Zydeco, which is expressed in glial processes (Melom and Littleton, 2013), and found Axed only in neuronal cell bodies, at or near the plasma membrane, but excluded from or expressed at extremely low levels in neuronal nuclei (Figure 3.1-C). To more specifically target expression in axons, we visualized neuronal membranes of larval abdominal nerves with HRP and found that Axed localized to axons throughout the nerves (Figure 3.1-D). We also tagged Axed^{long} with a non-fluorescent 'spaghetti monster GFP' ('smGdP') consisting of 10 cMyc tags under the control of a 5xUAS promoter and expressed it in a subset of octopaminergic neurons using Tdc2-Gal4. Similar to Axed$^{EGFP::FLAG}$, Axed$^{smGdP\text{-}cMyc}$ is stably expressed in axons and notably excluded from neuronal nuclei. Within neuronal cell bodies, is punctate and closely matches membrane associate myr$^{smGdP\text{-}cMyc}$ (Figure 3.1-E). Taken together, we conclude that Axed is expressed in neurons, absent in neuronal nuclei, and enriched in neuronal processes.

Does Axed localization change after injury? To explore this possibility we performed unilateral antennal ablation and visualized Axed$^{GFP::FLAG}$ intensity over time in antennal lobes (Figure 3.1-F). Compared to wild type (i.e. non-GFP) brains, Axed basal levels remained unchanged for 2 hours post antennal ablation, but significantly increased at 4 and 6 hours, and returned to baseline at 24 hours (Figure 3.1-G). These data are

consistent with the notion that Axed$^{GFP::FLAG}$ localization or levels transiently change in response to axonal injury.

Results 3-2: Axed is not required for axonal developmental pruning or programmed cell death

We next determined whether Axed is required specifically for axon death or if it is also involved in other regressive events such as cell death or pruning. First, we used the eye-specific glass multimer reporter to ectopically express pro-apoptotic hid (GMR-hid^{10}) to induce widespread cell death in the developing visual system (Figure S3A) (Bergmann et al., 1998). While mutant clones of the Nedd2-like caspase dronc^{I29} were able to suppress hid mediated eye ablation, wild type or axed clones failed to do so (Figure 3.2-A). Likewise, we found that pruning of axons or dendrites in larval mushroom body (MB) γ neurons was not affected by axed mutations(Lee et al., 2000)(Figure 3.2-B). These observations confirm that Axed, like dSarm, is selectively required for axon degeneration after injury, but not axon degeneration during pruning or in cell death (Osterloh et al., 2012).

Results 3-3: Axed is required downstream of dSarm pro-degenerative signaling

We next sought to determine where axed functions with respect to the other known axon death genes. First we determined if there was any genetic interaction between *axed* and *dsarm* by producing transheterozygous animals. Null mutations in both genes are lethal, while transheterozygotes for *axed*^{0011}/*dsarm*^{4621} were viable and their axons underwent death with similar kinetics as observed in wild type axons, as fragments

of axons were readily observed at 7 dpa (Figure 3.3-A). Next, we attempted to rescue axon death *axed* and *dsarm* mutants with a bacterial artificial chromosome (BAC) containing a genomic copy of wild type *dsarm*. While the genomic copy of wild type *dsarm* was able to fully rescue the axon death phenotype in $dsarm^{4314}$ mutants, it failed to rescue $axed^{0011}$ or $axed^{2094}$ mutants (Figure 3.3-B). Overexpression of full length $dsarm^{P862Q}$ (dSarm with a single missense mutation) fully rescues degeneration in $dsarm^{896}$, but has no effect on preserved severed axons in $axed^{0011}$ (Figure 3.3-C).

dSarm consists of a conserved N-terminal armadillo (ARM), two sterile alpha motifs (2xSAM), and a C-terminal Toll/interleukin-1 receptor homology (TIR) domain. Consistent with structure/function studies in worms and mouse cultured neurons(Chuang and Bargmann, 2005; Gerdts et al., 2013, 2015; Yang et al., 2015), previous work in the Freeman lab found that the SAM and TIR functional domains were essential to rescue the axon death phenotype in $dsarm^{896}$ mutant clones (data not shown in thesis, see preface for unpublished work cited). Expression of constructs lacking the SAM or TIR domains did not dominantly alter axon death in wild type, or cause spontaneous axon degeneration in the absence of injury. However, clones expressing dSarm lacking the ARM domain ($dsarm^{\Delta ARM}$), proposed to be auto-inhibitory in C. elegans (Chuang and Bargmann, 2005), underwent spontaneous cell body and axon degeneration (Figure 3.3-D/E). To assess if $dsarm^{\Delta ARM}$ induced degeneration in Drosophila, we scored the number of intact cell bodies and axons in age-matched adults at 1 through 10 days post eclosion (dpe). We found that $dsarm^{\Delta ARM}$ triggered the spontaneous degeneration of cell bodies and axons within 2-3 dpe in wild type (Figure 3.3-D/E) and *dsarm* mutants lacking endogenous

dSarm (Figure 3.3-F). This dsarm$^{\Delta ARM}$ mediated neurodegenerative phenotype was not specific to glutamatergic sensory neuron clones in the wing. We also observed a similar phenotype in larva when transiently expressing *dsarm*$^{\Delta ARM}$ in ddaC neurons and in adult-specific postmitotic PDF+ neurons using temperature sensitive Gal80ts ON/OFF system to express dsarm$^{\Delta ARM}$ (data not shown in thesis). In all cell types co-expression of P35, a broad apoptosis inhibitor, did not alter neurodegeneration, while co-expression of Wld^{S}, a potent inhibitor of Wallerian degeneration, was able to partially suppress cell body and axon degeneration induced by *dsarm*$^{\Delta ARM}$ (Figure 3.3-F). Thus, *dsarm*$^{\Delta ARM}$ resembles a pro-degenerative gain-of-function allele of dSarm in vivo, similar to versions of the TIR domain that can be dimerized for activation (Gerdts et al., 2015; Yang et al., 2015). Together our data argue that dSarm$^{\Delta ARM}$ activates a Wallerian-like program of degeneration in vivo, and that Wld^{S} either acts downstream of *dsarm*$^{\Delta ARM}$, or in parallel, since its activity is sufficient to partially overcome the pro-degenerative effects of dSarm activation, as has been found in vitro (Gerdts et al., 2015). Finally, we found that hiw mutant clones did not alter the pro-degenerative *dsarm*$^{\Delta ARM}$ phenotype at 10 dpe (Figure 3.3-F), arguing that Hiw acts upstream or in parallel to dSarm.

To determine the position of axed in the axon death signaling cascade, we explored the possibility that Axed might function downstream of dSarm. We expressed *dsarm*$^{\Delta ARM}$ in clones of *axed*^{2094}, *axed*^{0011} and *BSC411*, uncovering the axed genomic locus, and scored cell body and axon survival at 10 dpe. Loss of Axed function completely suppressed *dsarm*$^{\Delta ARM}$–mediated cell body and axonal degeneration at 10 dpe and some neurons persisted to 50 dpe, despite continuous dSarm$^{\Delta ARM}$ production (Figure

3.3-F/G). *Axed* null mutant suppression of *dsarm*$^{\Delta ARM}$ appeared complete, with the exception of some swelling which more apparent in cell bodies than in axons, and was much stronger than afforded by Wld^{S}. Axed is required genetically downstream for all dSarm-mediated pro-degenerative functions.

Results 3-4: Axed is required downstream of degeneration induced by loss of Nmnat

The NAD+ biosynthetic enzyme Nmnat is required for axon survival, and one isoform in mammals, Nmnat2, functions as a labile axon survival factor whose depletion induces Wallerian-like degeneration of even uninjured axons (Fang et al., 2012; Gilley and Coleman, 2010). Intriguingly, while mouse *Nmnat2*$^{-/-}$ knock-out animals die during embryonic stages and exhibit short axons, *Sarm1*$^{-/-}$ knock-out mutations can fully rescue *Nmnat2*$^{-/-}$ animals to adulthood (Gilley et al., 2015). *Nmnat2*$^{-/-}$ animals likely survive due to the NAD+ biosynthetic activity of two additional mammalian Nmnat isoforms, Nmnat1 and Nmnat3 (Gilley and Coleman, 2010). A current model posits that activated Sarm1 triggers rapid NAD+ destruction and loss of NAD+ then promotes axon degeneration (Gerdts et al., 2015). To test this model we used RNA interference (RNAi) to knock down the sole Drosophila Nmnat. We analyzed Nmnat knock-down effects in clones expressing *nmnat*^{RNAi} by assessing the integrity of cell bodies and axons over time, as described above with *dsarm*$^{\Delta ARM}$: compared to control clones, clones expressing *nmnat*^{RNAi} underwent complete cell body and axon degeneration within 8-10 dpe (Figure 3.4-A/B). These findings are consistent with previous reports (Fang et al., 2012), but knock-down of Nmnat was less potent, probably due to a different Gal4 driver used in this study. Interestingly, *nmnat*^{RNAi}-mediated degeneration of cell bodies and axons was

completely suppressed in distinct *axed* null mutant clones at 10 dpe (Figure 3.4-C). We also found suppression, though less robust, in clones lacking *dsarm*. Importantly, $nmnat^{RNAi}$-mediated degeneration in $axed^{2094}$,$dsarm^{896}$ double mutants were similar compared to *axed* single mutants, suggesting that *axed* is epistatic to *dsarm*. In contrast, loss of *hiw* was not able to significantly suppress $nmnat^{RNAi}$-mediated degeneration at 10dpe, however significantly delayed degeneration compared to wild type at 5dpe, consistent with previous findings and supporting a model with Hiw/Phr1 function upstream of Nmnat/Nmnat2 depletion (Babetto et al., 2010; Xiong et al., 2012). While Nmnat-RNAi induced whole neuron degeneration, we also wanted to see if suppression of death was also afforded to severed axons in this background. While we were unable to sever control axons at 5 dpe because most were already degenerated, we found approximately 90+% and 75% of anucleated axons in null alleles of *axed* and *dsarm*, respectively, remained intact to 7dpa.

RNAi-mediated knock-down often leads to partial phenotypes as compared to loss of function mutations. To determine the fate of neurons completely devoid of Nmnat activity and therefore lacking all NAD+ biosynthetic activity (Rongvaux et al., 2003; Sasaki et al., 2016), we analyzed cell body and axon integrity over time in clones of the a deletion uncovering most of *Nmnat*, $Nmnat^{4790\text{-}1}$ (Zhai et al., 2006). As compared to wild type, $Nmnat^{4790\text{-}1}$ clones in either wild type, *axed* heterozygote, or *dsarm* heterozygote backgrounds underwent rapid neurodegeneration within by 5dpe (Figure 3.5-A, right arm). Heterozygous $Nmnat^{4790\text{-}1}$ had no effect on uninjured axon or cell body survival and did not attenuate axon survival after injury in *axed* or *dsarm* null alleles (Figure 3.5-A,

left arm & 3.5B). Next, we used a heat-shock mediated approach to stochastically generate low numbers of GFP+-labeled *Nmnat* null clones, additionally homozygous for either wild type or unique *axed* or *dsarm* alleles. At 5 dpe, while *Nmnat* clones underwent complete neurodegeneration, double clones lacking *Nmnat* and *axed* remained morphologically preserved (Figure 3.5-C/D), arguing that execution of loss-of-nmnat triggered neurodegeneration requires axed. In contrast, loss-of-*Nmnat* triggered neurodegeneration was not altered in *dsarm* alleles, $dsarm^{896}$ & $dsarm^{4621}$, suggesting that loss of dsarm is not sufficient to block neurodegeneration induced by cellular depletion of Nmnat (Figure 3.5-C/D). Importantly, *axed, dsarm* double clones completely blocked *Nmnat*-mediated neurodegeneration, supporting a function for *axed* downstream of *dsarm*. When $axed^{long}$ was re-expressed in double null clones, *Nmnat*-loss induced degeneration is completely restored, further confirming a requirement for Axed to participated in the degenerative process (Figure 3.6-A). We also expressed $Nmnat^{RNAi}$ in a double null clonal background to ensure all *Nmnat* was eliminated and still observed protection with *axed*. Neurons lacking *axed* and *Nmnat* even remained intact to 30dpe (Figure 3.6-D). Taken together, we conclude that Axed is essential for neurodegeneration triggered by loss of Nmnat.

We demonstrated a requirement for Axed downstream of pro-degenerative dSarm and also downstream of loss of Nmnat. These two insults are occurring within an axon after injury, likely at the same time, and possibly from two parallel signaling pathways. In order to determine Axed is required for both processes within a single neuron, we expressed $dsarm^{\Delta ARM}$ in an *axed, Nmnat* null background and observed no degeneration

compared to rapid death in wild type at 5dpe (Figure 3.6-A), confirming both degenerative events converge on Axed.

Our epistatic analyses were derived from manipulated genetic environments, such as expression of a gain-of-function-dSarm or knock-down of Nmnat, which caused degeneration of whole neurons. In order to confirm the position of Axed in injury-induced axon degeneration signaling, we axotomized clones lacking *axed* and *Nmnat*, additionally expressing GFP or dsarm$^{\Delta ARM}$ and found the majority of severed axons remained morphologically preserved at 7 dpa in (Figure 3.6-B/C). These findings clearly suggest that both known axon death events after injury require Axed to promote the disassembly of severed axons.

Results 3-5: Genetic interactions with other axon death genes

Highwire/Phr1 is an ubiquitin E3 ligase that plays an essential role in regulating turnover of Nmnat and elimination results in long term suppression of axon death, primarily as a result of persistently higher Nmnat levels within the axonal compartment. We sought to assess whether overexpressing Hiw, theoretically increasing Nmnat proteasomal degradation, could rescue degeneration in severed *axed* null axons. We found overexpression of Hiw to levels sufficient to rescue degeneration in *hiw*$^{\Delta N}$ null background, had no effect on anucleated axon preservation in *axed*^{0011} (Figure 3.7).

The C. elegans dSarm/Sarm1 homologue tir-1 has been shown to act upstream of MAPK as well as c-Jun N terminal kinases (JNKs) during regulation of asymmetric odorant receptor expression (Chuang and Bargmann, 2005). Consistent with these findings, the mammalian MAPK kinases Mkk4 and Mkk7 as well JNK1-3 were recently

implicated in early events of axon death signaling downstream of Sarm1 (Yang et al., 2015), suggesting that axon degenerative signaling may parallel a signaling cascade in C. elegans. We found that the Drosophila null alleles of these genes ($MKK4^{e01485}$, $MKK4^{Exel6149}$, $MKK7/hep^{r75}$, $JNK/bsk^{flp170B}$ & bsk^{2}, respectively) were not able to suppress pro-degenerative $dsarm^{\Delta ARM}$ signaling at 10 dpe, nor were they defective in axon death in our wing assay at 7 dpa (Glise et al., 1995; Sluss et al., 1996; Thibault et al., 2004) (Table 3.2). Given that Drosophila has a single JNK ortholog (*bsk*), our data argue strongly against a requirement for JNK signaling in axon death in vivo.

Chapter III: Materials & Methods

Wing injury assays:
See Materials & Methods in Chapter II.

Immunohistochemistry:
Immunolabeling: Anti HRP (Horseradish Peroxidase) antibody (AB) staining of dorsal dendrite arborization (dda) sensory neurons was performed as described(Wong et al., 2013), Anti FasII (Fasciclin II) AB staining of unpruned α/ß MB neurons in(Tasdemir-Yilmaz and Freeman, 2014), anti PDF (Pigment dispersing factor) AB staining of PDF+ neurons in (Muthukumar et al., 2014), and anti GFP staining in (MacDonald et al., 2006). GFP and CsChrimson::mVenus detection in adult brains: 1st AB: 1:1,000 Chicken anti-GFP (Rockland 600-901-215S) at 4° C overnight, 2nd AB: 1:100 Goat anti Chicken Dylight® 488 (Abcam ab96947) at room temperature for 1h.

$Axed^{EGFP::FLAG}$ detection in larval brains: the central nervous system was dissected from third instar larvae, and fixed for 5 minutes in cold 100% methanol, washed in PBS, and subsequently subjected to immunostaining with primary antibodies in PBS + 0.1% Triton X-100 (PTX) overnight at 4º C. Brains were washed with PTX, followed by any secondary antibody incubation in PTX at 4º C overnight. $Axed^{EGFP::FLAG}$ signals were not enhanced with antibodies. The following ABs were used for colocalization with AxedeGFP::FLAG: 1st ABs: Cy5 conjugated goat anti-HRP (Jackson ImmunoResearch Laboratories, 1:500), mouse anti-Bruchpilot (nc82, Developmental Studies Hybridoma Bank, 1:20), and rabbit anti-GAT ((Stork et al., 2014),1:3,000). The following Cy5 conjugated 2nd ABs were used: goat anti-mouse (nc82) and goat anti-rabbit (GAT) (Jackson ImmunoResearch). CNS samples were washed in PTX and mounted in Vectashield mounting medium reagent (Vector Laboratories). Confocal images were obtained on Innovative Imaging Innovations (3I) spinning-disc confocal microscope equipped with a Yokogawa CSX-X1 scan head.

$Axed^{EGFP::FLAG}$ detection in adult brains: the third antennal segments of adult Drosophila were unilaterally removed using a pair of #5 forceps under a dissection microscope. Flies were decapitated at 2, 4, 6, and 24 h post antennal ablation, as well as without injury for non-injury controls (*y,w ; ; axed*$^{EGFP::FLAG}$ and *y,w*). Heads were fixed and permeabilized in 4% formaldehyde in PTX for 20 min at room temperature, and washed with PTX. Brains were dissected in cold PTX, and incubated with 1st AB (mouse anti-Bruchpilot (nc82, Developmental Studies Hybridoma Bank, 1:20)) in PTX at 4° C overnight, washed with PTX, and incubated with Cy3 conjugated 2nd AB goat anti-mouse at 4º C in PTX

overnight. Brains were washed with PTX, mounted with Vectashield mounting medium (Vector Laboratories), and ipsilateral antennal lobes were imaged on the 3I spinning-disc confocal.

Western Blot: Primary antibodies (AB) were applied at 4°C overnight, secondary antibodies at room temperature for 1h. GFP detection: 1st AB: 1:2000 Rabbit anti-GFP (Abcam ab6556), 2nd AB: 1:5000 Goat anti-rabbit HRP (Abcam ab6721). FLAG detection: 1st AB: 1:1000 Mouse anti FLAG (Sigma F1804), 2nd AB: 1:2000 Rabbit anti Mouse HRP (Abcam ab6728). Tubulin detection: 1st AB: 1:5000 Mouse anti-Tubulin (Sigma, clone DM1A, T9026), 2nd AB: 1:2000 Rabbit anti-Mouse HRP (Abcam ab6728).

Confocal microscopy:
See Materials & Methods in Chapter II.

Heat shock treatment:
Crosses for MARCM double clones were passed every day, and 1 h heat shock application at 37° C performed at 5 days post initial cross set up.

Drosophila Stocks and Genotypes in Display Items:
In addition to stocks listed in Materials & Methods section of Chapter II, stocks used in Chapter III are listed below.

X chromosome:
5xUAS-Wld^{S} (Hoopfer et al., 2006), *Mkk7 allele: hep^{r75}* (Glise et al., 1995).

Chromosome 2:
GMR-hid^{10} (Bergmann et al., 1998), *5xUAS-P35* (Hay et al., 1994), *5xUAS-Dcr-2* (Dietzl et al., 2007), *5xUAS-Nmnat$^{RNAi(GD32255)}$* (Dietzl et al., 2007), bacterial artificial chromosome containing genomic *dsarm* (landing site: *VK00037*): *BAC$^{CH321-38D07}$* (Osterloh et al., 2012), *5xUAS-dsarm^{P862Q}* (Lukas Neukomm), *5xUAS-dsarm$^{\Delta ARM}$::myc* (based of cDNA, isoform D(Amy Sheehan)), JNK alleles: *bsk^{flp170B}* & *bsk^{2}* (Sluss et al., 1996), *10xUAS-IVS-myr::smGdP-cMyc*(Nern et al., 2015).

Chromosome 3:
dronc^{I29} (Xu et al., 2005), *Nmnat$^{\Delta 4790-1}$* (Zhai et al., 2006), *nSyb-Gal4* {NagarkarJaiswal:2015gp}, *5xUAS-P35* (Hay et al., 1994), *5xUAS-Wld^{S}* (Hoopfer et al., 2006), *ase-FLP^{3a}* & *ase-FLP^{3b}* (Neukomm et al., 2014), *5xUAS-dsarm$^{\Delta ARM}$::EGFP* (based

of cDNA, isoform D (Amy Sheehan)), *Mkk4* alleles: *Mkk4*^{e01458} and *Df(3R)Exel6149* (Rallis et al., 2010), *dsarm*^{896} & *dsarm*^{4621} (Osterloh et al., 2012), *Tdc2-Gal4*(Cole et al., 2005), *5xUAS-CD8::mCherry*(Roy et al., 2011).

Chapter III: Figures & Tables

Figure 3.1: *Axed* is expressed in neurons

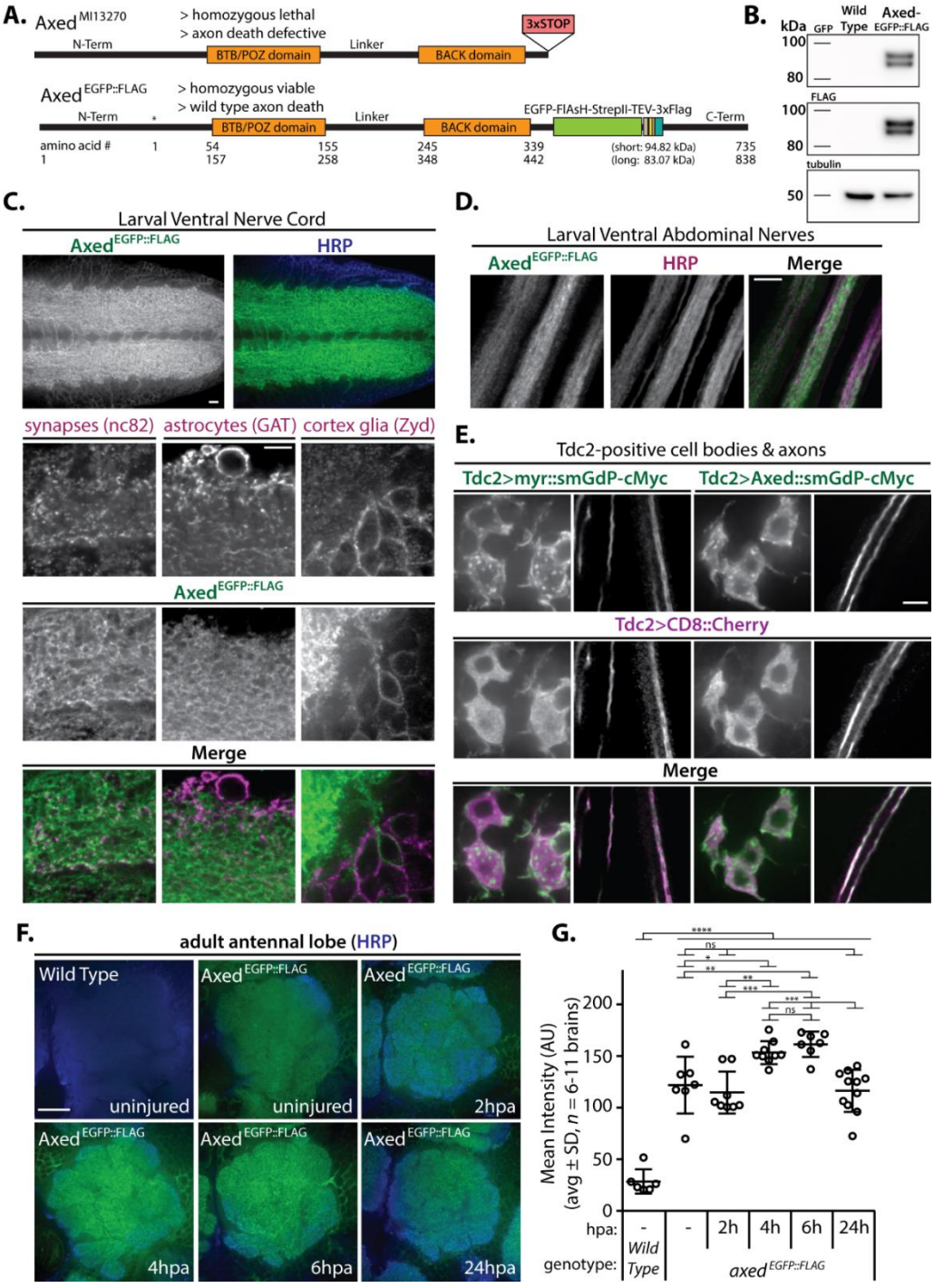

Figure 3.1:

A. Generation of a functional EGFP::FLAG tag knock-in to the genomic locus of Axed. Recombination Mediated Cassette Exchange (RMCE) of 3xStop with an EGFP::FLAG tag. While *axed*^{MI13270} mutants are homozygous lethal & axon death defective, *axed*$^{EGFP::FLAG}$ flies regain viability & the ability to drive axon degeneration.

B. Western blots of *axed*$^{EGFP::FLAG}$ fly heads confirm the expression of both long and short Axed isoforms.

C. Axed is enriched in the larval neuropil. Top: Axed$^{EGFP::FLAG}$ and merge with HRP staining. Bottom: Axed is found in close proximity to synapses (nc82 staining, top), and to mostly excluded from glia (astrocytes & cortex glia, middle & bottom, respectively). Scale bar, 10µm.

D. Axed is expressed in nerves. Top to bottom: Axed$^{EGFP::FLAG}$, larval ventral abdominal nerves (HRP staining) and merge. Scale bar, 10µm.

E. Tdc2-Gal4 driven overexpression of Axed$^{smGdP\text{-}cMyc}$ in Tdc2 positive neurons localizes to axons and in punctate clusters in cell soma. Top to bottom: Axed$^{smGdP\text{-}cMyc}$, CD8::cherry, and merge. Scale bar, 10µm.

F. Axed is upregulated upon axon injury in adult brains. Bilateral antennal ablation was performed to sever cell bodies from axons, and the antennal lobe in brains analyzed before, and 2, 4, 6 & 24 hour post axotomy (hpa). Green: Axed$^{EGFP::FLAG}$, Blue: nc82 staining. Scale bar, 20µm.

G. Quantification of Axed$^{EGFP::FLAG}$ levels pre- and post-injury. Ordinary one-way ANOVA with multiple comparisons test (* = $p < 0.05$, ** = $p < 0.01$, *** = $p < 0.001$, **** = $p < 0.0001$).

Figure 3.2: *Axed* is not involved in programmed cell death or developmental neurite pruning of MB γ neurons

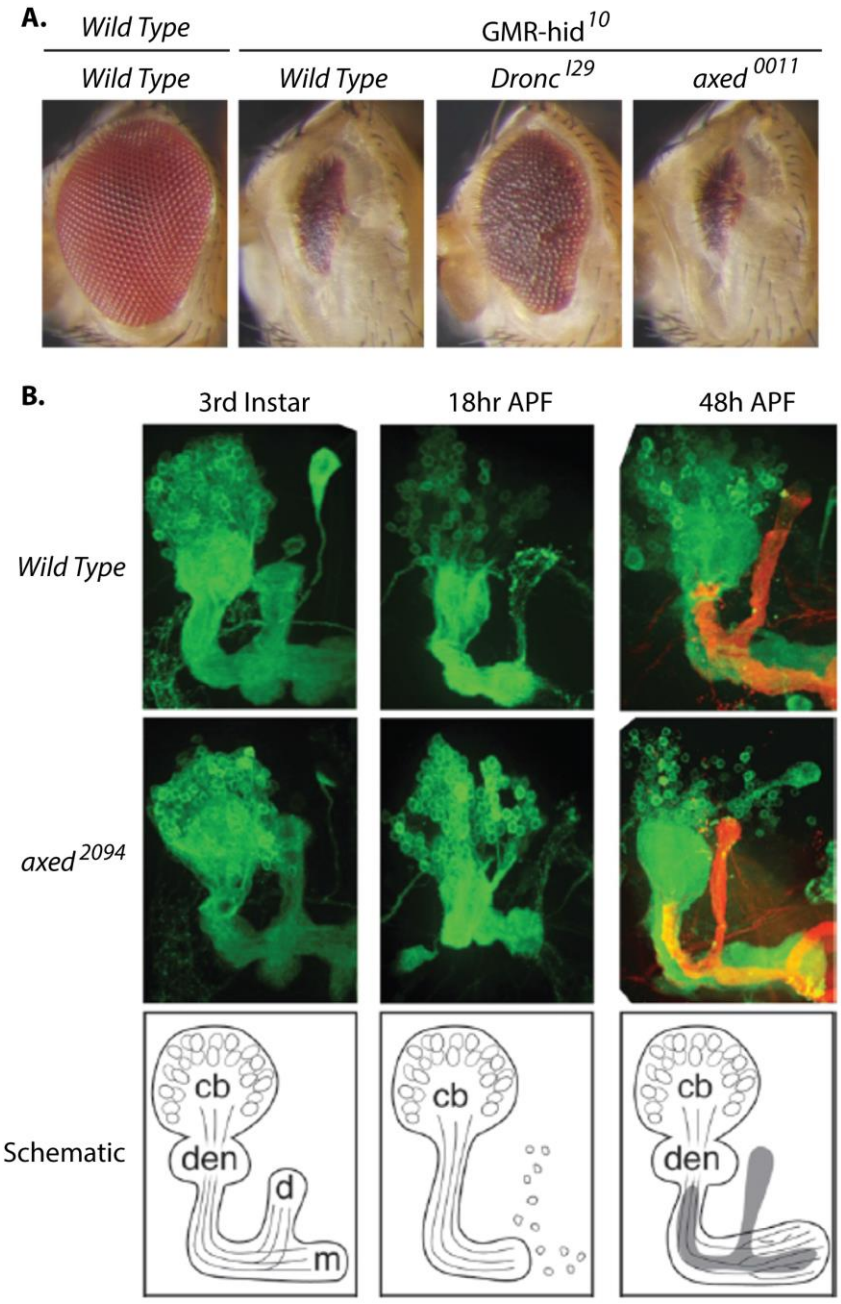

Figure 3.2:

A. *Axed* is not required for programmed cell death in the eye. *GMR-hid* induced pro-apoptotic signaling in the eye destroys eye morphology. Clones of the null allele *dronc*^{I29}, the *Drosophila* Nedd2-like initiator caspase, suppress this phenotype, while wild type or *axed*^{2094} mutant clones do not.

B. *Axed* is not required for developmental pruning of mushroom body (MB) γ neurons. Time points: 3rd larval stage, 18h & 48h after puparium formation (APF). MARCM clones of wild type and *axed*^{0011} mutants, showing cell bodies (cb), proximal dendritic arbors (den) and distal bifurcated axons projecting both medially and dorsally (m & d, respectively). In both genotypes, at 18h APF, dendrites and distal axons undergo fragmentation and are cleared. By 48h APF, medial axons regrow to form the adult-specific medial lobe. Red/grey: adult, unpruned α/ß MB neurons (anti-FasII staining).

Figure 3.3: *Axed* functions downstream of *dSarm* pro-degenerative signaling

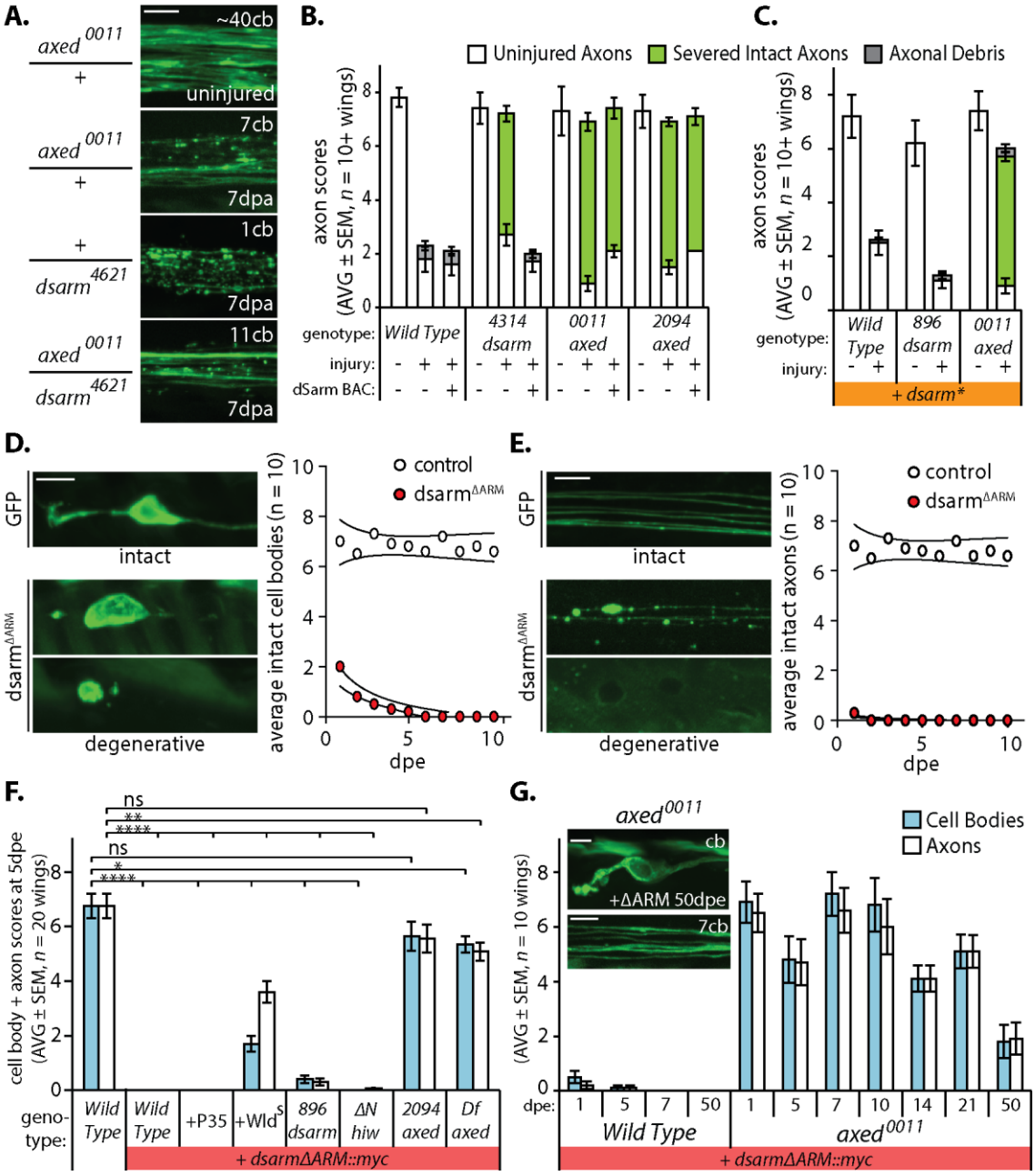

Figure 3.3:

A. Complementation test in axon degeneration assays. Glutamatergic axons (*OK371-Gal4, 5xUAS-mCD8::GFP*) were severed, and the onset of axon fragmentation visualized 7 days post axotomy (7 dpa). Severed axons either heterozygous for $dsarm^{4621}$, heterozygous for $axed^{0011}$, or trans-heterozygous for $dsarm^{4621}/axed^{0011}$ underwent fragmentation at 7 dpa.

B. Genomic *dsarm* fails to rescue axon degeneration in *axed* mutant alleles. Degeneration of axons, homozygous for *wild type*, $dsarm^{4314}$, $axed^{0011}$ or $axed^{2094}$, was assessed at 7 dpa, with or without an extra copy of a bacterial artificial chromosome (BAC) containing genomic *dsarm* ($BAC^{CH321\text{-}38D07}$). Uninjured axons served as internal controls (white bars).

C. Overexpression of *dsarm* fails to rescue axon degeneration in *axed* mutant alleles. Degeneration of axons homozygous for *wild type*, $dsarm^{4314}$, $axed^{0011}$ or $axed^{2094}$, was assessed at 7 dpa, with *dsarm** ($5xUAS\text{-}dsarm^{P862Q}$). Uninjured axons served as internal controls (white bars).

D. $dsarm^{\Delta ARM}$-mediated degeneration of sensory neuron cell bodies. Left side: top, intact control neuron; center and bottom, early and late examples of degenerative neurons. Dendrites and axons, left and right, respectively. Scale bar, 5 µm. Right side: the average numbers of intact cell bodies are plotted on each day post eclosion (dpe) expressing either $dsarm^{\Delta ARM}$ or *GFP* as a control (n = 10 wings each). Lines: interpolation of 95% confidence interval (CI).

E. $dsarm^{\Delta ARM}$-mediated degeneration of sensory axons. Left side: top, intact control axons; center and bottom, early and late examples of degenerative axons. Scale bar, 5 µm. Right side: the average numbers of intact axons are plotted at each dpe, expressing either $dsarm^{\Delta ARM}$ or *GFP* as a control (n = 10 each). Lines: interpolation of 95% CI.

F. *Axed* functions downstream of $dsarm^{\Delta ARM}$-mediated degeneration. Axons undergo Wallerian-like degeneration after $dSarm^{\Delta ARM}$ expression, they are partially protected by Wld^{S}. At 10 dpe, clones of both $axed^{2094}$ and the deficiency *BSC411* suppress $dsarm^{\Delta ARM}$-mediated degeneration of sensory neurons and their axons (n = 20 each).

G. Axons are morphologically preserved to 50 dpe in $axed^{0011}$ mutant alleles expressing $dsarm^{\Delta ARM}$ (n = 10 each). Inset: top and bottom, representative cell body and axons at 50 dpe, respectively. *Wild type* at 10, 14, and 21 dpe data not shown; 100% of cell bodies and axons are degenerated at these time points.

F. 2-way ANOVA with Sidak's multiple comparisons test (* = $p < 0.05$, ** = $p < 0.01$, *** = $p < 0.001$, **** = $p < 0.0001$).

Figure 3.4: *Axed* functions downstream of *Nmnat* depletion

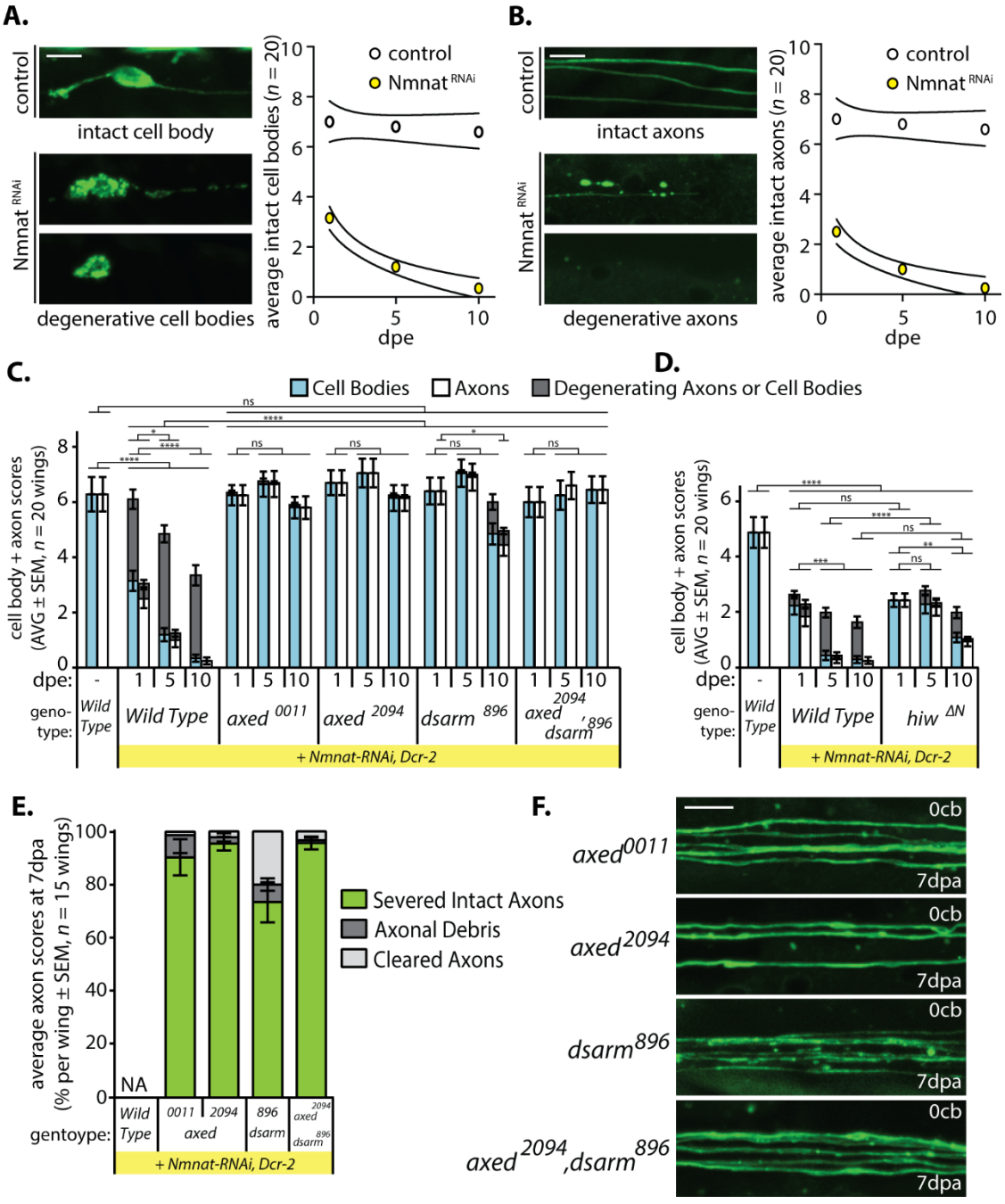

Figure 3.4:

A. RNAi-mediated knock-down of Nmnat (*Nmnat*^{RNAi}) induces degeneration of sensory neuron cell bodies. Left side: top, intact control axons; center and bottom, early and late examples of degenerative axons. Scale bar, 5 µm. Right side: the average numbers of intact axons are plotted at each dpe, expressing either *dsarm*$^{\Delta ARM}$ or *GFP* as a control (n = 20 each). Lines: interpolation of 95% CI.

B. *Nmnat*^{RNAi} & *Dcr2*-mediated degeneration of axons. Left side: top, intact control axons; center and bottom, early and late examples of degenerative axons. Scale bar, 5 µm. Right side: the average numbers of intact axons are plotted at each dpe, expressing either *dsarm*$^{\Delta ARM}$ or *GFP* as a control (n = 20 each). Lines: interpolation of 95% CI.

C. *Axed* functions downstream of *Nmnat*^{RNAi}-mediated neurodegeneration. To 10 dpe, *axed*^{2094} and *axed, dsarm* double mutants suppress *Nmnat* ^{RNAi}-mediated cell body and axonal degeneration. At 10 dpe *dsarm*^{896} mutants show axonal degeneration (n = 20 each).

D. *Hiw* cannot suppress *Nmnat*^{RNAi}-mediated neurodegeneration (n = 20 each).

E. Severed *axed* or *dsarm* mutant axons expressing Nmnat^{RNAi} & Dcr2 are preserved at 7 dpa (n = 15 each).

F. Representative pictures of severed axons at 7 dpa. Number of cb proximal to cut site is indicated in the upper right. Scale bar, 5 µm.

C-D. 2-way ANOVA with Sidak's multiple comparisons test on either cell bodies or axons, degenerating cell bodies and axons were excluded. (* = $p < 0.05$, ** = $p < 0.01$, *** = $p < 0.001$, **** = $p < 0.0001$).

Figure 3.5: Death induced by complete loss of *Nmnat* is suppressed in *axed* nulls, but not *dSarm.*

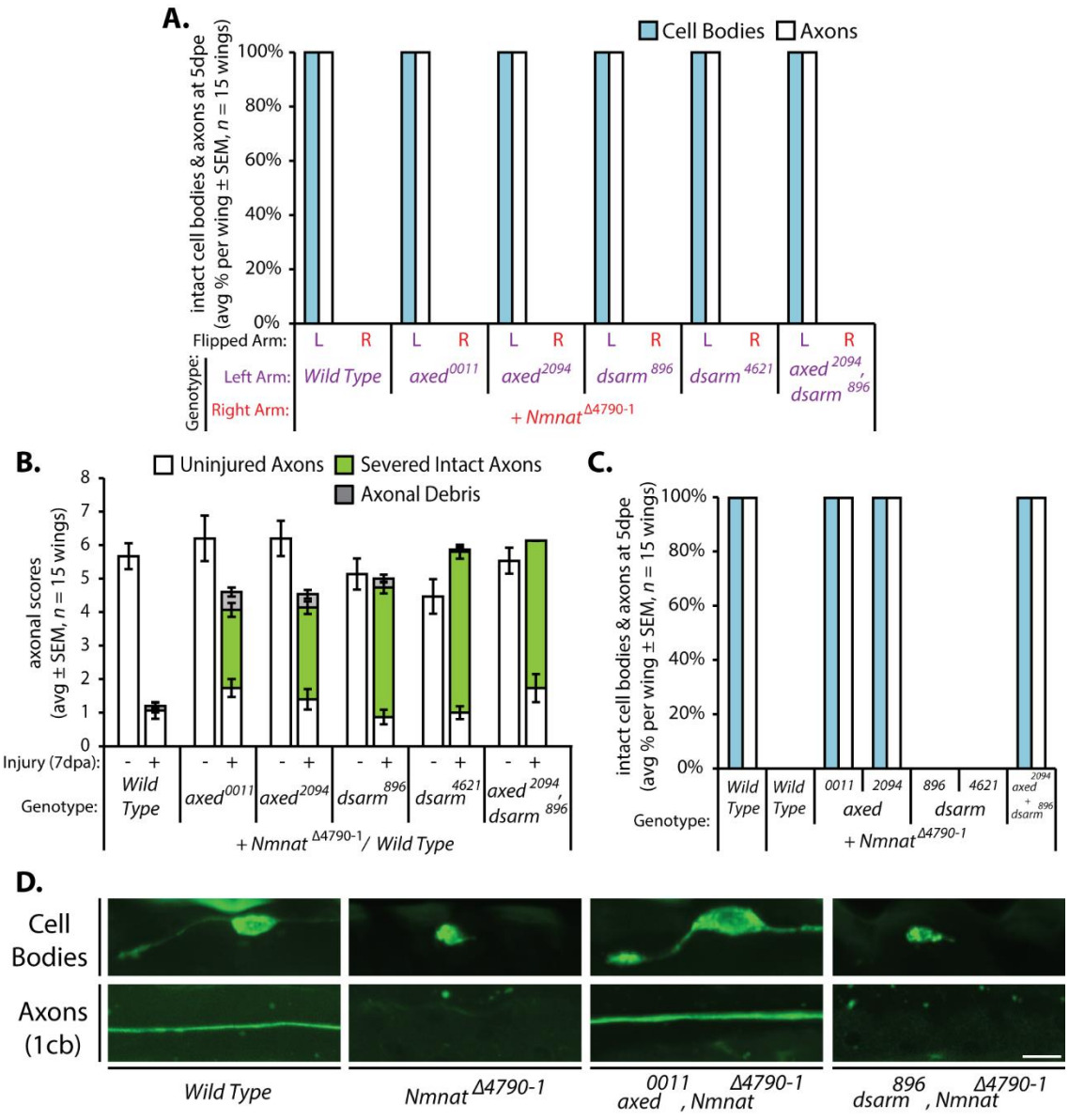

Figure 3.5:
A. Neurons in all backgrounds are morphologically unaffected by loss of one copy of *Nmnat* (left arm, mutant alleles, is flipped homozygous, purple). Conversely, complete neuron death in *Nmnat* mutant clones is unaffected by removal of one copy of *axed* or *dsarm* (right arm, *Nmnat*, is flipped homozygous, red). (*n* = 15 wings each).
B. Severed *axed* & *dsarm* axons heterozygous for *Nmnat* remain intact at 7 dpa. (*n* = 15 wings each).
C. *Axed* functions downstream of *Nmnat*-mediated neurodegeneration. Two unique alleles of *axed* block *Nmnat*$^{\Delta 4790}$-mediated neurodegeneration, while two separate alleles of *dsarm* fail to do so. *Axed, dsarm* double mutant clones also block *Nmnat*-mediated neurodegeneration. Percentage of clones with intact cell bodies & axons at 5 dpe (*n* = 15 wings each).
D. Representative images of cell bodies and axons double mutant clones Scale bar, 5 µm.

Figure 3.6: *Axed*, *Nmnat* double null axons are preserved in multiple contexts.

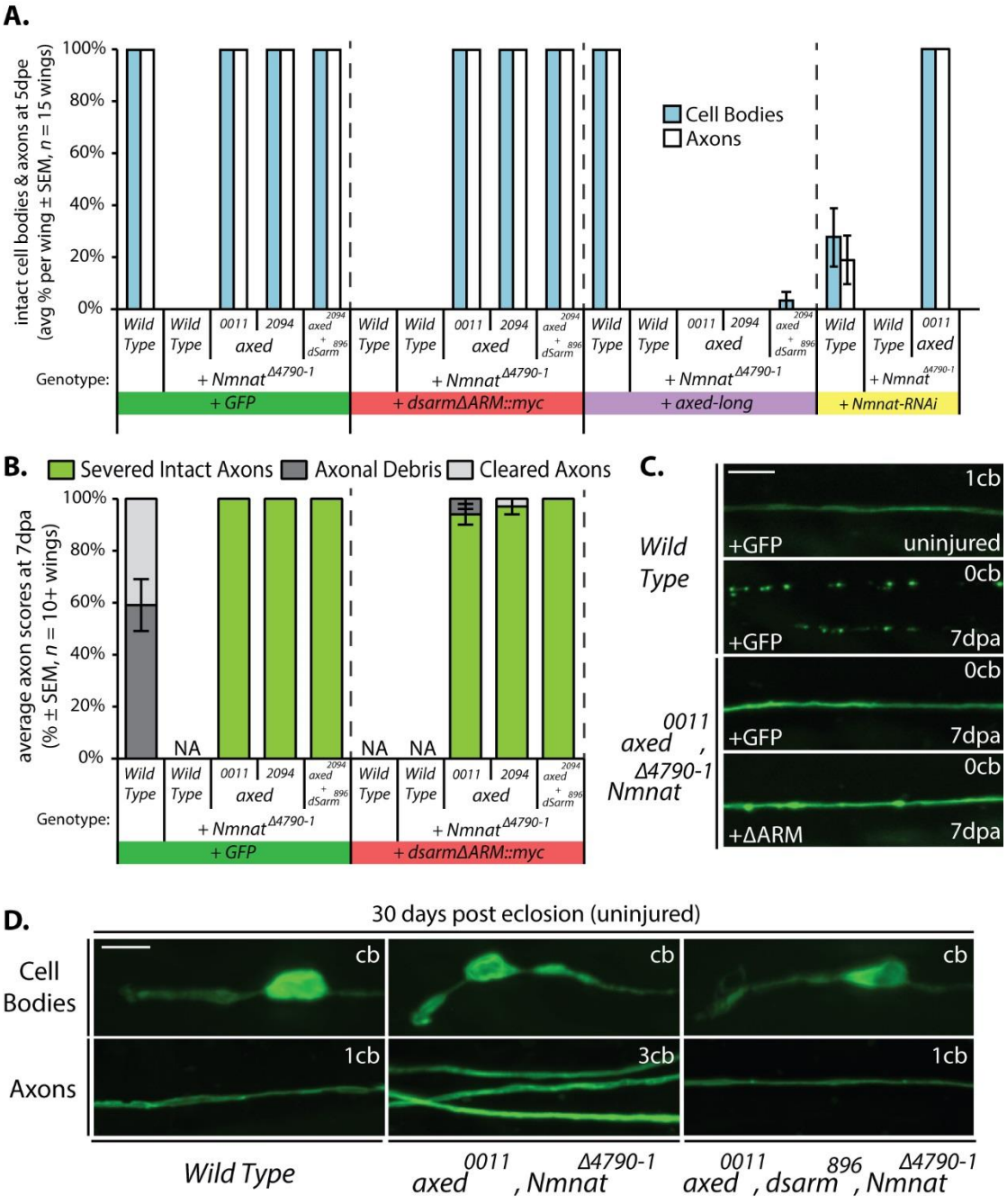

Figure 3.6:
A. *Axed, Nmnat* double null neuronal clones expressing GFP, dsarm$^{\Delta ARM}$, or Nmnat^{RNAi} & Dcr2 are preserved to 5 dpe, while those expressing Axed$^{long(attP40)}$ degenerate. Percentage of clones with intact cell bodies & axons. (*n* = 15 wings each)
B. Axon death is suppressed in severed *axed, Nmnat* double null axons expressing GFP, dsarm$^{\Delta ARM}$ at 7 dpa. (*n* = 10-15 wings each)
C. Wild type axons: Uninjured at 5dpe and 7dpa. *Axed, Nmnat* double null axons expressing GFP or dsarm$^{\Delta ARM}$. Scale bar, 5µm.
D. *Axed, Nmnat* double null neuronal clones expressing GFP remain morphologically intact at 30 days post eclosion. Scale bar, 5µm.

Figure 3.7: Hiw expression cannot rescue axon death in *axed* nulls

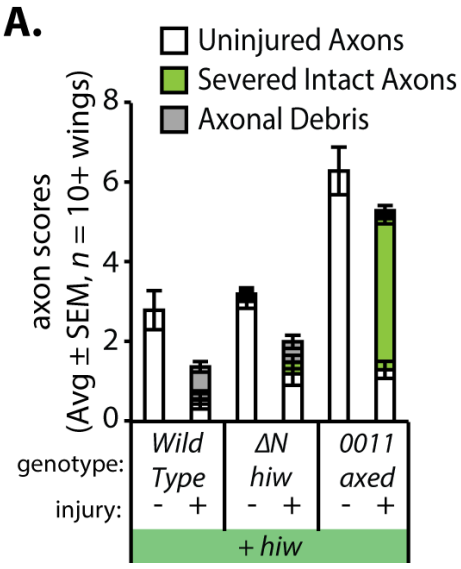

Figure 3.7:
A. Severed *axed* axons expressing *hiw* remain intact at 7 dpa. (*n* = 10 wings each).

Table 3.1: *Axed* alleles suppress axon degeneration downstream of *dSarm* & *Nmnat*

Axed allele	Detailed description	*dsarm*$^{\Delta ARM}$ suppression	*Nmnat*^{RNAi} *or* null suppression
axed^{0011}	EMS mutagenesis, 16bp deletion exon 3	yes	yes
axed^{2094}	EMS mutagenesis	yes	yes
BSC411	Deficiency uncovering genomic *axed*	yes	ND
axed^{MI13270}	Minos transposon *Mi{MIC}CG8398*^{MI13270}	yes	ND
axed^{Ex05}	Precise Minos excision	no	ND
axed^{Ex07}	Imprecise Minos excision	yes	ND
axed^{Ex65}	Imprecise Minos excision	yes	ND
axed^{Ex96}	Imprecise Minos excision	yes	ND
axed$^{eGFP::FLAG}$	Functional endogenous eGFP::FLAG fusion	no	ND
axed^{CrisprA}	CRISPR/Cas9, 194bp deletion, exon 2	yes	ND
axed^{CrisprB}	CRISPR/Cas9, 14bp deletion, exon 2	yes	ND
axed^{CrisprC}	CRISPR/Cas9, 14bp deletion, exon 2	yes	ND

Table 3.1:
Summary of all *axed* alleles generated and their abilities to suppress *dsarm*$^{\Delta ARM}$-mediated Wallerian-like degeneration or *Nmnat*^{RNAi}-triggered degeneration. If known, the molecular nature of each lesion is indicated. ND, not determined.

Table 3.2: MAPK alleles tested for deficits in axon death

Gene / allele	Detailed description	Axon death phenotype	*dsarm*$^{\Delta ARM}$ suppression
MAPK alleles			
bsk^{2}	*JNK* null allele, early stop mutation	no	no
bsk^{flp170B}	Deficiency uncovering *JNK*	no	no
MKK4^{e01485}	P element transposon	no	no
Df(3R)Exel6149	Deficiency uncovering *MKK4*	no	no
hep^{r75}	*MKK7* null allele	no	no

Table 3.2:
The MAPK genes in the table tested were null alleles or deficiencies recombined with FRT sites. Each was assessed for an axon death at 7 dpa and whole cell death after expression of dsarm$^{\Delta ARM}$.

Table 3.3: Genotypes in figures/experiments

Abbreviations: *Y: Y* chromosome, *w: w^{1118}* or *w^{-}*, *OK371: OK371-Gal4*, *mCD8::GFP: 5xUAS-mCD8::GFP*

Figure 3.1:
wild type: *yw ; + ; +*
Axed$^{EGFP::FLAG}$: *yw ; + ; axed$^{EGFP\text{-}FlAsH\text{-}StrepII\text{-}TEV\text{-}3xFlag}$*
w/Y ; 5xUAS-axed::smGdP-cMyc ; Tdc2-Gal4,5xUAS-CD8::mCherry
Spaghetti monster control: *w/Y ; 10xUAS-IVS-myr::smGdP-cMyc ; Tdc2-Gal4,5xUAS-CD8::mCherry*
Spaghetti monster *axed*: *w/Y ; 5xUAS-axed::smGdP-cMyc ; Tdc2-Gal4,5xUAS-CD8::mCherry*
Figure 3.2:
A. wild type: Canton S
A. *GMR-hid^{10}* wild type: *w,eyFLP^{2}/Y ; GMR-hid^{10}/+ ; FRT2A/tub-Gal80,FRT2A*
A. *GMR-hid^{10} dronc^{I29}*: *w,eyFLP^{2}/Y ; GMR-hid^{10}/+ ; dronc^{I29},FRT2A/tub-Gal80,FRT2A*
A. *GMR-hid^{10} axed^{2094}*: *w,eyFLP^{2}/Y ; GMR-hid^{10}/+ ; axed^{2094},FRT2A/tub-Gal80,FRT2A*
B. wild type: *w,hs-FLP^{12}/Y ; 201Y-gal4,mCD8::GFP/+ ; FRT2A/tub-Gal80,FRT2A*
B. *axed^{0011}*: *w,hs-FLP^{12}/Y ; 201Y-gal4,mCD8::GFP/+ ; axed^{0011},FRT2A/tub-Gal80,FRT2A*
Figure 3.3:
A. *axed^{0011}/+*: *w/Y ; OK371,mCD8::GFP/+ ; axed^{0011},FRT2A/FRT2A*
A. *+/dsarm^{4621}*: *w/Y ; OK371,mCD8::GFP/+ ; FRT2A/FRT2A,dsarm^{4621}*
A. *axed^{4621}/dsarm^{4621}*: *w/Y ; OK371,mCD8::GFP/+ ; axed^{4621},FRT2A/dsarm^{4621},FRT2A*
B. *wild type*: *w/Y ; OK371,mCD8::GFP,aseFLP^{2e}/+ ; FRT2A/tub-Gal80,FRT2A*
B. *wild type + genomic dsarm*: *w/Y ; OK371,mCD8::GFP,aseFLP^{2e}/BAC$^{CH321\text{-}38D07}$; FRT2A/tub-Gal80,FRT2A*
B. *dsarm^{4314}*: *w/Y ; OK371,mCD8::GFP,aseFLP^{2e}/+ ; dsarm^{4314},FRT2A/tub-Gal80,FRT2A*
B. *dsarm^{4314}* + genomic *dsarm*: *w/Y ; OK371,mCD8::GFP,aseFLP^{2e}/BAC$^{CH321\text{-}38D07}$; dsarm^{4314},FRT2A/tub-Gal80,FRT2A*
B. *axed^{0011} & axed^{2094}*: as above
C. *wild type + 5xUAS-dsarm*: *w/Y ; OK371,mCD8::GFP,aseFLP^{2e}/5xUAS-dsarm^{P862Q}; FRT2A/tub-Gal80,FRT2A*
C. *dsarm^{4314} + 5xUAS-dsarm*: *w/Y ; OK371,mCD8::GFP,aseFLP^{2e}/5xUAS-dsarm^{P862Q}; dsarm^{4314},FRT2A/tub-Gal80,FRT2A*
C. *axed^{0011} + 5xUAS-dsarm*: *w/Y ; OK371,mCD8::GFP,aseFLP^{2e}/5xUAS-dsarm^{P862Q}; axed^{0011},FRT2A/tub-Gal80,FRT2A*
D-E. *GFP*: *w/Y ; OK371,mCD8::GFP,aseFLP^{2e}/mCD8::GFP ; FRT2A/tub-Gal80,FRT2A*
D-E. *dsarm$^{\Delta ARM}$*: *w/Y ; OK371,mCD8::GFP,aseFLP^{2e}//5xUAS-dsarm$^{\Delta ARM}$::myc ; FRT2A/tub-Gal80,FRT2A*
F. *wild type + mCD8::GFP*: *w/Y ; OK371,mCD8::GFP,aseFLP^{2e}/mCD8::GFP ; FRT2A/tub-Gal80,FRT2A*
F. *wild type + 5xUAS-dsarm$^{\Delta ARM}$::myc*: *w/Y ; OK371,mCD8::GFP,aseFLP^{2e}//5xUAS-dsarm$^{\Delta ARM}$::myc ; FRT2A/tub-Gal80,FRT2A*
F. P35: *w/Y ; OK371,mCD8::GFP,aseFLP^{2e}/5xUAS-dsarm$^{\Delta ARM}$::myc,5xUAS-P35 ; FRT2A/tub-Gal80,FRT2A*
F. Wld^{S}: *w,5xUAS-Wld^{S}/Y ; OK371,mCD8::GFP,aseFLP^{2e}/5xUAS-dsarm$^{\Delta ARM}$::myc ; FRT2A/tub-Gal80,FRT2A*
F. *dsarm^{896}*: *w/Y ; OK371,mCD8::GFP,aseFLP^{2e}/5xUAS-dsarm$^{\Delta ARM}$::myc ; dsarm^{896},FRT2A/tub-Gal80,FRT2A*
F. *hiw$^{\Delta N}$*: *w,tub-Gal80,FRT19A/w,hiw$^{\Delta N}$,FRT19A ; OK371,mCD8::GFP,aseFLP^{2e}/5xUAS-dsarm$^{\Delta ARM}$::myc ; mCD8::GFP,aseFLP^{3b}/+*
F. *axed^{2094}*: *w/Y ; OK371,mCD8::GFP,aseFLP^{2e}/5xUAS-dsarm$^{\Delta ARM}$::myc ; axed^{2094},FRT2A/tub-Gal80,FRT2A*
F. *BSC411*: *w/Y ; OK371,mCD8::GFP,aseFLP^{2e}/5xUAS-dsarm$^{\Delta ARM}$::myc ; BSC411,FRT2A/tub-Gal80,FRT2A*
G. *wild type + 5xUAS-dsarm$^{\Delta ARM}$::myc*: *w/Y ; OK371,mCD8::GFP,aseFLP^{2e}//5xUAS-dsarm$^{\Delta ARM}$::myc ; FRT2A/tub-Gal80,FRT2A*
G. *axed^{2094}*: *w/Y ; OK371,mCD8::GFP,aseFLP^{2e}/5xUAS-dsarm$^{\Delta ARM}$::myc ; axed^{2094},FRT2A/tub-Gal80,FRT2A*
Figure 3.4:
A-B. control: *w/Y ; OK371,mCD8::GFP,aseFLP^{2e}/mCD8::GFP ; FRT2A/tub-Gal80,FRT2A*
A-B. *Nmnat^{RNAi}*: *w/Y ; OK371,mCD8::GFP,aseFLP^{2e}/10xUAS-Nmnat$^{RNAi(GD32255)}$,5xUAS-Dcr-2 ; FRT2A/tub-Gal80,FRT2A*
C. wild type: *w/Y ; OK371,mCD8::GFP,aseFLP^{2e}/mCD8::GFP ; FRT2A/tub-Gal80,FRT2A*
C. *Nmnat^{RNAi}*: *w/Y ; OK371,mCD8::GFP,aseFLP^{2e}/10xUAS-Nmnat$^{RNAi(GD32255)}$,5xUAS-Dcr2 ; FRT2A/tub-Gal80,FRT2A*
C. *axed^{0011}*: *w/Y ; OK371,mCD8::GFP,aseFLP^{2e}/10xUAS-Nmnat$^{RNAi(GD32255)}$,5xUAS-Dcr2 ; axed^{0011},FRT2A/tub-Gal80,FRT2A*
C. *axed^{2094}, dsarm^{896} & axed^{2094},dsarm^{896}*: as above
D. wild type: *w,19A/w,tubGal80,19A; 10xUAS-Nmnat$^{RNAi(GD32255)}$,5xUAS-Dcr2/Ok371-Gal4,mCD8::GFP ; aseFLP^{3b}/+*
D. *hiw$^{\Delta N}$*: *w,hsFLP,hiw$^{\Delta N}$,19A/w,tubGal80,19A; 10xUAS-Nmnat$^{RNAi(GD32255)}$,5xUAS-Dcr2/Ok371-Gal4,mCD8::GFP ; aseFLP^{3b}/+*

E-F. *axed^{0011}, axed^{2094}, dsarm^{896} & axed^{2094},dsarm^{896}:* as above in C.
Figure 3.5:
A. *Nmnat $^{\Delta 4790\text{-}1}$/+ and wild type 3L clones: w/Y ; OK371,mCD8::GFP,aseFLP^{2e}/+ ; FRT2A,FRT82B,Nmnat$^{\Delta 4790\text{-}1}$/tub-Gal80,FRT2A*
A. *Nmnat $^{\Delta 4790\text{-}1}$ and wild type/+ 3R clones: w/Y ; OK371,mCD8::GFP,aseFLP^{2a}/+ ; FRT2A,FRT82B,Nmnat$^{\Delta 4790\text{-}1}$/FRT82B,tub-Gal80*
A. *Nmnat $^{\Delta 4790\text{-}1}$/+ and axed^{0011} 3L clones: w/Y ; OK371,mCD8::GFP,aseFLP^{2e}/+ ; axed^{0011},FRT2A,FRT82B,Nmnat$^{\Delta 4790\text{-}1}$/tub-Gal80,FRT2A*
A. *Nmnat $^{\Delta 4790\text{-}1}$ and axed^{0011}/+ 3R clones: w/Y ; OK371,mCD8::GFP,aseFLP^{2a}/+ ; axed^{0011},FRT2A,FRT82B,Nmnat$^{\Delta 4790\text{-}1}$FRT82B,tub-Gal80*
A. *Nmnat $^{\Delta 4790\text{-}1}$/+ OR Nmnat axed^{0011}, axed^{2094}, dsarm^{896}, dsarm^{896}, & dsarm^{896} & axed^{2094} 3L OR 3R clones:* as above
B. *Axotomy in Nmnat $^{\Delta 4790\text{-}1}$/+ and wild type, axed^{0011}, axed^{2094}, dsarm^{896}, dsarm^{4621}, & dsarm^{896} & axed^{2094} 3L clones:* as above
C-D. *wild type 3L & 3R double clones: y,w,hsFLP ; Ok371,mCD::GFP,aseFLP^{2a}/+ ; FRT2A,FRT82B/tubGal80,FRT2A,FRT82b,tubGal80*
C-D. *wild type and Nmnat $^{\Delta 4790\text{-}1}$ 3L & 3R double clones: y,w,hsFLP ; Ok371,mCD::GFP,aseFLP^{2a}/+ ; FRT2A,FRT82B,Nmnat$^{\Delta 4790\text{-}1}$/tubGal80,FRT2A,FRT82b,tubGal80*
C-D. *axed^{0011} and Nmnat $^{\Delta 4790\text{-}1}$ 3L & 3R double clones: y,w,hsFLP ; Ok371,mCD::GFP,aseFLP^{2a}/+; FRT2A,FRT82B,Nmnat$^{\Delta 4790\text{-}1}$/tubGal80,FRT2A,FRT82b,tubGal80*
C-D. *axed^{2094}, dsarm^{896}, dsarm^{4621}, & dsarm^{896} & axed^{2094} 3L & 3R double clones:* as above
Figure 3-6:
A-D. *wild type 3L & 3R double clones + GFP: y,w,hsFLP ; Ok371,mCD::GFP,aseFLP^{2a}/mCD8::GFP ; FRT2A,FRT82B/tubGal80,FRT2A,FRT82b,tubGal80*
A-D. *wild type and Nmnat $^{\Delta 4790\text{-}1}$ 3L & 3R double clones + GFP: y,w,hsFLP ; Ok371,mCD::GFP,aseFLP^{2a}/mCD8::GFP ; FRT2A,FRT82B,Nmnat$^{\Delta 4790\text{-}1}$/tubGal80,FRT2A,FRT82b,tubGal80*
A-D. *axed^{0011} and Nmnat $^{\Delta 4790\text{-}1}$ 3L & 3R double clones + GFP: y,w,hsFLP ; Ok371,mCD::GFP,aseFLP^{2a}/mCD8::GFP ; FRT2A,FRT82B,Nmnat$^{\Delta 4790\text{-}1}$/tubGal80,FRT2A,FRT82b,tubGal80*
A-D. *axed^{2094}, & dsarm^{896} & axed^{2094} and Nmnat $^{\Delta 4790\text{-}1}$ 3L & 3R double clones + GFP:* as above
A-D. *wild type 3L & 3R double clones + ΔARM: y,w,hsFLP ; Ok371,mCD::GFP,aseFLP^{2a}/5xUAS-dsarm$^{\Delta ARM}$::myc ; FRT2A,FRT82B/tubGal80,FRT2A,FRT82b,tubGal80*
A-D. *wild type and Nmnat $^{\Delta 4790\text{-}1}$ 3L & 3R double clones + ΔARM: y,w,hsFLP ; Ok371,mCD::GFP,aseFLP^{2a}/5xUAS-dsarm$^{\Delta ARM}$::myc ; FRT2A,FRT82B,Nmnat$^{\Delta 4790\text{-}1}$/tubGal80,FRT2A,FRT82b,tubGal80*
A-D. *axed^{0011} and Nmnat $^{\Delta 4790\text{-}1}$ 3L & 3R double clones + ΔARM: y,w,hsFLP ; Ok371,mCD::GFP,aseFLP^{2a}/5xUAS-dsarm$^{\Delta ARM}$::myc ; FRT2A,FRT82B,Nmnat$^{\Delta 4790\text{-}1}$/tubGal80,FRT2A,FRT82b,tubGal80*
A-D. *axed^{2094}, & dsarm^{896} & axed^{2094} and Nmnat $^{\Delta 4790\text{-}1}$ 3L & 3R double clones + ΔARM:* as above
A. *wild type 3L & 3R double clones + axed$^{long(attp40)}$: y,w,hsFLP ; Ok371,mCD::GFP,aseFLP^{2a}/5xUAS-axed^{fl}(attP40) ; FRT2A,FRT82B/tubGal80,FRT2A,FRT82b,tubGal80*
A. *wild type and Nmnat $^{\Delta 4790\text{-}1}$ 3L & 3R double clones + axed$^{long(attp40)}$: y,w,hsFLP ; Ok371,mCD::GFP,aseFLP^{2a}/5xUAS-axed^{fl}(attP40); FRT2A,FRT82B,Nmnat$^{\Delta 4790\text{-}1}$/tubGal80,FRT2A,FRT82b,tubGal80*
A. *axed^{0011} and Nmnat $^{\Delta 4790\text{-}1}$ 3L & 3R double clones + axed$^{long(attp40)}$: y,w,hsFLP ; Ok371,mCD::GFP,aseFLP^{2a}/5xUAS-axed^{fl}(attP40); FRT2A,FRT82B,Nmnat$^{\Delta 4790\text{-}1}$/tubGal80,FRT2A,FRT82b,tubGal80*
A. *axed^{2094}, & dsarm^{896} & axed^{2094} and Nmnat $^{\Delta 4790\text{-}1}$ 3L & 3R double clones + axed$^{long(attp40)}$:* as above
A. *wild type 3L & 3R double clones + Nmnat-RNAi: y,w,hsFLP ; Ok371,mCD::GFP,aseFLP^{2a}/10xUAS-Nmnat$^{RNAi(GD32255)}$,5xUAS-Dcr2 ; FRT2A,FRT82B,Nmnat$^{\Delta 4790\text{-}1}$/tubGal80,FRT2A,FRT82b,tubGal80*
A. *wild type and Nmnat $^{\Delta 4790\text{-}1}$ 3L & 3R double clones + Nmnat-RNAi: y,w,hsFLP ; Ok371,mCD::GFP,aseFLP^{2a}/10xUAS-Nmnat$^{RNAi(GD32255)}$,5xUAS-Dcr2 ; FRT2A,FRT82B,Nmnat$^{\Delta 4790\text{-}1}$/tubGal80,FRT2A,FRT82b,tubGal80*
A. *axed^{0011} and Nmnat $^{\Delta 4790\text{-}1}$ 3L & 3R double clones + Nmnat-RNAi: y,w,hsFLP ; Ok371,mCD::GFP,aseFLP^{2a}/10xUAS-Nmnat$^{RNAi(GD32255)}$,5xUAS-Dcr2 ; FRT2A,FRT82B,Nmnat$^{\Delta 4790\text{-}1}$/tubGal80,FRT2A,FRT82b,tubGal80*
Table 3-1:
dsarm$^{\Delta ARM}$: w/Y ; OK371,mCD8::GFP,aseFLP^{2e}//5xUAS-dsarm$^{\Delta ARM}$::myc ; axed^{alleles},FRT2A/tub-Gal80,FRT2A
Nmnat^{RNAi}: w/Y ; OK371,mCD8::GFP,aseFLP^{2e}/10xUAS-Nmnat$^{RNAi(GD32255)}$,5xUAS-Dcr2 ; axed^{alleles},FRT2A/tub-Gal80,FRT2A
Figure 3-7:
A. wild type + *5xUAS-hiw: w,19A/w,tubGal80,19A ; Ok371-Gal4,mCD8::GFP/5xUAS-hiw^{fl} ; aseFLP^{3b}/+*
A. *hiw$^{\Delta N}$ + 5xUAS-hiw: w,hsFLP,hiw$^{\Delta N}$,19A/w,tubGal80,19A; Ok371-Gal4,mCD8::GFP /5xUAS-hiw^{fl} ; aseFLP^{3b}/+*
A. *axed^{0011} + 5xUAS-hiw: w/Y ; OK371,mCD8::GFP,aseFLP^{2e}/5xUAS-hiw^{fl} ; axed^{0011},FRT2A/tub-Gal80,FRT2A*
Table 3-2:
Axotomy:
JNK: *bsk^{flp170B} & bsk^{2}: w/Y ; JNK^{allelels},FRT40A/tub-Gal80,FRT40A ; nSyb-Gal4,mCD8::GFP,aseFLP^{3a}/nSyb-Gal4,mCD8::GFP*
Mkk4: *Mkk4^{e01485} & Df(3R)Exel6149: w/Y ; OK371,mCD8::GFP,aseFLP^{2a}/mCD8::GFP ; FRT82B,Mkk4^{alleles}/FRT82B,tub-Gal80*

Mkk7: *hep^{r75}:* *w,hs-FLP^{12},tub-Gal80,FRT19A/w,hep^{r75},FRT19A; OK371,mCD8::GFP,aseFLP^{2a}/+ ; mCD8::GFP,aseFLP^{3b}/+*
***dsarm$^{\Delta ARM}$* suppression:**
JNK: *bsk^{flp170B} & bsk^{2}:* *w/Y ; JNK^{allelels},FRT40A/tub-Gal80,FRT40A ; nSyb-Gal4,mCD8::GFP,aseFLP^{3a}/5xUAS-dsarm$^{\Delta ARM}$::EGFP*
Mkk4: *Mkk4^{e01485} & Df(3R)Exel6149:* *w/Y ; OK371,mCD8::GFP,aseFLP^{2a}/5xUAS-dsarm$^{\Delta ARM}$::myc ; FRT82B,Mkk4^{alleles}/FRT82B,tub-Gal80*
Mkk7: *hep^{r75}:* *w,hs FLP^{12},tub Gal80,FRT19A/w,hep^{r75},FRT19A ; OK371,mCD8::GFP,aseFLP^{2a}/+ ; 5xUAS dsarm$^{\Delta ARM}$::EGFP*

CHAPTER IV: Defining Axed Domains & Molecular Partners Required for Axon Death.

This work was conducted in the laboratory of Marc Freeman. I performed all of the *Drosophila* experiments in this chapter. Amy Sheehan cloned *axed* domain deletions constructs and Jon Farley tested expression in S2 cells.

The following publication is in preparation as follows:

Axon death pathways converge on Axed to promote functional and structural axon disassembly

Lukas J. Neukomm* & Thomas C. Burdett*, Jaeda Coutinho-Budd, Andrew M. Seeds, Stefanie Hampel, Jack Wong, Yonca Karadeniz, Jeannette M. Osterloh, Amy E. Sheehan, and Marc R. Freeman

Abstract

In the previous two chapters we identified and defined a downstream role for Axed within an axon death program activated after injury. In this chapter, I present experiments designed to elucidate which structural features of Axed are required for degenerative function. To do this we attempted to rescue degeneration in an *axed* null background with Axed constructs lacking conserved domains and found that the C-terminal region is essential for function. Additionally, we investigate whether common BTB domain protein binding partners are required for function and found that Axed likely does not integrate into Cullin-RING-ligase complex, since disrupting complex components had no effect on the progression axon death after injury or dSarm$^{\Delta ARM}$ induction. Furthermore, we find that the ubiquitin proteasome is not required for downstream degenerative processes in axons.

Chapter IV: Results & Discussion

Results 4-1: Defining Axed domains required for function

Axed contains two evolutionary conserved domains, BTB (bric-à-brac, tramtrack, broad complex), and BACK (BTB and C-terminal Kelch), respectively(Stogios and Privé, 2004). To determine the domains in Axed essential for axon death, we generated deletion constructs lacking either the BTB, the BACK, or the C terminal domain using $Axed^{long}$ as a reference (Figure 4.1-A). To avoid artificial localization or stabilization changes we did not tag the deletion constructs, but without a functional antibody, we were unable to confirm these constructs resulted in stably expressed protein. To confirm the protein was actually produced we tagged each deletion construct with N-terminal FLAG tags and expressed them in S2 cells under the actin promotor. Western blot revealed each construct produced protein of the expected size (Figure 4.1-B). FLAG-tagged constructs will be retested for function and subcellular localization *in vivo* in the future. Each deletion construct was site specifically inserted and expressed in wild type clones, as well as in several distinct axed mutant backgrounds, and assayed for axon death (Figure 4.1C/D/E/F). While full length $Axed^{long}$ was able to entirely rescue axon death, constructs lacking either BTB or BACK domains were only partially functional, whereas expression of Axed lacking the C terminus completely failed to rescue axon death. Our findings suggest that the BTB and BACK domains are important, but partially redundant for Axed function, while the C terminus, which harbors a substrate binding domain in many BTB molecules, is absolutely required for axon death signaling or protein stability *in vivo*.

Many BTB-containing proteins are involved in the recruitment of substrates to Cullin-RING ligase (CRL) complexes for ubiquitin tagging and proteasome degradation(Bennett et al., 2010; Pintard et al., 2004; Zhuang et al., 2009). We tested an array of Drosophila CRL complex mutants in our wing axotomy assay, we found none of them to be defective in axon death (Table 4.1). These data suggest CRL complexes are not involved in axon death, or that genetic redundancy among CRL components might mask their axon death involvement.

Results 4-2: Disrupting the proteasome fails to suppress axon death in multiple contexts

Despite the Cullin-RING-ligase complex components failing to display any axon death defects at all, we thought Axed may still play a role in the ubiquitin proteasome system with functionally redundant cullins or other E3 ligases. In order bypass an extensive candidate survey of *Drosophila* E3 ligase genes, we decided to alter the UPS itself, reasoning that if Axed functions within the UPS, disruptions should phenocopy *axed* null alleles. Previous studies have demonstrated pharmacological blockade of the UPS moderately preserves axons *in vivo* and antagonizing ubiquitin chain formation with yeast de-ubiquitinating yeast UBP2 strongly protects axons *in vivo* (Baker et al., 1992; Xiong et al., 2012; Zhai et al., 2003).

We first attempted to replicate UBP2 axon protection in adult glutamatergic neurons in the wing. We found the overexpressing UBP2 in adult glutamatergic sensory neurons led to spontaneous whole cell loss over the course of 5 days, not seen in axons expressing a GFP control (Figure 4.2-A), that could be almost fully suppressed by co-expression of apoptotic inhibitor P35 (Figure 4.2-B/D, uninjured at 5dpe). While death is

suppressed, cells are still morphologically altered with swollen and enlarged cell bodies and axonal membranes that are irregular compared to wild type (Figure 4.2-C). Since degeneration of axons and cell bodies before injury, expression of dsarm$^{\Delta ARM}$, or knock out of *Nmnat* would complicate our interpretation of suppression of a Wallerian-like death program, we co-expressed P35 with UBP2 or a control GFP in all experiments. Consistent with previous reports, we found UBP2 strongly suppressed injury-induced axon death after injury for at least 7 dpa (Figure 4.2-B/C).

We next wanted to assess whether this protective effect was applicable to downstream pro-degenerative processes. To do this we co-expressed UBP2 & P35 in an *Nmnat* null background and found that while UBP2 could delay spontaneous degeneration at 1 day, the majority of cell bodies and axons fully degenerated by 5 days (Figure 4.2-D). The few surviving cell bodies were severely swollen, while the axons were dimmer and thinned compared to controls, indicating a progressive degeneration (Figure 4.2-E). Additionally, we assessed whether UBP2 & P35 could suppress dsarm$^{\Delta ARM}$ induced degeneration and found no significant suppression of neuron death (Figure 4.2-F/G). The small amount of remaining neurons in control and UBP2 clones is likely due to the dilution of dsarm$^{\Delta ARM}$ production when using four UAS constructs. These data argue that axon protective effects of UBP2 occur upstream of *dsarm* activation and *Nmnat* loss.

Since UBP2 only reversed ubiquitination processes, we wanted to determine if whole proteasome disruption led to stronger axon protective effects possibly extending further downstream in the axon pathway. To do this we used ovexpression of temperature

sensitive dominant negative 20S proteasomal subunits, *prosβ6*^{1} & *prosβ2*^{1}, or 20S proteasome particle repressor 31kDA (*PI31*) (Cho-Park and Steller, 2013; Schweisguth, 1999). Previous reports demonstrated that proteasome disruption increased Nmnat levels modestly, but less than levels induced by UBP2. However, they did not test whether the Nmnat increase resulted in axon survival after injury. To our surprise none of the proteasome disruptions we attempted led to persistence of intact anucleated axons after axotomy or suppression of whole neuron death after gain of function *dsarm* signaling or loss of *Nmnat* (Figure 4.5). Even expression of *prosβ6*^{1} & *prosβ2*^{1} together failed to produce even partial suppression of axon death after injury at 7 dpa (Figure 4.3-A). As we could not directly assess proteasome activity within sensory neurons, it is possible some residual proteasome activity remained. However, taken together these data suggest that the proteasome plays no essential role in axon death and that the ubiquitin addition process may play essential roles beyond proteasomal degradation as proposed in previous reports (Xiong et al., 2012).

Chapter IV: Materials & Methods

Wing injury & assays and Confocal Microscopy:
See Materials & Methods in Chapter II.

Temperature sensitive alleles:
Use of temperature sensitive alleles to disrupt the proteasome is noted in figures. When assessing injury induced axon death, adult flies were shifted to 29°C immediately post eclosion for 5 days. Axotomy was applied and flies were maintained at 29°C for the remainder of the testing period. When assessing death induced by dSarm$^{\Delta ARM}$ or loss of Nmnat, both crosses and adults were maintained at 29°C.

Cloning:
For structure/function analyses, Gibson assembly was used to clone the *axed^{long}* PCR product into *pUAST(attB)* (Bischof et al., 2007) using the following primers:
pLN292 p(5x)UAST-axed^{long},w^{+},attB
5' primer: GCTAGCGGATCCAAAAGCTTtccggatccaagcttgcatgcc,
3' primer: GGTACCCTCGAGCCGCGGCCGCggatccgatccagacatgataag
Domain deletion versions as indicated:
pLN297 p(5x)UAST-axed$^{\Delta BTB(aa157-258)}$,w^{+},attB;
pLN298 p(5x)UAST-axed$^{\Delta BACK(aa348-442)}$,w^{+},attB;
pLN299 p(5x)UAST-axed$^{Nterm(aa442-537)}$,w^{+},attB.
Phi31-mediated integration was performed by (Bestgene).

S2 cells:
$8x10^5$ cells were plated out in 12-well plate 24 hr prior to transfection. Cells were co-transfected with 5xUAS deletion constructs and pAc-GAL4 to a final concentration of 1 µg DNA using Mirus *Trans*IT-Insect (Mirus Bio, Madison, WI). Cells were harvested 48 hours after transfection and protein expression was assessed using Western blot. (pAC-GAL4 was a gift from Liqun Luo - Addgene plasmid # 24344 -).

Immunohistochemistry
Western Blot: Primary antibodies (AB) were applied at 4°C overnight, secondary antibodies at room temperature for 1h. FLAG detection: 1st AB: 1:1000 Mouse anti FLAG (Sigma F1804), 2nd AB: 1:2000 Rabbit anti Mouse HRP (Abcam ab6728).

Drosophila Stocks and Genotypes in Display Items

In addition to stocks listed in Materials & Methods section of Chapter II & III, stocks used in Chapter IV are listed below.

X chromosome:
Df(1)G1 (uncovering *Roc1a*^{G1}) (Noureddine et al., 2002).

Chromosome 2:
axed structure/function (including endogenous 5' & 3' UTR, landing site: *attP40*): 5xUAS-*axed*^{long}, *5xUAS-axed*$^{\Delta BTB}$, *5xUAS-axed*$^{\Delta BACK}$, *5xUAS-axed*$^{\Delta Cterm}$ (Amy Sheehan), *cul1*^{K01207} (Spradling et al., 1999), *cul3*^{gft2} (Ou et al., 2002), *cul3*^{06430} (Mistry et al., 2004), *cul3*^{EY11031}(Bellen et al., 2004), *cul4*^{11L} (Hu et al., 2008), *cul4*^{KG02900} (Lin et al., 2009), *Uba1*^{S3484} (Spradling et al., 1999), *Uba1*^{LL03617} (Schuldiner et al., 2008), *Nedd8*^{KG03071} (Spradling et al., 1999), *5xUAS- UAS-UBP2.D* (Liqun Luo), *5xUAS-ProsB6*^{1} (Belote and Fortier, 2002), *5xUAS-PI31::HA* (Bader et al., 2011).

Chromosome 3:
Roc1b^{dc3} (Donaldson et al., 2004), *5xUAS-GFP::gft*^{K717R} (Zhu et al., 2005), *5xUAS-ProsB2*^{1} (Belote and Fortier, 2002), *5xUAS-PI31* (Provided by the Stellar Lab), *sina*^{2} (Carthew and Rubin, 1990), *eff*^{S1782} (Fauvarque et al., 2001).

Chapter IV: Figures & Tables

Figure 4.1: Axed conserved domains required for function

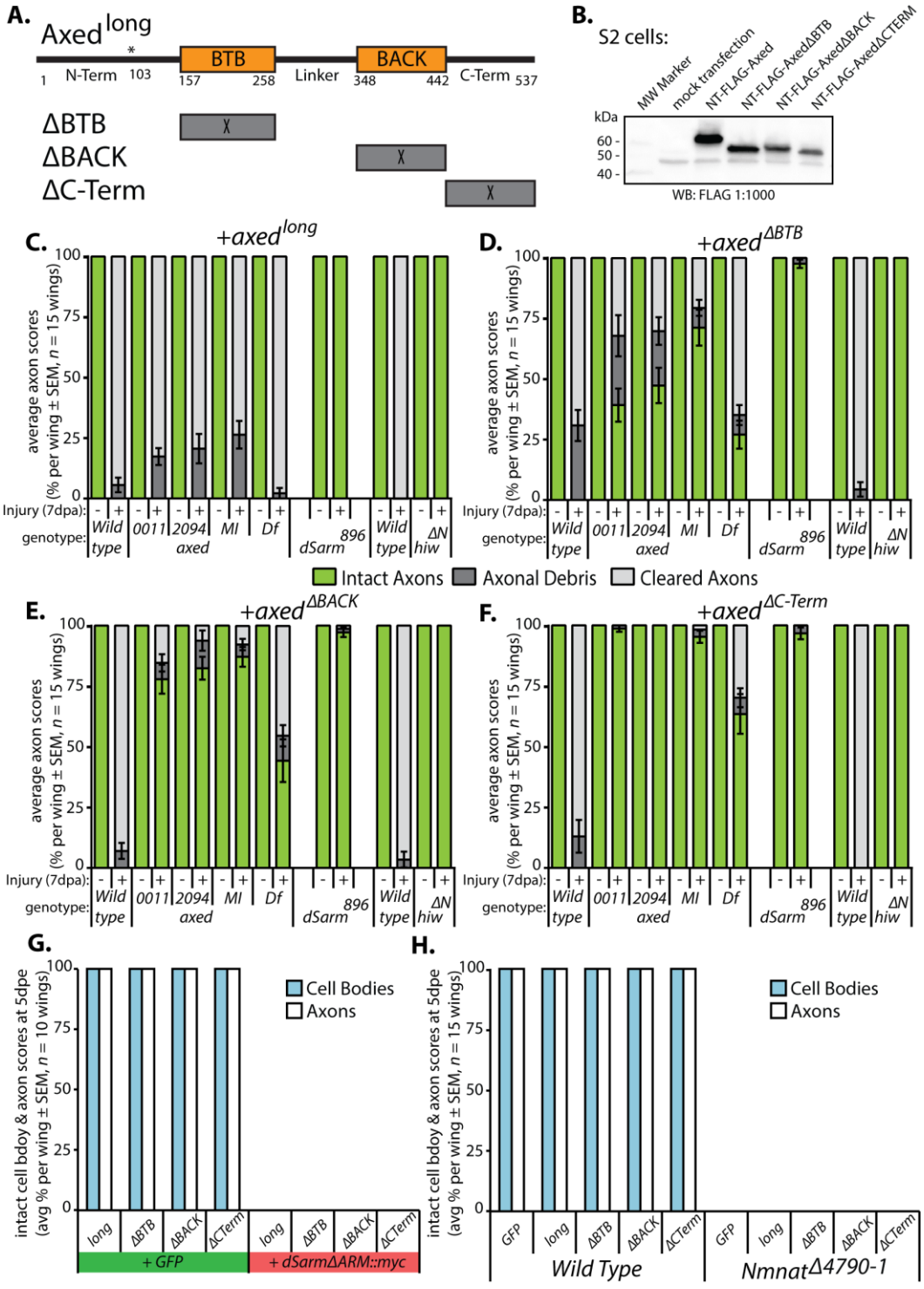

Figure 4.1:

A. Depicted are the conserved domains of Axed^{long} (537 amino acids (aa)), * indicates the start codon of Axed^{short} (434 aa). Indicated deletions are shown below (aa deleted: ΔBTB(157-258), ΔBACK(348-442), ΔCTerm(442-537)).

B. N-terminal FLAG tagged deletion constructs under an actin promoter produce stable protein species S2 cells. Deletions constructs were co-transfected with a pAc in S2 cells, lysed, and assessed using Western blot and anti-FLAG (Expected molecular weights: Axed^{long}: ~60kDa, Axed$^{\Delta BTB}$: ~49kDa, Axed$^{\Delta BACK}$: ~49.5kDa, Axed$^{\Delta CTerm}$: ~49.5kDa).

C-F. To determine if Axed^{long} or Axed deletion constructs caused spontaneous degeneration or dominant negative effects, or could rescue axon degeneration we assessed axon integrity in uninjured axons and axons at 7dpa in *wild type*, *axed* null, *dsarm* null, and *hiw* null clones:

C. Axed^{long} recues axon death at 7dpa in *axed* null clones, yet fails to attenuate axon protection afforded in severed *dsarm* or *hiw* null axons. Expression in *wild type* has no effect on uninjured neuronal morphology or on the progression of axon death after injury (*n* = 15 wings each).

D. Axed$^{\Delta BTB}$ partially recues axon death at 7dpa in *axed* null clones and fails to attenuate axon protection afforded in severed *dsarm* or *hiw* null axons. Expression in *wild type* has no effect on uninjured neuronal morphology or on the progression of axon death after injury (*n* = 15 wings each).

E. Axed$^{\Delta BACK}$ partially recues axon death at 7dpa in *axed* null clones and fails to attenuate axon protection afforded in severed *dsarm* or *hiw* null axons. Expression in *wild type* has no effect on uninjured neuronal morphology or on the progression of axon death after injury (*n* = 15 wings each).

F. Axed$^{\Delta CTerm}$ fails to rescue axon death at 7dpa in *axed*, *dsarm,* or *hiw* null axons. Expression in *wild type* has no effect on uninjured neuronal morphology or on the progression of axon death after injury (*n* = 15 wings each).

G. Axed deletion constructs, as well as Axed^{long}, fail to attenuate neuronal death induced by *dsarm$^{\Delta ARM}$* (*n* = 10 wings each).

H. Axed deletion constructs, as well as Axed^{long}, fail to attenuate neuronal death in *Nmnat* null clones (*n* = 15 wings each).

Figure 4.2: Disrupting the proteasome with *UBP2* suppresses axon death induced by injury, but not by Nmnat depletion or dSarm$^{\Delta ARM}$.

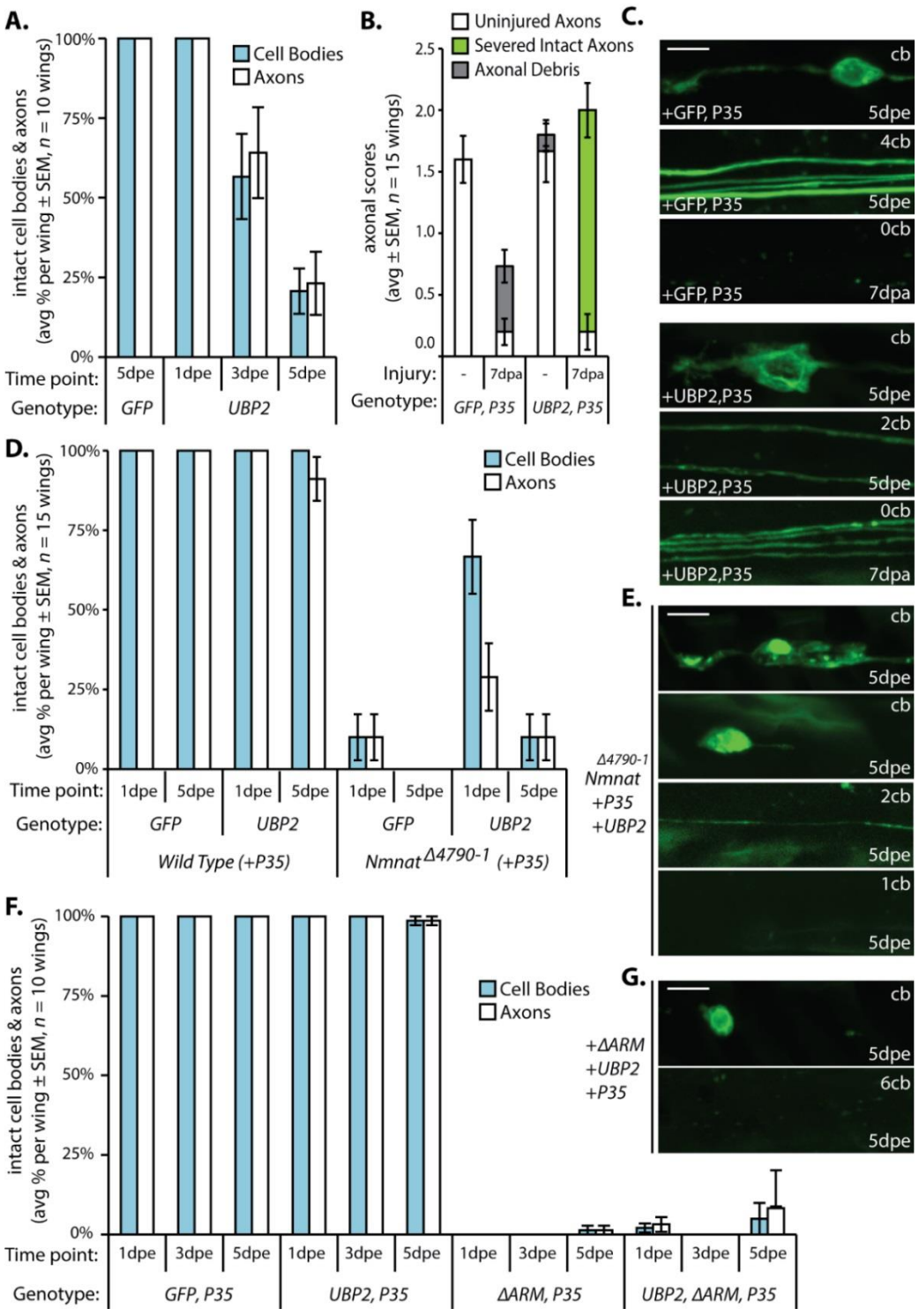

Figure 4.2:
A. Expression of the yeast de-ubiquitinating enzyme UBP2 in neurons causes spontaneous progressive degeneration of both cell bodies and axons. Intact cell bodies and axons were scored wild type expressing GFP or UBP2 (*n* = 10 wings each).
B. UBP2 completely inhibits axon degeneration to 7 days post axotomy. Apoptotic inhibitor P35 has no effect on axon degeneration and suppresses spontaneous neuronal death induced by UBP2 (*n* = 15 wings each).
C. Representative images of cell bodies (cb), uninjured axons at 5 dpe and severed axons at 7 days (expected axons, #cb). Scale bar, 5µm.
D. UBP2 delays neuronal death induced by deletion of *Nmnat*. Intact cell bodies and axons were scored wild type or *Nmnat* clones co-expressing P35 and either GFP or UBP2 (*n* = 15 wings each).
E. Representative image of partially (upper) and fully degenerated (lower) *Nmnat* null cell bodies and axons expressing P35 and UBP2 at 5 dpe. Scale bar, 5µm.
F. Expression of UBP2, P35, or both in tandem fail to attenuate death induced by $dsarm^{\Delta ARM}$. Intact cell bodies and axons were scored wild type clones co-expressing P35 and either GFP or UBP2 (*n* = 10 wings each).
G. Representative image of degenerated cell bodies and axons expressing P35, UBP2, $dsarm^{\Delta ARM}$ at 5 dpe. Scale bar, 5µm

Figure 4.3: Disrupting the proteasome with *prosβ2*^{1}, *prosβ6*^{1}, or *PI31* overexpression fails suppress axon death induced by injury, Nmnat depletion, or dSarm$^{\Delta ARM}$.

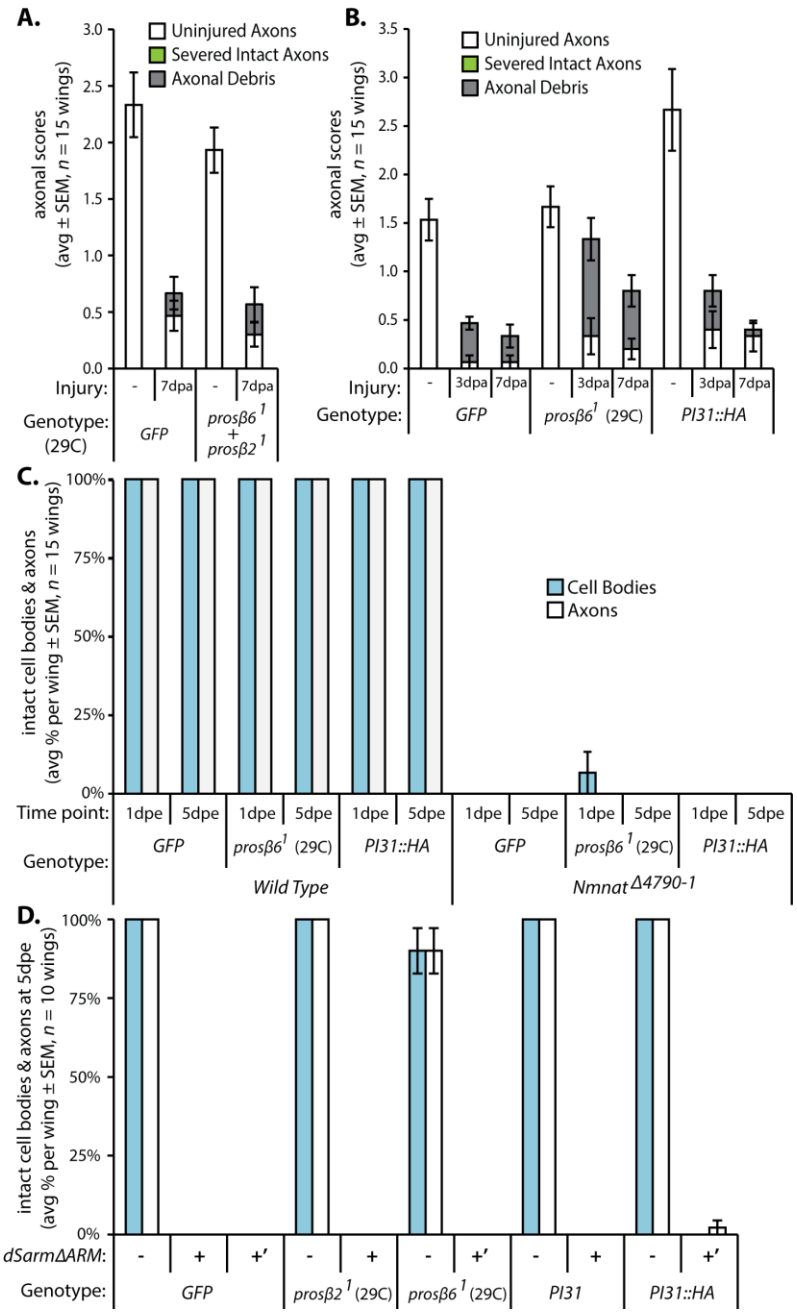

Figure 4.3:
A. Dual expression of temperature sensitive dominant negative proteasome 20S subunits *prosβ2*^{1} & *prosβ6*^{1} fails to inhibit axon degeneration at 29C. (*n* = 15 wings each).
B. Axon death is unaffected by expression of either *prosβ6*^{1} at 29C or *PI31*. (*n* = 15 wings each).
C. Overexpression of *prosβ6*^{1} at 29C or *PI31* fail to inhibit neuronal death in *Nmnat* null clones. (*n* = 15 wings each).
D. *dsarm*$^{\Delta ARM}$ induced neuronal death is unaffected by expression of either *prosβ6*^{1} at 29C or *PI31*. (*n* = 10 wings each)

Table 4.1: Cullin-RING-ligase complex component alleles tested for deficits in axon death

Gene / allele	Detailed description	Axon death phenotype	*dsarm*$^{\Delta ARM}$ suppression
Cullin-RING ligase complex mutants			
cul1^{K01207}	P element transposon	no	no
cul3^{gft2}	EMS mutant	no	no
cul3^{06430}	P element transposon	no	no
cul3^{EY11031}	P element transposon	no	no
UAS-GFP::gft^{K717R}	Cul3 mutation in *Nedd8* conjugation site	no	nd
cul4^{11L}	Imprecise excision	no	no
cul4^{KG02900}	P element transposon	no	no
Df(3R)Exel6211	Deficiency uncovering *cul5*	no	no
Df(3R)BSC3450	Deficiency uncovering *cul5*	no	no
Df(3R)BSC413	Deficiency uncovering *CG11261*	no	no
Df(3R)ED4486	Deficiency uncovering *CG11261*	no	no
Uba1^{S3484}	P element transposon	no	no
Uba1^{LL03617}	P element transposon	no	no
Df(1)G1	Deletion uncovering *Roc1a*	no	no
Roc1b^{dc3}	Deletion uncovering *Roc1b*	no	no
Df(3L)BSC247	Deficiency uncovering *Roc1b*	no	no
eff^{S1782}	P element transposon	no	no
sina^{2}	EMS mutant	no	no
Df(3L)Exel9004	Deficiency uncovering *sinah* & *sina*	no	no
Nedd8^{KG03071}	P element transposon	no	no

Table 4.1:

The Cullin-RING-ligase complex genes in the table tested were null alleles or deficiencies recombined with FRT sites. Each was assessed for an axon death at 7 dpa and whole cell death after expression of dsarm$^{\Delta ARM}$.

Table 4.2: Genotypes in figures/experiments

Abbreviations: *Y: Y* chromosome, *w: w*^{1118} or *w*$^{-}$, *OK371: OK371-Gal4*, *mCD8::GFP: 5xUAS-mCD8::GFP*

Figure 4-1:
A. -
B. wild type + *axed*^{long}: *w/Y ; OK371,mCD8::GFP,aseFLP*^{2e}*/5xUAS-axed*$^{long(attP40)}$ *; FRT2A/tub-Gal80,FRT2A*
B. *axed*^{0011} + *axed*^{long}: *w/Y ; OK371,mCD8::GFP,aseFLP*^{2e}*/5xUAS-axed*$^{long(attP40)}$ *; axed*^{0011}*,FRT2A/tub-Gal80,FRT2A*
B. *axed*^{2094}, *axed*^{MI13270}, *BSC411, & dsarm*^{896} + *axed*^{long} : as above
B. wild type + *axed*^{long}: *w,19A/w,tubGal80,19A ; Ok371-Gal4,mCD8::GFP/5xUAS-axed*$^{long(attP40)}$ *; aseFLP*^{3b}*/+*
B. *hiw*$^{\Delta N}$ + *axed*^{long}: *w,hsFLP,hiw*$^{\Delta N}$*,19A/w,tubGal80,19A; Ok371-Gal4,mCD8::GFP /5xUAS-axed*$^{long(attP40)}$ *; aseFLP*^{3b}*/+*
C. wild type + *axed*$^{\Delta BTB}$: *w/Y ; OK371,mCD8::GFP,aseFLP*^{2e}*/5xUAS-axed*$^{\Delta BTB(attP40)}$*; FRT2A/tub-Gal80,FRT2A*
C. *axed*^{0011} + *axed*$^{\Delta BTB}$: *w/Y ; OK371,mCD8::GFP,aseFLP*^{2e}*/5xUAS-axed*$^{\Delta BTB(attP40)}$ *; axed*^{0011}*,FRT2A/tub-Gal80,FRT2A*
C. *axed*^{2094}, *axed*^{MI13270}, *BSC411, & dsarm*^{896} + *axed*$^{\Delta BTB}$: as above
C. wild type + *axed*$^{\Delta BTB}$: *w,19A/w,tubGal80,19A ; Ok371-Gal4,mCD8::GFP/5xUAS-axed*$^{\Delta BTB(attP40)}$ *; aseFLP*^{3b}*/+*
C. *hiw*$^{\Delta N}$ + *axed*$^{\Delta BTB}$: *w,hsFLP,hiw*$^{\Delta N}$*,19A/w,tubGal80,19A; Ok371-Gal4,mCD8::GFP /5xUAS-axed*$^{\Delta BTB(attP40)}$ *; aseFLP*^{3b}*/+*
D. wild type + *axed*$^{\Delta BACK}$: *w/Y ; OK371,mCD8::GFP,aseFLP*^{2e}*/5xUAS-axed*$^{\Delta BACK(attP40)}$ *; FRT2A/tub-Gal80,FRT2A*
D. *axed*^{0011} + *axed*$^{\Delta BACK}$: *w/Y ; OK371,mCD8::GFP,aseFLP*^{2e}*/5xUAS-axed*$^{\Delta BACK(attP40)}$ *; axed*^{0011}*,FRT2A/tub-Gal80,FRT2A*
D. *axed*^{2094}, *axed*^{MI13270}, *BSC411, & dsarm*^{896} + *axed*$^{\Delta BTB}$: as above
D. wild type + *axed*$^{\Delta BACK}$: *w,19A/w,tubGal80,19A ; Ok371-Gal4,mCD8::GFP/5xUAS-axed*$^{\Delta BACK(attP40)}$ *; aseFLP*^{3b}*/+*
D. *hiw*$^{\Delta N}$ + *axed*$^{\Delta BACK}$: *w,hsFLP,hiw*$^{\Delta N}$*,19A/w,tubGal80,19A; Ok371-Gal4,mCD8::GFP /5xUAS-axed*$^{\Delta BACK(attP40)}$ *; aseFLP*^{3b}*/+*
E. wild type + *axed*$^{\Delta Cterm}$: *w/Y ; OK371,mCD8::GFP,aseFLP*^{2e}*/5xUAS-axed*$^{\Delta Cterm(attP40)}$ *; FRT2A/tub-Gal80,FRT2A*
E. *axed*^{0011} + *axed*$^{\Delta Cterm}$: *w/Y ; OK371,mCD8::GFP,aseFLP*^{2e}*/5xUAS-axed*$^{\Delta Cterm(attP40)}$ *; axed*^{0011}*,FRT2A/tub-Gal80,FRT2A*
E. *axed*^{2094}, *axed*^{MI13270}, *BSC411, & dsarm*^{896} + *axed*$^{\Delta Cterm}$: as above
E. wild type + *axed*$^{\Delta Cterm}$: *w,19A/w,tubGal80,19A ; Ok371-Gal4,mCD8::GFP/5xUAS-axed*$^{\Delta Cterm(attP40)}$ *; aseFLP*^{3b}*/+*
E. *hiw*$^{\Delta N}$ + *axed*$^{\Delta Cterm}$: *w,hsFLP,hiw*$^{\Delta N}$*,19A/w,tubGal80,19A; Ok371-Gal4,mCD8::GFP /5xUAS-axed*$^{\Delta Cterm(attP40)}$ *; aseFLP*^{3b}*/+*
F. *GFP + axed*^{long}: *FRT19A/tubGal80,hsFLP,FRT19A ; OK371,mCD8::GFP,aseFLP*^{2a}*/5xUAS-axed*$^{long(attP40)}$ *; mCD8::GFP,aseFLP*^{3b}*/mCD8::GFP*
F. *GFP + axed*$^{\Delta BTB}$*, axed*$^{\Delta BACK}$*, & axed*$^{\Delta Cterm}$: *as above*
F. *ΔARM + axed*^{long}: *FRT19A/tubGal80,hsFLP,FRT19A ; OK371,mCD8::GFP,aseFLP*^{2a}*/5xUAS-axed*$^{long(attP40)}$ *; mCD8::GFP,aseFLP*^{3b}*/5xUAS-dsarm*$^{\Delta ARM}$*::EGFP*
F. *ΔARM + axed*$^{\Delta BTB}$*, axed*$^{\Delta BACK}$*, & axed*$^{\Delta Cterm}$: *as above*
G. *wild type + GFP: w/Y ; OK371,mCD8::GFP,aseFLP*^{2e}*/mCD8::GFP ; FRT82B/FRT82B,tub-Gal80*
G. *Nmnat*$^{\Delta 4790-1}$ *+ GFP: w/Y ; OK371,mCD8::GFP,aseFLP*^{2e}*/mCD8::GFP ; FRT82B,Nmnat*$^{\Delta 4790-1}$*/FRT82B,tub-Gal80*
G. *wild type + axed*^{long}: *w/Y ; OK371,mCD8::GFP,aseFLP*^{2e}*/5xUAS-axed*$^{long(attP40)}$*; FRT82B/FRT82B,tub-Gal80*
G. *wild type + axed*$^{\Delta BTB}$*, axed*$^{\Delta BACK}$*, & axed*$^{\Delta Cterm}$: *as above*
G. *Nmnat*$^{\Delta 4790-1}$ *+ axed*^{long}: *w/Y ; OK371,mCD8::GFP,aseFLP*^{2e}*/5xUAS-axed*$^{long(attP40)}$*; FRT82B,Nmnat*$^{\Delta 4790-1}$*/FRT82B,tub-Gal80*
G. *Nmnat*$^{\Delta 4790-1}$ *+ axed*$^{\Delta BTB}$*, axed*$^{\Delta BACK}$*, & axed*$^{\Delta Cterm}$: *as above*
Table 4-1:
Axotomy:
Cul1: *cul1*^{k01207}: *w/Y ; FRT42D,tub-Gal80/FRT42D,cul1*^{k01207} *; nSyb-Gal4,mCD8::GFP,aseFLP*^{3a}*/mCD8::GFP*
Cul3: *cul3*^{gft2}*, cul3*^{06430}*, cul3*^{EY11031}: *w/Y ; cul3*^{alleles}*,FRT40A/tub-Gal80,FRT40A ; nSyb-Gal4,mCD8::GFP,aseFLP*^{3a}*/mCD8::GFP*
Cul3: *5xUAS-GFP::gft*^{K717R}: *w/Y ; FRT40A/tub-Gal80,FRT40A ; nSyb-Gal4,mCD8::GFP,aseFLP*^{3a}*/5xUAS-GFP::gft*^{K717R}
Cul4: *cul4*^{11L}: *w,elav*^{C155}*-Gal4/Y ; FRTG13,tub-Gal80/FRTG13,cul4*^{11L} *; aseFLP*^{3b}*,mCD8::GFP/mCD8::GFP*
Cul4: *cul4*^{KG02900}: *w/Y ; FRT42D,tub-Gal80/FRT42D,cul4*^{KG02900} *; nSyb-Gal4,mCD8::GFP,aseFLP*^{3a}*/mCD8::GFP*
Cul5: *Df(3R)Exel6211 & Df(3R)BSC3450: w/Y ; OK371,mCD8::GFP,aseFLP*^{2a}*/mCD8::GFP ; FRT82B,Cul5*^{alleles}*/FRT82B,tub-Gal80*
CG11261: *Df(3R)BSC413 & Df(3R)ED4486: w/Y ; OK371,mCD8::GFP,aseFLP*^{2e}*/mCD8::GFP ; CG11261*^{alleles}*,FRT2A/tub-Gal80,FRT2A*
Uba1: *uba1*^{LL03617}: *w,elav*^{c155}*-Gal4/Y ; FRTG13,tub-Gal80/FRTG13,uba1*^{LL03617} *; aseFLP*^{3b}*,mCD8::GFP/mCD8::GFP*
Uba1: *uba1*^{S3484}: *w/Y ; FRT42D,tub-Gal80/FRT42D,uba1*^{S3484} *; nSyb-Gal4,mCD8::GFP,aseFLP*^{3a}*/mCD8::GFP*
Roc1a: *Df(1)G1: Df(1)G1,w,sn*^{1}*,FRT19A/w,hs-FLP*^{12}*,tub-Gal80,FRT19A ; OK371,mCD8::GFP,aseFLP*^{2a}*/+ ; mCD8::GFP,aseFLP*^{3b}
Roc1b: *roc1b*^{dc3} *& Df(3L)BSC247: w/Y ; OK371,mCD8::GFP,aseFLP*^{2e}*/mCD8::GFP ; Roc1b*^{alleles}*,FRT2A/tub-Gal80,FRT2A*

Eff: *w/Y ; OK371,mCD8::GFP,aseFLP^{2e}/mCD8::GFP ; eff^{S1782},FRT2A/tub-Gal80,FRT2A*
Sina: *w/Y ; OK371,mCD8::GFP,aseFLP^{2e}/mCD8::GFP ; sina^{2},FRT2A/tub-Gal80,FRT2A sina^{2}*
Sina & Sinah: *w/Y ; OK371,mCD8::GFP,aseFLP^{2e}/mCD8::GFP ; Df(3L)Exel9004,FRT2A/tub-Gal80,FRT2A*
Nedd8: *nedd8^{KG03071}: w/Y ; nedd8^{KG03071},FRT40A/tub-Gal80,FRT40A ; nSyb-Gal4,mCD8::GFP,aseFLP^{3a}/mCD8::GFP*
***dsarm$^{\Delta ARM}$* suppression:**
Cul1: *cul1^{k01207}: w/Y ; FRT42D,tub-Gal80/FRT42D,cul1^{k01207} ; nSyb-Gal4,mCD8::GFP,aseFLP^{3a}/5xUAS-dsarm$^{\Delta ARM}$::EGFP*
Cul3: *cul3^{gft2}, cul3^{06430}, cul3^{EY11031}: w/Y ; cul3^{alleles},FRT40A/tub-Gal80,FRT40A ; nSyb-Gal4,mCD8::GFP,aseFLP^{3a}/5xUAS-dsarm$^{\Delta ARM}$::EGFP*
Cul4: *cul4^{11L}: w,elav^{c155}-Gal4/Y ; FRTG13,tub-Gal80/FRTG13,cul4^{11L} ; aseFLP^{3b},mCD8::GFP/5xUAS-dsarm$^{\Delta ARM}$::EGFP*
Cul4: *cul4^{KG02900}: w/Y ; FRT42D,tub-Gal80/FRT42D,cul4^{KG02900} ; nSyb-Gal4,mCD8::GFP,aseFLP^{3a}/5xUAS-dsarm$^{\Delta ARM}$::EGFP*
Cul5: *Df(3R)Exel6211 & Df(3R)BSC3450: w/Y ; OK371,mCD8::GFP,aseFLP^{2a}/5xUAS-dsarm$^{\Delta ARM}$::myc ; FRT82B,Cul5^{alleles}/FRT82B,tub-Gal80*
CG11261: *Df(3R)BSC413 & Df(3R)ED4486: w/Y ; OK371,mCD8::GFP,aseFLP^{2e}/5xUAS-dsarm$^{\Delta ARM}$::myc ; CG11261^{alleles},FRT2A/tub-Gal80,FRT2A*
Uba1: *uba1^{LL03617}: w,elav^{c155}-Gal4/Y ; FRTG13,tub-Gal80/FRTG13,uba1^{LL03617} ; aseFLP^{3b},mCD8::GFP/5xUAS-dsarm$^{\Delta ARM}$::EGFP*
Uba1: *uba1^{S3484}: w/Y ; FRT42D,tub-Gal80/FRT42D,uba1^{S3484} ; nSyb-Gal4,mCD8::GFP,aseFLP^{3a}/5xUAS-dsarm$^{\Delta ARM}$::EGFP*
Roc1a: *Df(1)G1: Df(1)G1,w,sn^{1},FRT19A/w,hs-FLP^{12},tub-Gal80,FRT19A ; OK371,mCD8::GFP,aseFLP^{2a}/+ ; 5xUAS-dsarm$^{\Delta ARM}$::EGFP*
Roc1b: *roc1b^{dc3} & Df(3L)BSC247: w/Y ; OK371,mCD8::GFP,aseFLP^{2e}/5xUAS-dsarm$^{\Delta ARM}$::myc ; Roc1b^{alleles},FRT2A/tub-Gal80,FRT2A*
Eff: *w/Y ; OK371,mCD8::GFP,aseFLP^{2e}/5xUAS-dsarm$^{\Delta ARM}$::myc ; eff^{S1782},FRT2A/tub-Gal80,FRT2A*
Sina: *w/Y ; OK371,mCD8::GFP,aseFLP^{2e}/5xUAS-dsarm$^{\Delta ARM}$::myc ; sina^{2},FRT2A/tub-Gal80,FRT2A sina^{2}*
Sina & Sinah: *w/Y ; OK371,mCD8::GFP,aseFLP^{2e}/5xUAS-dsarm$^{\Delta ARM}$::myc ; Df(3L)Exel9004,FRT2A/tub-Gal80,FRT2A*
Nedd8: *nedd8^{KG03071}: w/Y ; nedd8^{KG03071},FRT40A/tub-Gal80,FRT40A ; nSyb-Gal4,mCD8::GFP,aseFLP^{3a}/5xUAS-dsarm$^{\Delta ARM}$::EGFP*
Figure 4-2:
A. *GFP: w,FRT19A/w,hsFLP,tubGal80,FRT19A ; mCD8::GFP/ OK371,mCD8::GFP ; mCD8::GFP/mCD8::GFP,aseFLP^{3b}*
A. *UBP2: w,FRT19A/w,hsFLP,tubGal80,FRT19A ; 5xUAS-UBP2.D/ OK371,mCD8::GFP ; mCD8::GFP/mCD8::GFP,aseFLP^{3b}*
B-C. *GFP,P35: w/Y ; OK371,mCD8::GFP,5xUAS-P35/mCD8::GFP ; FRT2A,FRT82b / FRT82b, tubGal80*
B-C. *GFP,UBP2: w/Y ; OK371,mCD8::GFP,5xUAS-P35/5xUAS-UBP2 ; FRT2A,FRT82b / FRT82b, tubGal80*
D-E. *wild type + GFP,P35: w/Y ; OK371,mCD8::GFP,5xUAS-P35/mCD8::GFP ; FRT2A,FRT82b / FRT82b, tubGal80*
D-E. *wild type + GFP,P35: GFP,UBP2: w/Y ; OK371,mCD8::GFP,5xUAS-P35/5xUAS-UBP2 ; FRT2A,FRT82b / FRT82b, tubGal80*
D-E. *Nmnat$^{\Delta 4790-1}$ + GFP,P35: w/Y ; OK371,mCD8::GFP,5xUAS-P35/mCD8::GFP ; FRT82b,Nmnat$^{\Delta 4790-1}$ / FRT82b, tubGal80*
D-E. *Nmnat$^{\Delta 4790-1}$ + GFP,P35: w/Y ; OK371,mCD8::GFP,5xUAS-P35/5xUAS-UBP2 ; FRT82b,Nmnat$^{\Delta 4790-1}$/FRT82b, tubGal80*
F-G. *GFP,P35: w,FRT19A/ w,hsFLP,tubGal80,FRT19A ; mCD8::GFP/mCD8::GFP,OK371,mCD8::GFP ; 5xUAS-P35/mCD8::GFP, aseFLP^{3b}*
F-G. *GFP,UBP2: w,FRT19A/ w,hsFLP,tubGal80,FRT19A ; 5xUAS-UBP2/mCD8::GFP,OK371,mCD8::GFP ; 5xUAS-P35/mCD8::GFP, aseFLP^{3b}*
F-G. *ΔARM,P35: w,FRT19A/ w,hsFLP,tubGal80,FRT19A ; mCD8::GFP/mCD8::GFP,OK371,mCD8::GFP ; 5xUAS-P35/5xUAS-dsarm$^{\Delta ARM}$::EGFP*
F-G. *UBP2,ΔARM,P35: w,FRT19A/ w,hsFLP,tubGal80,FRT19A ; 5xUAS-UBP2/mCD8::GFP,OK371,mCD8::GFP ; 5xUAS-P35/5xUAS-dsarm$^{\Delta ARM}$::EGFP*
Figure 4-3:
A. *GFP: w,hsFLP,FRT19/w,tubGal80,FRT19 ; OK371,mCD8::GFP/mCD8::GFP; aseFLP^{3b},mCD8::GFP / +*
A. *Proβ6^{1} + Prosβ2^{1}: w,hsFLP,FRT19/w,tubGal80,FRT19 ; OK371,mCD8::GFP/5xUAS-ProsB6^{1} ; aseFLP^{3b}/5xUAS-ProsB2^{1}*
B. *GFP: w/Y ; OK371,mCD8::GFP,5xUAS-P35/mCD8::GFP; FRT2A,FRT82b/FRT82b, tubGal80*
B. *Proβ6^{1}: w/Y ; OK371,mCD8::GFP,5xUAS-P35/5xUAS-Proβ6^{1}; FRT2A,FRT82b/FRT82b, tubGal80*
B. *PI31::HA: w/Y ; OK371,mCD8::GFP,5xUAS-P35/5xUAS-PI31::HA ; FRT2A,FRT82b/FRT82b, tubGal80*
C. *GFP, Proβ6^{1}, & PI31::HA: as above (B)*
C. *Nmnat$^{\Delta 4790-1}$ + GFP: w/Y ; OK371,mCD8::GFP,5xUAS-P35/mCD8::GFP; FRT82b,Nmnat$^{\Delta 4790-1}$/FRT82b, tubGal80*
C. *Nmnat$^{\Delta 4790-1}$ + Proβ6^{1}: w/Y ; OK371,mCD8::GFP,5xUAS-P35/5xUAS-Proβ6^{1}; FRT82b,Nmnat$^{\Delta 4790-1}$/FRT82b, tubGal80*
C. *Nmnat$^{\Delta 4790-1}$ + PI31::HA: w/Y ; OK371,mCD8::GFP,5xUAS-P35/5xUAS-PI31::HA ; FRT82b,Nmnat$^{\Delta 4790-1}$/FRT82b, tubGal80*
D. *GFP (-): w,hsFLP,FRT19/w,tubGal80,FRT19 ;OK371,mCD8::GFP/mCD8::GFP ; aseFLP^{3b}/mCD8::GFP*
D. *Prosβ2^{1}(-): w,hsFLP,FRT19/w,tubGal80,FRT19 ;OK371,mCD8::GFP/mCD8::GFP ; aseFLP^{3b}/5xUAS-Prosβ2^{1}*
D. *Proβ6^{1}(-): w,hsFLP,FRT19/w,tubGal80,FRT19 ;OK371,mCD8::GFP/5xUAS-Proβ6^{1}; aseFLP^{3b}/mCD8::GFP*
D. *PI31(-): w,hsFLP,FRT19/w,tubGal80,FRT19 ;OK371,mCD8::GFP/mCD8::GFP ; aseFLP^{3b}/5xUAS-PI31*
D. *PI31::HA(-): w,hsFLP,FRT19/w,tubGal80,FRT19 ;OK371,mCD8::GFP/5xUAS-PI31::HA; aseFLP^{3b}/mCD8::GFP*

D. *GFP (+):* *w,hsFLP,FRT19/w,tubGal80,FRT19 ;OK371,mCD8::GFP/5xUAS-dsarm$^{\Delta ARM}$::myc; aseFLP^{3b}/mCD8::GFP*
D. *GFP (+'):* *w,hsFLP,FRT19/w,tubGal80,FRT19 ;OK371,mCD8::GFP/mCD8::GFP ; aseFLP^{3b}/5xUAS-dsarm$^{\Delta ARM}$::EGFP*
D. *Prosβ2^{1}(+):* *w,hsFLP,FRT19/w,tubGal80,FRT19 ;OK371,mCD8::GFP/5xUAS-dsarm$^{\Delta ARM}$::myc; aseFLP^{3b}/5xUAS-Prosβ2^{1}*
D. *Proβ6^{1} (+'):* *w,hsFLP,FRT19/w,tubGal80,FRT19 ;OK371,mCD8::GFP/5xUAS-Proβ6^{1} ; aseFLP^{3b}/5xUAS-dsarm$^{\Delta ARM}$::EGFP*
D. *PI31 (+):* *w,hsFLP,FRT19/w,tubGal80,FRT19 ;OK371,mCD8::GFP/5xUAS-dsarm$^{\Delta ARM}$::myc; aseFLP^{3b}/5xUAS-PI31*
D. *PI31::HA (+'):* *w,hsFLP,FRT19/w,tubGal80,FRT19 ;OK371,mCD8::GFP/5xUAS-PI31::HA ; aseFLP^{3b}/5xUAS-dsarm$^{\Delta ARM}$::EGFP*

CHAPTER V: Discussion

Discussion 5-1: Screening for regulators of axon death and maintenance

In this thesis I describe the identification *axed,* a novel essential component of the axon death signaling pathway in *Drosophila.* In addition, I uncovered and identified two other mutant genes, one required for axon maintenance, the other required for normal axon death progression. Two distinct, unbiased forward genetic screens of axotomized neuronal clones in the *Drosophila* wing, combined with NGS technology and conventional genetic mapping, were used to identify these mutations. Unbiased screening, in contrast to a candidate screening approach, has the advantage of uncovering unexpected genes of interest. In retrospect, taking this strategy seems especially useful in the search for genes required for axon death, since no previous evidence would implicate a SAM/TIR domain- or a BTB domain-containing protein as pro-degenerative molecules, *dsarm* and *axed*, although a candidate strategy utilized by myself and others in the lab has ruled out a large swath of genes from essential participation in axon death signaling.

I first attempted to screen using chromosomal deficiency lines recombined with FRT sites that were generously provided by the Doe Lab (Oregon). Only one of 169 tested deficiencies was defective for axon death and this deficiency, Df(1)ED7289, uncovered *hiw*, a gene previously described for its role in axon death by the Collins Lab (Xiong et al., 2012) (Table 2.1). Lines were tested for an axon defective phenotype at 5-7 dpa, so it is possible we may have missed more subtle phenotypes. Although this strategy failed to uncover any novel candidates, it still provides evidence that genes within tested deficiencies are not essential for axon death to proceed and is therefore a useful resource to cross reference genes and proteins that may turn up as candidates in additional screens

for axon death, other degenerative screens, or protein interaction experiments. For more definitive evidence however, well characterized null mutations of individual genes would have to be tested.

Another group in lab, including myself, used ethyl methanesulfonate to induce random mutations across the *Drosophila* genome in the hope of disrupting a gene required for axon death. We attempted to saturate the genome and screened 40,000+ unique mutants. I recovered *gene-of-interest-#1*^{345x} (Figure 2.2) and *axed*^{0011}, while Lukas Neukomm recovered *axed*^{2094} (Figure 2.4). There is also an axon death gene on chromosome 2L, or possibly a dominant mutation located elsewhere, where both I and Jon Farley acquired in the screen, but failed to recover. I also recovered two alleles of a single gene required for axon maintenance, *gene-of-interest-#2*$^{596x\ \&1013x}$ (Figure 2.3).

Taken together combination of screening approaches attempted to test most *Drosophila* genes, however we may have missed some genes required for axon death for a few reasons. First, due to MARCM technical constraints we could not screen genes located between FRTs and telomeres as well as on the Y and 4th chromosomes, missing ~18% of the *Drosophila* genome, although Wallerian degeneration proceeds identically in males and females, so genes on the Y chromosome are unlikely to contribute to axon death. Second, it is also possible we could not recover more candidates because some axon death genes may have functionally redundant duplicates. For example, it would not have been surprising to recover a calcium activated protease (Glass et al., 2002; Ma et al., 2013; Yang et al., 2013), but *Drosophila* have three to four possibly redundant calpains on different chromosomes. Third, some genes may have failed to meet our stringent

requirements that axons survive to 7 dpa, thus limiting 'hits' to strong mutations in genes absolutely essential for axon death, but missing mutations with phenotypes that slightly delayed axon death. We also might miss phenotypes where only a subset of axons remained intact, especially in the F1 screen, where only one or two injured wings can be assessed. Successful recovery of partially protective *gene-of-interest-#1*^{345x} may have been due the X chromosome requiring an F2 screen and thus allowing several injured wings to be analyzed. On other chromosomes, we failed to recover any mutations in genes reported to participate in axon death such as *SkpA/Skp1a, DFsn/Fbxo45, wnd/Dlk*, *Mkk4*, *hep/Mkk7*, and *bsk/Jnk*, possibly due to very weak phenotypes and some MAPK redundancy (Brace et al., 2014; Miller et al., 2009; Wu et al., 2007; Yamagishi and Tessier-Lavigne, 2016; Yang et al., 2015). *Df(1)ED6443* is an example of a deficiency which uncovered a noted axon death gene in mammals, *SkpA/Skp1a*, but displayed no axon death deficit, possibly due to redundancy in the fly (Brace et al., 2014). In the future, it might be possible to use several RNAi constructs or Cas9/CRISPR multiple gene knockouts within clones, possibly in combination with null alleles to test functionally redundant genes. Also, weak genes in an axon death might be uncovered by screening in a sensitized background, such as one lacking one copy *axed* or *dsarm* or both or very slightly overexpressing *nmnat*. Going forward, it may also be prudent to use different methods to screen as certain chromosomal regions vary in susceptibility mutagens and other groups have pulled out non-overlapping groups of candidate genes using distinct methods (Yamamoto et al., 2014).

False negative results are also possible if certain genes, either within a tested deficiency or altered by mutagen, negate the phenotype of an axon death candidate gene by causing non-Wallerian cell death before axonal injury. This type of cell death, defects in neuronal differentiation, or the suppression of components required for MARCM in deficiency clones may produce no detectable neurons in wings or ORNs and render them untestable for axon death phenotypes. Indeed, some deficiencies produced no clones and were omitted.

Discussion 5-2: A novel gene required for axon maintenance

Mutagenesis screening on the 1st chromosome uncovered two distinct sets of missense mutations within the accessory and catalytic domain of *GOI#2* causing severe axonal membrane dysfunction and a progressive 'dying-back' from distal to proximal axonal regions. These mutations phenocopy available loss-of-function alleles and RNAi knockdown of GOI#2 in wing sensory neurons. It remains to be determined how long wild type GOI#2 protein remains after clone induction and if this is responsible for the 'dying back' pattern of degeneration. Since distal axonal regions display dysfunction before proximal regions and cell bodies appear normal, we might hypothesize GOI#2 must be transported from a remaining and diminishing pool of wild type protein in null clone cell somas. It will be interesting in the future to probe how product of GOI#2 governs membrane structural integrity. Since I will not continue this project, only the basic phenotype of GOI#2 loss is presented in this thesis.

Discussion 5-3: A single mutation partially suppresses axon degeneration

I identified a splice site mutation within the transcription factor, *GOI#1*, that results in a subset of axons remaining intact post injury as well as a delayed fragmentation in severed axon that do degenerate. Since *GOI#1* is a transcription factor we might hypothesize that it regulates levels of components in the axon death pathway and its loss leads to decrease of pro-degenerative factors such as *MAPKs, hiw, dsarm,* and/or *axed* or an increase of pro-survival *Nmnat*. In theory, reducing *Nmnat* or overexpressing other genes should rescue degeneration if this hypothesis is correct. If none of these experiments rescue degeneration, it is possible *GOI#1* may have other unknown targets required for axon death or have other non-transcriptional regulatory roles. Since this line of inquiry will be continued by Jon Farley, only the basic phenotype of *GOI#1* null is presented in this thesis.

Discussion 5-4: *Axed* is essential for axon death after injury

Two mutants were identified on 3L left chromosome that displayed strong suppression of axon degeneration in both wing glutamatergic sensory neurons and ORNs (Figure 2.4). In wing neurons, nearly 100% of severed axons were morphologically intact at 7 days, while in anucleated olfactory receptor axons persisted intact for 50 days post injury (Figure 2.4-C/D). The near complete suppression of axon death, for almost the lifetime of the fly, is only comparable to loss of function mutations *dSarm* and *hiw*, as well as expression of Wld^{s}, suggesting the mutations affected a gene or genes that were essential for axon death to proceed after injury (MacDonald et al., 2006; Osterloh et al.,

2012; Xiong et al., 2012). Since both mutations on the same chromosomal arm caused lethality at early larval stage 1 and were linked to the axon death defective phenotype through multiple outcrossed generations, we used lethality complementation testing to map both mutations to a single BTB domain containing gene *CG8398*, renamed *axundead* or *axed* (Figure 2.5-A/B). Importantly, genetic elements that disrupted *axed*, such as *Df BSC411* and $axed^{MI13270}$, were also defective for axon degeneration at 7 dpa (Figure 2.5-D). Furthermore, when the transposon in $axed^{MI13270}$ was precisely excised, removing an artificial intron containing stop codons, but not altering *axed* exons, the resulting animals are homozygous viable and have wild type axon death in contrast to imprecise Minos excision, which resulted in lethal, axon death defective, deletions in *axed*.

We also used two CRISPR guides co-injected with Cas9 to generate three distinct alleles, all harboring lethal deletion mutations in exon 2 of *axed*. While these mutations caused early frameshift deletions with early predicted stops, they only had a partial suppression of axon death in clones. Since our Axed antibody failed, we could not assess if any Axed protein was produced in the animals, however one of three ATG sites C-terminal to the last CRISPR guide site might produce a truncated protein containing the BACK and C-terminal regions that could phenocopy the partial axon death phenotype observed in our structural analyses (Figure 4.1). In the future, we might assess production of a truncated transcript in these animals with RT-PCR. It is also possible that the guides had one or more off targets in genes required for neuronal maintenance or metabolism, and axons were more susceptible to degeneration after injury.

To further confirm that the mutations in *axed* were responsible for the axon death phenotype, we re-expressed either $axed^{long}$ or $axed^{short}$ isoforms in *axed* null clones and fully rescued axon degeneration (Figure 2.5-D). Both isoforms are also expressed endogenously as detected in western blot for $Axed^{EGFP::FLAG}$ (Figure 3.1-B). Neither isoform when overexpressed in wild type or *axed* null clones caused any spontaneous degeneration, so there must be some injury-induced upstream post-translational modification to Axed or required co-factors for Axed to exert its pro-degenerative function. It remains to be determined if the isoforms serve any differential roles besides an alternative start site, but the 103 amino acids in the N-terminal region are completely dispensable for axon death and contain no conserved domains (Figure 4.1).

While we had strong genetic evidence that *axed* dysfunction was responsible for our phenotype, whole genome sequencing using NGS technology failed any chromosomal anomalies in the *CG8398* region. This could be due to low depth of sequencing coverage, miscalls of nucleotide variants or deletions compared to the reference genome, or complex rearrangements that are difficult to assemble with available software. Thus, we used focused Sanger sequencing identify a 16bp deletion in the 3rd exon of *CG8398*, in $axed^{0011}$, yet we still could not detect a causative mutation in the sequence of $axed^{2094}$. The 16bp deletion is exactly the type of small indel mutation that alignment-based software struggles to detect with NGS, while the Sanger method is more reliable due to longer sequencing reads (Abel and Duncavage, 2013). It might be plausible to assume the mutation affecting $axed^{2094}$ may alter a distant regulatory region, since, both Sanger and NGS failed to detect any mutation within *axed* coding regions. In

the future, we may return to whole genome sequencing data with new algorithms to detect indels in *axed*^{2094} or assess expression levels of Axed in this mutant, however between genetic rescue and generation of new alleles, we were confident loss of function mutations in *axed* were responsible for the lack of axon degeneration after injury.

We also attempted to target BTBD2, the closest mammalian homolog of *axed*, using lentivirus delivered short hairpin RNA knockdown in axotomized mammalian dorsal root ganglia neuron culture, but failed to confirm sufficient knockdown (data not in thesis). In addition, collaborators tried similar knock-down strategies as well as testing *BTBD2* knockouts generated with CRISPR/Cas9 with mixed results that failed upon repetition (Nick Hertz, Tessier-Lavigne Lab). It's possible that loss of BTBD2 function is compensated by closely related proteins BTBD3, BTBD6 or BTBD1. I also tried the reverse, but failed in an attempt to rescue degeneration in *axed* null clones with murine BTBD2. It is possible that BTBD2 is too structurally diverged from Axed for rescue, however a follow up failed to detect strong expression of BTBD2 with antibody staining (data not in thesis) which could be the result of technical issues such as non-optimized codons for *Drosophila* or lack of intron for splicing to enhance expression (Le Hir et al., 2003; Powell and Dion, 2015). If the former is the case, the negative result may still be informative by comparing structures between Axed and BTBD2. Notably, the BTBD2 includes a PHR/Hiw-like domain that is not present in Axed. PHR domains can interact with a variety of protein species (Grill et al., 2016) and may have evolved some regulatory mechanism in mammalian BTBD2, possibly hindering its function in *Drosophila*.

While the mammalian experiments above aimed primarily to demonstrate conservation, we also hoped to utilize a neuronal cell culture system to assess metabolic state and cytoskeletal structural integrity of axons after injury using a variety of markers, which we are unfortunately unable to assess in *Drosophila*. These culture systems allow for the axotomy of a large swath of axons, which can be collected over various time points and subjected to biochemical analyses. If we successfully knocked out Axed's mammalian equivalent (Axed^{m}) in this system, we would have assessed following: 1) Cytoskeletal integrity by assessing neurofilament light, medium, and heavy chains as well microtubule markers such as β-tubulin class III; 2) metabolic state by measuring levels of NAD+ & ATP; 3) levels of Nmnat2; 4) phosphorylation status of MAPKs especially, pS257/T261-MKK4 & pT183/Y185-JNK (Yang et al., 2015). We would expect severed neurons lacking an Axed homolog would definitely maintain cytoskeletal integrity, however the results of #2, 3, and 4 could vary and help to further define Axed^{m} function. For example, if ATP levels still decline in severed *axed^{m}* null axons, Axed^{m} may destroy axons similar to calpain induction and calcium inflow (Yang et al., 2013). It might be possible that Nmnat2 levels remain elevated in *axed^{m}* in contrast to *Sarm1* axons, possibly placing in a parallel pathway to Sarm1 action after injury (Gilley et al., 2015). Additionally, we could determine if Axed^{m} is regulating basal levels of Nmnat2 in a similar manner to Phr1 and MAPKs(Babetto et al., 2013; Walker et al., 2017). We could also attempt to determine an exact time point after axotomy when an Axed^{m} is required by packaging the protein in lentiviral-like particles and adding Axed^{m} back to *axed^{m}* null axons at different times points after injury (Gerdts et al., 2013). This

experiment would definitively allow us to place Axed^{m} function in the axon after injury and rule out a role regulating basal levels of Nmnat or other factors before injury. It is important to note that while these experiments would no doubt provide valuable mechanistic insight into Axed^{m}, phenotypes observed in *axed^{m}* null cell culture models may be substantially different than the observations *in vivo* due to cellular expression differences *in vitro* and lack unique exchange with the extracellular milieu including glia cells.

In order to gain insight into the function of Axed *in vivo*, we returned to *Drosophila* to visualize endogenous Axed protein. While our attempts to generate immunoreactive antibodies against Axed failed, we fluorescently tagged endogenous Axed using recombination mediated cassette exchange with *axed^{MI13270}* to create *axed$^{EGFP::FLAG}$*. As a back-up if Axed protein was expressed at exceedingly low levels, as seems to be the case with *dSarm*, we also generated a UAS controlled *axed::smGdP-cMyc*, although we must be careful interpreting data from this construct as protein overexpression commonly causes artificial localization patterns (Prelich, 2012). Available repositories for *Drosophila* expression analysis shows *axed* expression is favored in nervous tissue as well as gut, salivary gland, and very highly expressed in the testis (Broderick et al., 2014; Chintapalli et al., 2007; Hu et al., 2017). We observed robust expression of Axed$^{EGFP::FLAG}$ in *Drosophila* adult brains and in the larval ventral nerve cord (Figure 3.1-C/F). Axed was particularly enriched the neurite dense neuropil regions and did not co-localize with markers of astrocytes or cortex glia. BTBD2 and BTBD1 are similarly

expressed in mammalian neurons, but also expressed at lower levels in astrocytes, oligodendrocytes, and microglia (Zhang et al., 2014).

Since differentiating between dendritic and axonal arbors within the neuropil is challenging, we stained neuronal membranes with HRP to visualize axons in larval abdominal nerves and observed strong Axed expression (Figure 3.1-D). Axon targeting is also observed in Tdc2 positive neurons expressing Axed::smGdP-cMyc (Figure 3.1-E). We cannot observe $Axed^{EGFP::FLAG}$ within wing sensory neuron axons, however low level expression could be masked by observation through the thick auto-fluorescing cuticle. It is also possible that Axed might be more strongly located towards the distal synaptic ends of these long neurons within the thoracic ganglion and outside our field of view, since we also observed close association of Axed with synaptic markers in the larval neuropil (Figure 3.1-C). This close association to synapse may play a role in axon degeneration or have some unknown function, although to date, large scale screens to find determinants of synapse maintenance have not observed a role for *axed* or BTBD2 even after injury (Sieburth et al., 2005; Wishart et al., 2012). Both Hiw and Nmnat are also located in and around near synaptic compartments, and play roles in synapse formation and maintenance seemingly distinct from their roles in axon degeneration (Lauwers and Verstreken, 2013; Wan et al., 2000; Wu et al., 2005). In the future, examination of stereotyped larval neuromuscular junctions could uncover a role for Axed in synapse formation or maintenance.

Axed is also expressed in neuronal cell bodies, albeit excluded from neuronal nuclei, and patterning suggests an enrichment at the plasma membrane in both larval and adult

brains. This localization pattern is matched in Tdc2 positive neurons expressing Axed::smGdP-cMyc and notable that Axed is still excluded from neuronal nuclei even when overexpressed (Figure 3.1-E).). If we had found Axed located primarily in neuronal nuclei, we might more strongly consider the hypothesis that Axed is regulating basal levels of axon death pathway components, rather than acting in the axon post injury. This is not out of the realm of possibility as BTBD2/1/3 have described roles within the nucleus (Matsui et al., 2013; Xu et al., 2002). Additionally, we observe very similar punctate membrane localization when comparing Axed::smGdP-cMyc to membrane targeted myristoylated smGdP-cMyc (Figure 3.1.-E). Punctate patterning may be related to Axed packaging in vesicles for transport to axons, but further analysis is required such as co-staining for variety of specific vesicle markers. It would be interesting if Axed co-localized to vesicles harboring palmitoylated Nmnat, possibly hinting at role for Axed in Nmnat or NAD+ breakdown (Milde et al., 2013). We might also assess whether palmitoylation is also plays a role in localizing Axed to membranes as it also defines localization of Nmnat and DLK. In fact, Axed has three predicted palmitoylation sites at C442, C443, and C528 within the essential C-terminal region, while BTBD2 has two predicted sites at C363 and C364, with all sites located C-terminal to conserved BACK domain (Ren et al., 2008). Taken together, this evidence supports a cell-autonomous role for Axed within the axonal compartment axons after injury.

The key question remained, what does Axed do in an axon after injury? To address this question we ablated antennal cell bodies and found that $Axed^{EGFP::FLAG}$ signal significantly increased in antennal lobes from 4 to 6 hours post injury and returned to an

uninjured baseline by 24 hours. Increased signal at these time points is particularly of note since we have found that the majority of axons undergo explosive fragmentation after 4 post injury in multiple Drosophila neuron types (MacDonald et al., 2006; Neukomm et al., 2014; Rooney and Freeman, 2014; Xiong and Collins, 2012). The observed signal increase may arise for several reasons, not all with biological relevance. Since these axons are completely severed from their cell bodies, an actual increased level of Axed protein levels could be the result of either local translation or decreased turnover. Protein synthesis seems unlikely, as the energy intensive process would require ATP/GTP at the same time that levels are rapidly decreasing. This would be the first example of increased production of a pro-degenerative factor after an axon injury, in contrast to the auto-inhibited-to-activated strategy employed by dSarm/Sarm1 post injury. Interestingly, previous work has demonstrated that Sarm1 is upregulated in response to excitotoxic stress or viral infection and one study showed *axed* upregulation in gut epithelial cells by 1-2 fold after infection by several bacterial species (Broderick et al., 2014; Massoll et al., 2013; Mukherjee et al., 2013), although in these cases cells had transcriptional machinery intact.

It is also possible the increased $Axed^{EGFP::FLAG}$ signal is due to a relocalization or clustering of Axed. As noted previously, over-expression of Axed has no spontaneous degenerative effects, so some injury-induced cue must 'activate' its pro-degenerative function. It could be that activation requires a re-localization to some unknown organelle or intracellular complex that increases $Axed^{EGFP::FLAG}$ signal, however we could not resolve distinct clustering after injury. While localization to vesicular membranes plays a

role in neuroprotective ability and basal turnover of Nmnat2, active of relocalization after injury has not been described for Nmnat or for pro-degenerative axon death proteins (Gerdts et al., 2013; Milde et al., 2013). This is another case where large amounts of injured axonal material could be collected from a mammalian culture system at different time points, organellar compartments segregated and assessed for enrichment of Axed^{m}. It is also possible that Axed clustering is a byproduct of axons breaking down into condensed fragments. If Axed does relocate after injury, it will be necessary to determine if this is required for Axed pro-degenerative function in axons or an artifact of degeneration.

Discussion 5-5: The axon death pathway converges on Axed

We next sought to address how Axed genetically interacts with known axon death regulators, such as *dSarm*, *Nmnat*, *hiw*, and *MAPKs*. To do this we took several approaches to assess epistatic relationships among axon death components using null alleles, knock-down via RNAi, and overexpression of full length and gain of function proteins. Through the application of these techniques we demonstrated that Axed is absolutely required for spontaneous axon disintegration downstream of activated dSarm and loss of Nmnat (Figure 3.3/4/5/6/7). Either event causes rapid degeneration within days in wild type and *dsarm* null neurons, while *axed* null clones persist morphologically intact for well past the mean lifetime of the fly, 30 to 50 days. Amazingly, both events can be induced together in combination with injury and the vast majority of *axed* null axons persist for at least 7 days. Consistent with previous evidence Hiw play roles

upstream of both events and thus upstream of Axed function, likely regulating Nmnat turnover. Additionally, we find no essential role for MAPKs either after axotomy or after prodegenerative dSarm signaling, at least in *Drosophila* wing sensory neurons (Table 3.2). These findings clash with a number of proposed pathways of axon degeneration and also highlight possible conflicts when proposed conclusions cross between different models of axotomy and neuronal subtypes among *Drosophila* and mammal, both *in vitro* and *in vivo*.

Numerous labs have found a role for kinases, specifically MAPKs, in regulating axon death before and after injury. Studies have described pro-degenerative roles for Dlk, Mkk4, Mkk7, Jnk3 and a number of other weaker kinases as well as scaffolding molecules required for their function and pro-survival roles for Akt (Klinedinst et al., 2013; Rallis et al., 2010, 2013; Shin et al., 2012b; Wakatsuki et al., 2011; Walker et al., 2017; Yang et al., 2015). Outside of axon death, MAPK signaling cascades are required downstream of dSarm/Sarm1 in development and linker cell death and an obvious hypothesis would be to assume a similar signaling cascade occurs post injury (Chuang and Bargmann, 2005; Kinet et al., 2016). *Drosophila* have a single Jnk, *bsk*, and null alleles displayed no suppression of axon death after axotomy or dsarm$^{\Delta ARM}$ expression in sensory neurons. We saw similarly no protection in *Mkk4* and *hep*/*Mkk7* null alleles, however they may be functionally redundant and we were unable to test double nulls. This data conflicts with a proposed requirement for MAPK downstream of Sarm1 (Yang et al., 2015), although agrees with recent findings that MAPK aid in the regulation of basal levels of Nmnat/Nmnat2 (Walker et al., 2017). Walker et al. demonstrated altering

bsk by RNAi or expression of dominant negative directly leads to higher levels of Nmnat, but only when overexpressing HA tagged Nmnat (Walker et al., 2017). Absolute change in level of endogenous *Nmnat* may be not be sufficient for protection after injury or $dsarm^{\Delta ARM}$. Interestingly, constitutively active *hep* causes spontaneous neurodegeneration, which may result from increased Nmnat turnover (data not in thesis). They also showed MAPK alteration fails to affect progression of degeneration and energy deficit after gain of function Sarm1(Walker et al., 2017). Since we find no protective phenotype we are unable to describe a relationship to Axed and our data suggest MAPK signaling cascades likely play a non-essential role in axon death.

Degenerative dSarm signaling and loss of Nmnat remain central to the axon death pathway. The prevailing model in the field is that Nmnat2, by an unknown mechanism, keeps Sarm1 in an auto-inhibited state until injury eliminates Nmnat2 resupply from the cell soma to the distal axon (Gilley and Coleman, 2010; Gilley et al., 2015; Sasaki et al., 2016). Lack of new Nmnat2, combined with rapid Nmnat2 degradation, results in dSarm/Sarm1 activation in which dimerized TIR domains actively consume NAD+ (Gerdts et al., 2015; Sasaki et al., 2016; Summers et al., 2016; Yamagishi and Tessier-Lavigne, 2016). Accelerated NAD+ consumption cause local energy deficits likely from the breakdown of ATP production cycles that require NAD+/NADH redox reactions (Sasaki et al., 2016).

If we first consider that *dsarm* mutants delay degeneration induced by gradual Nmnat knock down by $Nmnat^{RNAi}$, but completely fail to attenuate rapid cell death when Nmnat is completely removed, it would seem like Nmnat is playing dual roles, both

upstream and downstream of dSarm. However, these data may still fit with the above model. For example, in the case of RNAi, it is possible that in wild type, Nmnat levels fall to a concentration that releases dSarm inhibition and then rapidly destroys axons, while in *dsarm* nulls, degeneration only takes place if local NAD+ concentrations cannot be replenished, since NAD+ is not actively consumed by dSarm. Degeneration is likely delayed in this case, especially since RNAi incompletely eliminates Nmnat. Conversely, complete loss of Nmnat causes degeneration in the absence of dSarm in contrast to mammals where Nmnat2$^{-/-}$ animals survive only in a Sarm1$^{-/-}$ background (Gilley et al., 2015). This may be due to the fact that *Drosophila* only have a single *Nmnat* to generate NAD+, while mammals have a nuclear, axonal or cytoplasmic, and mitochondrial Nmnat. Thus, mammalian Nmnat2 functions to inhibit Sarm1 and Nmnat2$^{-/-}$animals survive only when Sarm1 activity is eliminated, but Nmnat1/3 are enough to provide the cell with NAD+, especially within the mitochondria. Meanwhile, *Drosophila* neurons with no functional Nmnat enzymes simply perish due to the lack of NAD+ production, although we cannot definitely assess NAD+ levels. We attempted to generate a sensor for flies to assess steady state NAD+ levels, however it lacked the resolution to provide accurate measurement.

How then do *axed* null clones that survive with both supposed NAD+ consuming dSarm$^{\Delta ARM}$ activity and no intracellular Nmnat to provide NAD+? Since it is likely impossible for a cell to persist lacking NAD+, what scenarios preserve at least a modest amount NAD+ or conversely prevent rapid NAD+ consumption?

The most likely scenario might be that active dSarm requires Axed to deplete NAD+ or Axed itself depletes NAD+ downstream of dSarm. In this situation both 'loss of Nmnat activated' endogenous dSarm as well as constitutively active dSarm$^{\Delta ARM}$ do not consume NAD+ in absence of Axed. We could test this hypothesis with a construct, currently being injected into flies, to consume NAD+ on using an inducibly dimerizable Tankyrase1 (Tnk1) PARP domain to readily consume NAD+ on demand (Gerdts et al., 2015). If NAD+ loss drives degeneration, activating Tnk1-PARP domain should overcome protection afforded in *axed* mutants and phenocopy effects of dSarm$^{\Delta ARM}$ in wild type. If neurons still survive, NAD+ consumption is not driving degeneration or isn't sufficient for degeneration and Axed may be required for some other pro-degenerative downstream function, although this seems unlikely. Alternatively, we might also test whether dimerizable TIR domain from either mammals or *C. elegans* Sarm1/TIR-1 induce TIR specific NAD+ degradation in *Drosophila* Axed null background. If vastly different species TIR domains induce degeneration without Axed, it would support a model in which the TIR domain is responsible for NAD+ consumption. If they fail to elicit degeneration without Axed, we might attempt to define a physical interaction between Axed and TIR domains, or Axed acts itself as the NADase. Perhaps, Axed can consume NAD+ without dSarm and this explains why *Nmnat, dsarm* double null neurons degenerate, but *Nmnat, axed* double null neurons do not. How the structure of either Axed or dSarm or a combination of the two might consume NAD+ is still an open question and is further discussed.

It might also be possible that Axed is responsible for releasing NAD+ from axonal compartments not accessible to cytoplasmic dSarm consumption. A candidate compartment for this could be mitochondria with approximately 50% of the cellular NAD+ pool. Partial mitochondrial localization of Wld^{s} seems to grant it exceptional axon protective power and mPTP blockers offer modest delays in axon degeneration(Avery et al., 2012; Barrientos et al., 2011). A previous study in HEK293T cells also demonstrated that maintaining mitochondrial levels of NAD+ could delay overall cellular death even when both cytoplasmic and nuclear pools were depleted (Yang et al., 2007). Although unlikely, Axed might form a pore itself similar to the BTB tetramerisation domain in the potassium channel (Doyle et al., 1998; Stogios et al., 2005). Maybe the increase in $Axed^{EGFP::FLAG}$ signal after injury is due to a clustering at mitochondria or some other membrane and future experiment could test this hypothesis. We also might test this by targeting our NAD+ consumption construct to different cellular compartments. Curiously dSarm/Sarm1 has a mitochondrial localization sequence that is completely dispensable for axon death.

In these scenarios, it still remains to be determined how neurons are surviving with no internal NAD+ production since Hiw should still be actively destroying Nmnat in severed axons and no Nmnat is present in nulls. It is possible NAD+ could be imported either from the extracellular space or from glia via through $P2X_7$-gated channels. These channels are present and active in both neurons and glia, specifically astrocytes, and facilitate the transport of NAD+ and NADH across plasma membranes (Alano et al., 2010)(Lu et al., 2007). Even if $P2X_7$ channels are not responsible, others have

demonstrated that NAD+ can enter axons in culture so there is some structure to facilitate transfer (Araki et al., 2004; Wang et al., 2005). There are no homologs of $P2X_7$-gated channels in *Drosophila*, however channels within the degenerin/epithelial Na^+ channel superfamily may be functional equivalents (Fountain and Burnstock, 2009; Schwiebert et al., 2005). In the second situation, required NAD+ is sequestered in mitochondria away from dSarm consumption and neurons can be supplied with pyruvate abrogating the need for large pools of cytoplasmic NAD+, at least for glycolysis. Methyl pyruvate already has been shown to delay axon degeneration and pyruvate or lactate can be transferred from axons to glia via MCT2/1 channels (Bros et al., 2014; Fünfschilling et al., 2012; Yang et al., 2015).

One may also argue that Axed is required for Nmnat turnover before and after injury such as Hiw, but to a stronger degree, and *axed* nulls have exceedingly high levels of Nmnat. While we were unable to assess Nmnat levels in an Axed null background, this hypothesis seems unlikely since UPS disruptions cannot phenocopy Axed nulls, discussed in detail below, cannot suppress from active dSarm or loss of Nmnat. This matches proposed Hiw function in which nulls seem to only protect due the combination of higher baseline levels of Nmnat pre-injury and the eliminated turnover post injury, and provide no suppression of $dSarm^{\Delta ARM}$ or Nmnat loss induced degeneration.

Discussion 5-6: How does Axed precipitate axon death?

In addition to genetically positioning Axed within an axon death cascade, we also sought to address which Axed domains were absolutely required and if Axed required

other protein partners to execute pro-degenerative function. First, we assessed whether a series of *axed* deletion constructs could rescue wild type degeneration in severed null *axed* axons (Figure 4.1-A). We targeted the conserved BTB and BACK domains of *axed*, as well as the C-terminal region. Structural studies of other BTB proteins suggested that the BTB domain would be required for dimerization with another BTB domain, the BACK domain would be required to interact with a cullin E3 ligase via a '3 box', and the C-terminal region would impart substrate specificity (Canning et al., 2013; Zhuang et al., 2009). Consistent with structural evidence suggesting BTB dimer unites two CRL complexes to increase efficiency, we observed severed axons with Axed lacking the BTB domain could still undergo axon degeneration, but only half as well as full length Axed (Figure 4.1-D). Since we were unable to definitively define a '3-box' required for Cul3 binding, possibly located within the linker region between the BTB and BACK domains, the BTB and BACK deletion constructs may retain their interactions with a CRL complex and partially function. Axed lacking the BACK domain had very little function with only a 1 of 5 severed axon degenerating (Figure 4.1-E). Since it retains some function, $Axed^{\Delta BACK}$ may incorporate into the complex but fail to efficiently orient a substrate for ubiquitylation. Consistent with this hypothesis, we found that the proposed substrate binding region somewhere in the C-terminus is absolutely required for function (Figure 4.1-F). None of the constructs tested had any dominant axon protective phenotype and failed to alter the course of degeneration induced by $dSarm^{\Delta ARM}$ or loss of Nmnat (Figure 4.1-G/H).

Going forward with structural analysis it would be informative to determine if the linker region, possibly containing the cullin binding region, is required for all function. Also, if the C-terminus is actually binding a substrate required for axon survival, could overexpression of this region sequester a substrate away from ubiquitination and dominantly protect axons similar to the phenotype observed with mutations in the RING domain of *hiw* (Neukomm et al., 2014; Xiong et al., 2012). If so, we might be able to identify the substrate by crosslinking followed by affinity purification and mass spectrometry techniques (Jüschke and Knoblich, 2008). Determining protein interactions in *Drosophila in vivo* in cell types of interest, namely adult neurons, is challenging because of the required starting material. I therefore tried to find binding partners with an unbiased yeast two hybrid assay. I identified Cul3 in a yeast two hybrid screen for protein-protein interactions with mouse BTBD2, however failed to detect any interaction in using *Drosophila* counterparts (data not presented in this thesis). In the future we could attempt to confirm these interactions in mammalian tissue using immunoprecipitation or antibody-bound column purification.

Based on the this data and several previous studies describing functional interactions between BTB domain containing proteins and Cul3, along with the linker cell death pathway in *C. elegans* which requires *axed* homolog BTBD2 downstream of *dsarm* homolog TIR-1, we hypothesized *axed* would interact with Cullin 3 in a CRL complex to ubiquitinate a target, possibly for degradation by the proteasome (Kinet et al., 2016; Pintard et al., 2004). We therefore tested loss of function mutants or deletions of the CRL complex components, anticipating that those utilized by Axed would phenocopy

axed mutant alleles and preserve axons after axotomy and dsarm$^{\Delta ARM}$ expression. Unfortunately, *cul3* mutant alleles were wild type for axon death and could not suppress dsarm$^{\Delta ARM}$ induced death. We did not test for suppression of death induced by Nmnat loss due to constraints governing the genetic tools available. We also tested other cullins (*cul1, cul4, cul5, cul6, CG11261*) and CRL components such as the RING box *regulators of cullins* (*Roc1a, Roc1b*), the E1 *uba1*, the ubiquitin conjugating E2 *eff*, a deficiency uncovering E3 ligase *sina*/*siah*, and the CRL activator *Nedd8* (Table 4.1) (Kinet et al., 2016; Zhuang et al., 2009). None suppressed death in our two assays. It is possible that we did not uncover any genes required for E3 CRL complex in our original screen or candidate screening in axotomy or after Sarm pro-degenerative signaling due to genetic redundancy in the fly. While this hypothesis is likely in the case of E1 and E2 proteins, this seems unlikely for the cullins and ring box proteins, as their evolved variations persisted primarily to enhance specificity. Going forward, additional candidates to be tested may be the TRIM family of ubiquitin E3 ligases based on their relationship to BTBD2 in mammals and protein interaction candidates from the yeast two hybrid screen.

Before continuing to test more candidate ubiquitin ligases, we wanted to determine if Axed actually worked with the ubiquitin-proteasome system. We reasoned that disruptions to the UPS should phenocopy Axed null mutations and protect axons after axotomy as well as from death induced by Nmnat loss or knockdown and dSarm$^{\Delta ARM}$ expression. To date, UPS inhibitors have, with few exceptions, only been tested models of axotomy with mixed, cell-type specific results (Yang et al., 2013; Zhai et al., 2003). In *Drosophila,* incorporation of dominant negative proteasomal subunits can

significantly increase Nmnat levels, but by only small amounts relative to the increase observed in *hiw* nulls, while countering global ubiquitination by overexpression of the yeast de-ubiquitinating enzyme UBP2 can strongly suppress axon death, but not death from loss of Nmnat (Xiong et al., 2012).

Therefore, I first tested whether severed axons with *UBP2* remained intact after injury. Consistent with previous evidence in larval nerves at 24h, axon death was suppressed and intact axons persisted until at least 7 dpa (Figure 4.2-B/C) (Xiong et al., 2012). Despite strongly suppressing axon death after injury, UBP2 failed to suppress death in Nmnat null clones after 5 days, but significantly delayed progression of degeneration (Figure 4.2D/E), matching observations that UBP2 could not suppress death induced by Nmnat-RNAi (Xiong et al., 2012). The delay in death might be attributed to significantly higher basal levels of Nmnat in neurons with UBP2 (Xiong et al., 2012), probably due to decreased turnover, and consistent with slight delay in death observed in *hiw* null clones expressing Nmnat-RNAi (Figure 3.4-D). While UBP2 delayed progression of death after loss of Nmnat, it showed no significant suppression or delay of degeneration induced by activated dSarm (Figure 4.2-F/G). It is possible that UBP2 cannot block degeneration downstream of dSarm or Nmnat because it is overwhelmed by massive up-regulation of ubiquitination processes during degenerative events, although to date, there is little direct evidence implicating a massive upregulation of UPS activity after axon injury or after pro-degenerative dSarm/Sarm1 signaling. To test this, it would be reasonable to simply transect axons *in vitro* or activate Sarm1 signaling, block the proteasome with a selective inhibitor such lactacystin, and assess the amount of ubiquitin

conjugated proteins. It might be possible to excise certain bands of interest and use mass spectrometry to identify these proteins. It is also possible that K48 ubiquitin chains, used primarily for recognition by the 26S proteasome, play outsized roles after injury signaling compared to K63 chains and no blockade is achieved because UBP2 preferentially targets K63 versus K48 ubiquitin chains (Kee et al., 2005). While this is possible, at high enough concentrations, UBP2 also deconstructs K48 chains, though UBP2 concentration present in neuronal clones *in vivo* is unknown (Kee et al., 2005). These experiments suggest that ubiquitination is not required beyond regulating baseline levels of Nmnat, as previously described (Brace et al., 2014; Xiong et al., 2012).

Since the ubiquitination process can affect other processes outside of protein turnover, we attempted to disrupt the proteasome core to determine if proteolysis is specifically required in axon degeneration. To do this we expressed proteasome inhibitor 31 kDa (PI31) (Bader et al., 2011) as well as temperature sensitive dominant negative β2 and β6 subunits of the of the 20S core particle of the protein. When shifted to 29°C the mutated subunits severely hamper the function of the proteasome as evidenced in the *Drosophila* eye and wing (Schweisguth, 1999; Velentzas et al., 2013). We would have expected to find at least some slight axon protection with double $\beta2^{ts}$ and $\beta6^{ts}$, due to previously demonstrated increased Nmnat levels (Xiong et al., 2012), however neither $\beta2^{ts}$, $\beta6^{ts}$, or PI31 could suppress axon death after axotomy, Nmnat loss, or and $dSarm^{\Delta ARM}$ expression. Interestingly this data aligns well with previous work showing Nmnat levels are only slightly higher after proteasome inhibition, but not as high as in UBP2 expression or loss of *hiw,* suggesting that Hiw may alter Nmnat with ubiquitin in

ways other than directing it to the proteasome (Xiong et al., 2012). It might be possible that ubiquitination alters cellular localization of Nmnat in a similar fashion to recently described palmitoylation events (Lau et al., 2010; Mayer et al., 2010; Milde et al., 2013). It is also possible that the proteasome wasn't fully incapacitated using these constructs, especially since expressing neither $\beta2^{ts}$ together with $\beta6^{ts}$ leads to more severe dysfunction in eye development compared to either alone (Velentzas et al., 2013), and axon death only requires little functional proteasome to proceed. To disrupt the proteasome more completely, we might try null clones or RNAi knockdown of the α5, β2 or β6 subunits of 20S core or the Rpn1, Rpn2, Rpn6 of the 19S cap. It remains to be seen if neuronal clones would be produced or how dysfunctional they might be without an active proteasome. Global dysfunction could mask any axon death phenotype and more specific targeting might be required.

Of note, co-expression of apoptotic inhibitor P35 with UBP2 was required to attenuate progressive spontaneous death in neurons (Figure 4.2-A), possibly similar to a degenerative phenotypes observed with UPS inhibition during wing and eye development (Hay et al., 1994; Velentzas et al., 2013), and suggesting that ubiquitin homeostasis in a mature neuron is required to avoid the activation of an apoptotic death program. However, other apoptotic inhibitors such as BclXL or Z-VAD-FMK, P35 had no effect on axon degeneration induced by axotomy, $dsarm^{\Delta ARM}$ expression, or Nmnat loss (Gerdts et al., 2013).

Taken together, these data argue that the UPS system is not required for axon degeneration to proceed downstream of activated dSarm or Nmnat-loss and any axon

protective phenotypes result from increased basal levels of Nmnat. The failure of proteasome perturbation to prevent death downstream of pro-degenerative dSarm signaling is not particularly surprising since proteasome assembly, activation, and enzymatic coupling requires ATP, levels of which drop precipitously after dSarm induction (Liu et al., 2006; Peth et al., 2013). We might actually expect proteasome function to decrease after dSarm induction as the 26S proteasome dissociates when bound ATP is removed (Liu et al., 2006). From an evolutionary standpoint it seems puzzling to utilize the proteasome to recycle protein components in a doomed axon rather than simply cleaving structural proteins as in the case of calpains in late stage axon fragmentation for later recycling by glia or caspases in programmed cell death (George et al., 1995; Yang et al., 2013). However, utilizing components other than caspases to other forms of non-apoptotic programmed cell death has been hypothesized to be an evolutionarily conserved back-up to apoptotic processes (Kutscher and Shaham, 2017). For example, possible compensation by non-apoptotic death programs enables some *bak/bax* double knockout mice to develop and survive to adulthood lacking all apoptotic activity (Kutscher and Shaham, 2017; Lindsten et al., 2000). One example of non-apoptotic death is linker cell death which requires proteasome activation and BTBD2 downstream of TIR-1, although we cannot find a role for the proteasome in downstream axon death process, in addition to finding no roles for genes in this pathway (Table 4.1) (Kinet et al., 2016). While it seems almost too coincidental to have two axon death genes participate in another pathway, Sarm1/dSarm/TIR-1 has demonstrated signaling in multiple contexts depending on the cellular environment and its possible Axed/BTBD2

may have other roles as well (Chuang and Bargmann, 2005; Murata et al., 2013; Panneerselvam et al., 2013; Shivers et al., 2009).

Since none of these experimental alterations to the UPS could phenocopy loss of Axed, we must then ask if Axed actually functions as an adaptor to ubiquitinate proteins in a CRL complex or with some other E3 ligase for degradation by the proteasome. While this hypothesis seems increasingly unlikely, we could attempt to assess ubiquitinated proteins species after overexpressing Axed while also blocking the proteasome. If Axed is required for the addition of ubiquitin to many different proteins we would expect to see a smear in a Western block stained for ubiquitin in Axed overexpressing cells. Ideally this experiment would be run in neurons and specifically axons. Although biochemical analyses like this are more amendable to a mammalian cell culture system than *Drosophila*. Also, Axed seems require some impetus for pro-degenerative function and carrying out the above experiment in axons challenged by injury or cellular stressors, such as activated Sarm1, could provide more valuable protein targets.

In light of the data above, we might abandon completely our hypothesis that Axed requires the UPS or CRL complexes and speculate as to the structural requirements for Axed to actively degrade NAD+, possibly in complex with dSarm. Recent work has proposed that Sarm1 directly consumes NAD+ through NADase activity of a Sarm-specific loop in the TIR domain, similar to the function of PARP1 in other forms of cell death, however definitive evidence such as activated Sarm1 directly interacting and destroying NAD+ in a minimal environment has yet to be demonstrated (Summers et al., 2016). Axed may have its own intrinsic NADase activity, possibly in the C-terminal

region, or works in tandem with dSarm, however no structural elements seem to suggest this and we have been unable to produce a gain of function Axed.

Discussion 5-7: Therapeutically Targeting Axon Death Components

Axons are primary therapeutic targets in peripheral neuropathies and traumatic brain injury, and possibly secondary targets in neurodegenerative diseases with axon dysfunction occurring before the onset of whole cell neuronal death such as Parkinson's disease (Geisler et al., 2016; Henninger et al., 2016; Meyer zu Horste et al., 2011). The ultimate goal of fully elucidating the entire axon death pathway is to logically target specific components in certain traumatic and neurodegenerative disease. In the manuscript describing Axed function, Lukas Neukomm, with Stefanie Hampel and Andrew Seeds, also demonstrated that severed axons are not only morphologically preserved in *axed*, *dsarm*, or *hiw* null backgrounds, but remain highly functional and integrated into complex circuits, confirming previous data showing severed Wld^{s} preserved axons can sustain evoked axon potentials weeks after injury (Lunn et al., 1989). This was achieved by expressing csChrimson in neurons controlling *Drosophila* grooming, performing axotomy by removing cell bodies in the antenna, and stimulating severed axons with red light to evoke a grooming response days and even weeks later (Hampel et al., 2015). These data suggest that therapies targeting the axon death pathway would retain not just cytoskeletal corpse, but a functional axon with preserved synaptic structure and integration.

Two obvious strategies emerge, either enhancing pro-survival Nmnat function or dampening the degenerative responses from molecules like Axed, Sarm1, Phr1, and a number of weaker players such as MAPKs, calpains, calcium channels, ROS formation and mPTP opening. It is worth noting that particular strategies to inhibit axon death may be successful in one condition, yet fail in another simply due to the environment in which degeneration is occurring and the side effects or delivery mechanisms of the treatment.

Axed may be a particularly good target, as it is required at a potential bottleneck in the pathway downstream of both pro-degenerative dSarm activity and Nmnat loss. We still do not know exactly how Axed elicits degeneration, so targeting specific structures is limited to targeting the C-terminal region, which is essential for function, or broadly knocking down expression of Axed's mammalian homolog. The interface between BTB domain homo- or hetero-dimerization could also provide an attractive druggable target, since the BTB/BACK domains play some role in function. Unfortunately, Axed may have multiple functionally redundant mammalian counterparts, BTBD2/1/3/6/etc. which may complicate targeting and also explain why it may have been missed mammalian screens for axon death components. It also remains to be determined what other roles BTBD2/1 may play in neurons when uninjured, especially in complex with TRIM5δ or TOPI (Xu et al., 2002, 2003).

Sarm1 is also an especially attractive to target for broad knock down of expression or domain specific inhibition. Sarm1 is auto-inhibited by its N-terminus by a physical interaction with its TIR domain, so therapeutics might be developed that mimic N-terminal inhibition or that target the unknown mechanism by which inhibition is

released (Summers et al., 2016). Also, since TIR domains must dimerize for destructive Sarm1 function, whether by pro-degenerative signaling or NADase activity, small molecules interfering with SAM or TIR domain dimerization should strongly inhibit axon death. While Sarm1 null mice survive into adulthood, they do have subtle alterations in neuronal morphology and immune response, so therapeutically targeting Sarm1 may have similar side effects (Chen et al., 2011; Lin and Hsueh, 2014; Lin et al., 2014a, 2014b). However, acute Sarm1 inhibitors could target degenerative TIR activity, which may be separable from TIR MAPK signaling and avoid off target side effects (Chen et al., 2011; Summers et al., 2016).

In contrast to inhibiting degenerative molecules, axon protection may be achieved through multiple strategies that enhance Nmnat production of NAD+. One method could be to increase overall levels of Nmnat2 by inhibiting the Phr1/Skp1a/Fbxo45 complex formation or its ability to position Nmnat2 for ubiquitination and subsequent degradation by the proteasome (Babetto et al., 2013; Yamagishi and Tessier-Lavigne, 2016). Broad application UPS inhibitors are probably not useful as they cause extensive dysregulation of protein homeostasis leading to neuronal dysfunction and death (McNaught et al., 2004; Velentzas et al., 2013; Vernon et al., 2010); also see UBP2 data. Another strategy to decrease Nmnat2 turnover may be to eliminate membrane attachment by increasing de-palmitoylated cytoplasmic form, possibly by increasing the activity of APT1/2 thioesterases, decreasing the activity of zDHHC family of palmitoyltransferases, or blocking Nmnat2 palmitoylation sites (Milde and Coleman, 2014; Milde et al., 2013). However, palmitoylation is also required for vesicular transport, so strategies would

somehow still allow Nmnat2 transport to occur while increasing cytosolic forms in the axonal compartment. It may be possible to introduce strongly protective forms of Nmnat by gene therapy or introducing protein directly using a nanoparticles or cell penetrating peptide delivery systems (Asteriti et al., 2015; Bolhassani et al., 2017). Since the ultimate goal is to increase NAD+, we can also attempt to provide Nmnat2 with excess NMN to convert NAD+. This can be achieved by supplementation with NR plus increased NRK1/2 activity or with increased activity of NAMPT. These manipulations protect axons *in vitro* and the small molecule P7C3 has demonstrated neuroprotective ability in a variety of contexts by activating NAMPT (Sasaki et al., 2016; Wang et al., 2014). The multiple strategies presented above provide hope that therapeutically preventing axon death should be feasible in the near future.

Discussion 5-8: Concluding Remarks:

This thesis has described the discovery of *Drosophila* BTB domain protein, Axed, as novel and essential component of injury induced axon death. Severed *axed* null axons remain intact for weeks *in vivo* and an equivalent suppression of axon degeneration axon is only observed *dSarm* and *hiw* null axons or after overexpression of Nmnat or Wld^{s}. Furthermore, we demonstrate a requirement for Axed downstream of pro-degenerative dSarm function as well as death induced by loss of Nmnat. This poses a potential conflict with a proposed mechanism in the field positing that an uninhibited dSarm/Sarm1 TIR domain actively depletes NAD+. Since Axed is required downstream of dSarm, either NAD+ depletion is not a driving force in degeneration or Axed is required, with or

without dSarm, to deplete NAD+. While additional study is required to elucidate the exact mechanism of Axed function, we have demonstrated the C-terminal region plays an essential, yet unknown role and the canonical BTB protein interaction with UPS is likely not involved in axon death downstream of dSarm or Nmnat loss. Future experiments will to clarify interactions governed by the C-terminal region and also definitively identify a mammalian homolog Axed, likely BTBD2. Once functionally defined in mammals, Axed, as well as other components such as Sarm1, will be an attractive therapeutic targets in diseases with axon degeneration and dysfunction.

References

Abel, H.J., and Duncavage, E.J. (2013). Detection of structural DNA variation from next generation sequencing data: a review of informatic approaches. Cancer Genet *206*, 432–440.

Alano, C.C., Garnier, P., Ying, W., Higashi, Y., Kauppinen, T.M., and Swanson, R.A. (2010). NAD+ depletion is necessary and sufficient for poly(ADP-ribose) polymerase-1-mediated neuronal death. J Neurosci *30*, 2967–2978.

Alobuia, W.M., Xia, W., and Vohra, B.P.S. (2013). Axon degeneration is key component of neuronal death in amyloid-β toxicity. Neurochem Int *63*, 782–789.

Anderson, K.V., and Nüsslein-Volhard, C. (1984). Information for the dorsal--ventral pattern of the Drosophila embryo is stored as maternal mRNA. Nature *311*, 223–227.

Araki, T., Sasaki, Y., and Milbrandt, J. (2004). Increased nuclear NAD biosynthesis and SIRT1 activation prevent axonal degeneration. Science *305*, 1010–1013.

Asteriti, S., Dal Cortivo, G., Pontelli, V., Cangiano, L., Buffelli, M., and Dell'Orco, D. (2015). Effective delivery of recombinant proteins to rod photoreceptors via lipid nanovesicles. Biochem Biophys Res Commun *461*, 665–670.

Avery, M.A., Sheehan, A.E., Kerr, K.S., Wang, J., and Freeman, M.R. (2009). Wld S requires Nmnat1 enzymatic activity and N16-VCP interactions to suppress Wallerian degeneration. J Cell Biol *184*, 501–513.

Avery, M.A., Rooney, T.M., Pandya, J.D., Wishart, T.M., Gillingwater, T.H., Geddes, J.W., Sullivan, P.G., and Freeman, M.R. (2012). WldS prevents axon degeneration through increased mitochondrial flux and enhanced mitochondrial Ca2+ buffering. Curr Biol *22*, 596–600.

Babetto, E., Beirowski, B., Janeckova, L., Brown, R., Gilley, J., Thomson, D., Ribchester, R.R., and Coleman, M.P. (2010). Targeting NMNAT1 to axons and synapses transforms its neuroprotective potency in vivo. J Neurosci *30*, 13291–13304.

Babetto, E., Beirowski, B., Russler, E.V., Milbrandt, J., and DiAntonio, A. (2013). The Phr1 ubiquitin ligase promotes injury-induced axon self-destruction. Cell Rep *3*, 1422–1429.

Bader, M., Benjamin, S., Wapinski, O.L., Smith, D.M., Goldberg, A.L., and Steller, H. (2011). A conserved F box regulatory complex controls proteasome activity in Drosophila. Cell *145*, 371–382.

Baker, R.T., Tobias, J.W., and Varshavsky, A. (1992). Ubiquitin-specific proteases of Saccharomyces cerevisiae. Cloning of UBP2 and UBP3, and functional analysis of the UBP gene family. J Biol Chem *267*, 23364–23375.

Baker, S.T., Opperman, K.J., Tulgren, E.D., Turgeon, S.M., Bienvenut, W., and Grill, B. (2014). RPM-1 uses both ubiquitin ligase and phosphatase-based mechanisms to regulate DLK-1 during neuronal development. PLoS Genet *10*, e1004297.

Ballinger, M.L., and Bittner, G.D. (1980). Ultrastructural studies of severed medial giant and other CNS axons in crayfish. Cell Tissue Res *208*, 123–133.

Banerjee, A., and Gerondakis, S. (2007). Coordinating TLR-activated signaling pathways in cells of the immune system. Immunol Cell Biol *85*, 420–424.
Barrientos, S.A., Martinez, N.W., Yoo, S., Jara, J.S., Zamorano, S., Hetz, C., Twiss, J.L., Alvarez, J., and Court, F.A. (2011). Axonal degeneration is mediated by the mitochondrial permeability transition pore. J Neurosci *31*, 966–978.
Bellen, H.J., Levis, R.W., Liao, G., He, Y., Carlson, J.W., Tsang, G., Evans-Holm, M., Hiesinger, P.R., Schulze, K.L., Rubin, G.M., et al. (2004). The BDGP gene disruption project: single transposon insertions associated with 40% of Drosophila genes. Genetics *167*, 761–781.
Belote, J.M., and Fortier, E. (2002). Targeted expression of dominant negative proteasome mutants in Drosophila melanogaster. Genesis *34*, 80–82.
Bennett, E.J., Rush, J., Gygi, S.P., and Harper, J.W. (2010). Dynamics of cullin-RING ubiquitin ligase network revealed by systematic quantitative proteomics. Cell *143*, 951–965.
Berbusse, G.W., Woods, L.C., Vohra, B.P.S., and Naylor, K. (2016). Mitochondrial Dynamics Decrease Prior to Axon Degeneration Induced by Vincristine and are Partially Rescued by Overexpressed cytNmnat1. Front Cell Neurosci *10*, 179.
Bergmann, A., Agapite, J., McCall, K., and Steller, H. (1998). The Drosophila gene hid is a direct molecular target of Ras-dependent survival signaling. Cell *95*, 331–341.
Bischof, J., Maeda, R.K., Hediger, M., Karch, F., and Basler, K. (2007). An optimized transgenesis system for Drosophila using germ-line-specific phiC31 integrases. Proc Natl Acad Sci U S A *104*, 3312–3317.
Bolhassani, A., Jafarzade, B.S., and Mardani, G. (2017). In vitro and in vivo delivery of therapeutic proteins using cell penetrating peptides. Peptides *87*, 50–63.
Bommel, H., Xie, G., Rossoll, W., Wiese, S., Jablonka, S., Boehm, T., and Sendtner, M. (2002). Missense mutation in the tubulin-specific chaperone E (Tbce) gene in the mouse mutant progressive motor neuronopathy, a model of human motoneuron disease. J Cell Biol *159*, 563–569.
Bomont, P., Cavalier, L., Blondeau, F., Ben Hamida, C., Belal, S., Tazir, M., Demir, E., Topaloglu, H., Korinthenberg, R., Tüysüz, B., et al. (2000). The gene encoding gigaxonin, a new member of the cytoskeletal BTB/kelch repeat family, is mutated in giant axonal neuropathy. Nat Genet *26*, 370–374.
Brace, E.J., Wu, C., Valakh, V., and DiAntonio, A. (2014). SkpA restrains synaptic terminal growth during development and promotes axonal degeneration following injury. J Neurosci *34*, 8398–8410.
Brand, A.H., and Perrimon, N. (1993). Targeted gene expression as a means of altering cell fates and generating dominant phenotypes. Development *118*, 401–415.
Broderick, N.A., Buchon, N., and Lemaitre, B. (2014). Microbiota-induced changes in drosophila melanogaster host gene expression and gut morphology. MBio *5*, e01117–14.

Bros, H., Millward, J.M., Paul, F., Niesner, R., and Infante-Duarte, C. (2014). Oxidative damage to mitochondria at the nodes of Ranvier precedes axon degeneration in ex vivo transected axons. Exp Neurol *261*, 127–135.
Buckmaster, E.A., Perry, V.H., and Brown, M.C. (1995). The rate of Wallerian degeneration in cultured neurons from wild type and C57BL/WldS mice depends on time in culture and may be extended in the presence of elevated K+ levels. Eur J Neurosci *7*, 1596–1602.
Campenot, R.B. (1977). Local control of neurite development by nerve growth factor. Proc Natl Acad Sci U S A *74*, 4516–4519.
Cancalon, P. (1982). Slow flow in axons detached from their perikarya. J Cell Biol *95*, 989–992.
Canning, P., Cooper, C.D.O., Krojer, T., Murray, J.W., Pike, A.C.W., Chaikuad, A., Keates, T., Thangaratnarajah, C., Hojzan, V., Ayinampudi, V., et al. (2013). Structural basis for Cul3 protein assembly with the BTB-Kelch family of E3 ubiquitin ligases. J Biol Chem *288*, 7803–7814.
Carlsson, E., Ding, J.L., and Byrne, B. (2016). SARM modulates MyD88-mediated TLR activation through BB-loop dependent TIR-TIR interactions. Biochim Biophys Acta *1863*, 244–253.
Carthew, R.W., and Rubin, G.M. (1990). seven in absentia, a gene required for specification of R7 cell fate in the Drosophila eye. Cell *63*, 561–577.
Chang, C., Hsieh, Y.-W., Lesch, B.J., Bargmann, C.I., and Chuang, C.-F. (2011). Microtubule-based localization of a synaptic calcium-signaling complex is required for left-right neuronal asymmetry in C. elegans. Development *138*, 3509–3518.
Chen, C.-Y., Lin, C.-W., Chang, C.-Y., Jiang, S.-T., and Hsueh, Y.-P. (2011). Sarm1, a negative regulator of innate immunity, interacts with syndecan-2 and regulates neuronal morphology. J Cell Biol *193*, 769–784.
Chintapalli, V.R., Wang, J., and Dow, J.A.T. (2007). Using FlyAtlas to identify better Drosophila melanogaster models of human disease. Nat Genet *39*, 715–720.
Cho-Park, P.F., and Steller, H. (2013). Proteasome regulation by ADP-ribosylation. Cell *153*, 614–627.
Chou, T.B., and Perrimon, N. (1996). The autosomal FLP-DFS technique for generating germline mosaics in Drosophila melanogaster. Genetics *144*, 1673–1679.
Chuang, C.-F., and Bargmann, C.I. (2005). A Toll-interleukin 1 repeat protein at the synapse specifies asymmetric odorant receptor expression via ASK1 MAPKKK signaling. Genes Dev *19*, 270–281.
Chung, T., Park, J.S., Kim, S., Montes, N., Walston, J., and Höke, A. (2016). Evidence for dying-back axonal degeneration in age-associated skeletal muscle decline. Muscle Nerve.
Cole, S.H., Carney, G.E., McClung, C.A., Willard, S.S., Taylor, B.J., and Hirsh, J. (2005). Two functional but noncomplementing Drosophila tyrosine decarboxylase genes:

distinct roles for neural tyramine and octopamine in female fertility. J Biol Chem *280*, 14948–14955.
Coleman, M.P., and Perry, V.H. (2002). Axon pathology in neurological disease: a neglected therapeutic target. Trends Neurosci *25*, 532–537.
Collins, C.A., Wairkar, Y.P., Johnson, S.L., and DiAntonio, A. (2006). Highwire restrains synaptic growth by attenuating a MAP kinase signal. Neuron *51*, 57–69.
Conforti, L., Wilbrey, A., Morreale, G., Janeckova, L., Beirowski, B., Adalbert, R., Mazzola, F., Di Stefano, M., Hartley, R., Babetto, E., et al. (2009). Wld S protein requires Nmnat activity and a short N-terminal sequence to protect axons in mice. J Cell Biol *184*, 491–500.
Conforti, L., Gilley, J., and Coleman, M.P. (2014). Wallerian degeneration: an emerging axon death pathway linking injury and disease. Nat Rev Neurosci *15*, 394–409.
Cook, R.K., Deal, M.E., Deal, J.A., Garton, R.D., Brown, C.A., Ward, M.E., Andrade, R.S., Spana, E.P., Kaufman, T.C., and Cook, K.R. (2010). A new resource for characterizing X-linked genes in Drosophila melanogaster: systematic coverage and subdivision of the X chromosome with nested, Y-linked duplications. Genetics *186*, 1095–1109.
Cook, R.K., Christensen, S.J., Deal, J.A., Coburn, R.A., Deal, M.E., Gresens, J.M., Kaufman, T.C., and Cook, K.R. (2012). The generation of chromosomal deletions to provide extensive coverage and subdivision of the Drosophila melanogaster genome. Genome Biol *13*, R21.
Coutinho-Budd, J., and Freeman, M.R. (2013). Probing the enigma: unraveling glial cell biology in invertebrates. Curr Opin Neurobiol *23*, 1073–1079.
Cusack, C.L., Swahari, V., Hampton Henley, W., Michael Ramsey, J., and Deshmukh, M. (2013). Distinct pathways mediate axon degeneration during apoptosis and axon-specific pruning. Nat Commun *4*, 1876.
Davis, C.O., Kim, K.-Y., Bushong, E.A., Mills, E.A., Boassa, D., Shih, T., Kinebuchi, M., Phan, S., Zhou, Y., Bihlmeyer, N.A., et al. (2014). Transcellular degradation of axonal mitochondria. Proc Natl Acad Sci U S A *111*, 9633–9638.
Dietzl, G., Chen, D., Schnorrer, F., Su, K.-C., Barinova, Y., Fellner, M., Gasser, B., Kinsey, K., Oppel, S., Scheiblauer, S., et al. (2007). A genome-wide transgenic RNAi library for conditional gene inactivation in Drosophila. Nature *448*, 151–156.
Dikranian, K., Cohen, R., Mac Donald, C., Pan, Y., Brakefield, D., Bayly, P., and Parsadanian, A. (2008). Mild traumatic brain injury to the infant mouse causes robust white matter axonal degeneration which precedes apoptotic death of cortical and thalamic neurons. Exp Neurol *211*, 551–560.
Dobritsa, A.A., van der Goes van Naters, W., Warr, C.G., Steinbrecht, R.A., and Carlson, J.R. (2003). Integrating the molecular and cellular basis of odor coding in the Drosophila antenna. Neuron *37*, 827–841.

Donaldson, T.D., Noureddine, M.A., Reynolds, P.J., Bradford, W., and Duronio, R.J. (2004). Targeted disruption of Drosophila Roc1b reveals functional differences in the Roc subunit of Cullin-dependent E3 ubiquitin ligases. Mol Biol Cell *15*, 4892–4903.
Doyle, D.A., Morais Cabral, J., Pfuetzner, R.A., Kuo, A., Gulbis, J.M., Cohen, S.L., Chait, B.T., and MacKinnon, R. (1998). The structure of the potassium channel: molecular basis of K+ conduction and selectivity. Science *280*, 69–77.
Errington, W.J., Khan, M.Q., Bueler, S.A., Rubinstein, J.L., Chakrabartty, A., and Privé, G.G. (2012). Adaptor protein self-assembly drives the control of a cullin-RING ubiquitin ligase. Structure *20*, 1141–1153.
Fang, Y., Soares, L., Teng, X., Geary, M., and Bonini, N.M. (2012). A novel Drosophila model of nerve injury reveals an essential role of Nmnat in maintaining axonal integrity. Curr Biol *22*, 590–595.
Fauvarque, M.-O., Laurenti, P., Boivin, A., Bloyer, S., Griffin-Shea, R., Bourbon, H.-M., and Dura, J.-M. (2001). Dominant modifiers of the polyhomeotic extra-sex-combs phenotype induced by marked P element insertional mutagenesis in Drosophila. Genet Res (Camb) *78*.
Finn, J.T., Weil, M., Archer, F., Siman, R., Srinivasan, A., and Raff, M.C. (2000). Evidence that Wallerian degeneration and localized axon degeneration induced by local neurotrophin deprivation do not involve caspases. J Neurosci *20*, 1333–1341.
Fountain, S.J., and Burnstock, G. (2009). An evolutionary history of P2X receptors. Purinergic Signal *5*, 269–272.
Frühbeis, C., Fröhlich, D., Kuo, W.P., and Krämer-Albers, E.-M. (2013). Extracellular vesicles as mediators of neuron-glia communication. Front Cell Neurosci *7*, 182.
Fünfschilling, U., Supplie, L.M., Mahad, D., Boretius, S., Saab, A.S., Edgar, J., Brinkmann, B.G., Kassmann, C.M., Tzvetanova, I.D., Möbius, W., et al. (2012). Glycolytic oligodendrocytes maintain myelin and long-term axonal integrity. Nature *485*, 517–521.
Geisler, S., Doan, R.A., Strickland, A., Huang, X., Milbrandt, J., and DiAntonio, A. (2016). Prevention of vincristine-induced peripheral neuropathy by genetic deletion of SARM1 in mice. Brain *139*, 3092–3108.
George, E.B., Glass, J.D., and Griffin, J.W. (1995). Axotomy-induced axonal degeneration is mediated by calcium influx through ion-specific channels. J Neurosci *15*, 6445–6452.
Gerdts, J., Summers, D.W., Sasaki, Y., DiAntonio, A., and Milbrandt, J. (2013). Sarm1-mediated axon degeneration requires both SAM and TIR interactions. J Neurosci *33*, 13569–13580.
Gerdts, J., Brace, E.J., Sasaki, Y., DiAntonio, A., and Milbrandt, J. (2015). SARM1 activation triggers axon degeneration locally via NAD^+ destruction. Science *348*, 453–457.
Gilley, J., and Coleman, M.P. (2010). Endogenous Nmnat2 is an essential survival factor for maintenance of healthy axons. PLoS Biol *8*, e1000300.

Gilley, J., Orsomando, G., Nascimento-Ferreira, I., and Coleman, M.P. (2015). Absence of SARM1 rescues development and survival of NMNAT2-deficient axons. Cell Rep *10*, 1974–1981.
Gillingwater, T.H., Ingham, C.A., Parry, K.E., Wright, A.K., Haley, J.E., Wishart, T.M., Arbuthnott, G.W., and Ribchester, R.R. (2006). Delayed synaptic degeneration in the CNS of Wlds mice after cortical lesion. Brain *129*, 1546–1556.
Glass, J.D., Culver, D.G., Levey, A.I., and Nash, N.R. (2002). Very early activation of m-calpain in peripheral nerve during Wallerian degeneration. J Neurol Sci *196*, 9–20.
Glise, B., Bourbon, H., and Noselli, S. (1995). hemipterous encodes a novel Drosophila MAP kinase kinase, required for epithelial cell sheet movement. Cell *83*, 451–461.
Gonzalez, M.A., Van Booven, D., Hulme, W., Ulloa, R.H., Lebrigio, R.F.A., Osterloh, J., Logan, M., Freeman, M., and Zuchner, S. (2012). Whole Genome Sequencing and a New Bioinformatics Platform Allow for Rapid Gene Identification in D. melanogaster EMS Screens. Biology *1*, 766–777.
Grill, B., Murphey, R.K., and Borgen, M.A. (2016). The PHR proteins: intracellular signaling hubs in neuronal development and axon degeneration. Neural Dev *11*, 8.
Gyoneva, S., and Ransohoff, R.M. (2015). Inflammatory reaction after traumatic brain injury: therapeutic potential of targeting cell-cell communication by chemokines. Trends Pharmacol Sci *36*, 471–480.
Hampel, S., Franconville, R., Simpson, J.H., and Seeds, A.M. (2015). A neural command circuit for grooming movement control. Elife *4*, e08758.
Hay, B.A., Wolff, T., and Rubin, G.M. (1994). Expression of baculovirus P35 prevents cell death in Drosophila. Development *120*, 2121–2129.
Henninger, N., Bouley, J., Sikoglu, E.M., An, J., Moore, C.M., King, J.A., Bowser, R., Freeman, M.R., and Brown, R.H. (2016). Attenuated traumatic axonal injury and improved functional outcome after traumatic brain injury in mice lacking Sarm1. Brain *139*, 1094–1105.
Hicks, A.N., Lorenzetti, D., Gilley, J., Lu, B., Andersson, K.-E., Miligan, C., Overbeek, P.A., Oppenheim, R., and Bishop, C.E. (2012). Nicotinamide mononucleotide adenylyltransferase 2 (Nmnat2) regulates axon integrity in the mouse embryo. PLoS ONE *7*, e47869.
Le Hir, H., Nott, A., and Moore, M.J. (2003). How introns influence and enhance eukaryotic gene expression. Trends Biochem Sci *28*, 215–220.
Hoopfer, E.D., McLaughlin, T., Watts, R.J., Schuldiner, O., O'Leary, D.D.M., and Luo, L. (2006). Wlds protection distinguishes axon degeneration following injury from naturally occurring developmental pruning. Neuron *50*, 883–895.
Hou, Y.-J., Banerjee, R., Thomas, B., Nathan, C., García-Sastre, A., Ding, A., and Uccellini, M.B. (2013). SARM is required for neuronal injury and cytokine production in response to central nervous system viral infection. J Immunol *191*, 875–883.

Hu, J., Zacharek, S., He, Y.J., Lee, H., Shumway, S., Duronio, R.J., and Xiong, Y. (2008). WD40 protein FBW5 promotes ubiquitination of tumor suppressor TSC2 by DDB1-CUL4-ROC1 ligase. Genes Dev *22*, 866–871.
Hu, Y., Comjean, A., Perrimon, N., and Mohr, S.E. (2017). The Drosophila Gene Expression Tool (DGET) for expression analyses. BMC Bioinformatics *18*, 98.
Joseph, B.S. (1973). Somatofugal events in Wallerian degeneration: a conceptual overview. Brain Res *59*, 1–18.
Jüschke, C., and Knoblich, J.A. (2008). Purification of Drosophila protein complexes for mass spectrometry. Methods Mol Biol *420*, 347–358.
Kee, Y., Lyon, N., and Huibregtse, J.M. (2005). The Rsp5 ubiquitin ligase is coupled to and antagonized by the Ubp2 deubiquitinating enzyme. EMBO J *24*, 2414–2424.
Kerckhove, N., Collin, A., Condé, S., Chaleteix, C., Pezet, D., and Balayssac, D. (2017). Long-Term Effects, Pathophysiological Mechanisms, and Risk Factors of Chemotherapy-Induced Peripheral Neuropathies: A Comprehensive Literature Review. Frontiers in Pharmacology *8*, 86.
Khurana, B., Zhuang, L., Moitra, P.K., Stantchev, T.S., Broder, C.C., Cutler, M.L., and D'Arpa, P. (2010). Human TOP1 residues implicated in species specificity of HIV-1 infection are required for interaction with BTBD2, and RNAi of BTBD2 in old world monkey and human cells increases permissiveness to HIV-1 infection. Virol J *7*, 332.
Kinet, M.J., Malin, J.A., Abraham, M.C., Blum, E.S., Silverman, M.R., Lu, Y., and Shaham, S. (2016). HSF-1 activates the ubiquitin proteasome system to promote non-apoptotic developmental cell death in C. elegans. Elife *5*.
Klinedinst, S., Wang, X., Xiong, X., Haenfler, J.M., and Collins, C.A. (2013). Independent pathways downstream of the Wnd/DLK MAPKKK regulate synaptic structure, axonal transport, and injury signaling. J Neurosci *33*, 12764–12778.
Knöferle, J., Koch, J.C., Ostendorf, T., Michel, U., Planchamp, V., Vutova, P., Tönges, L., Stadelmann, C., Brück, W., Bähr, M., et al. (2010). Mechanisms of acute axonal degeneration in the optic nerve in vivo. Proc Natl Acad Sci U S A *107*, 6064–6069.
Kreusch, A., Pfaffinger, P.J., Stevens, C.F., and Choe, S. (1998). Crystal structure of the tetramerization domain of the Shaker potassium channel. Nature *392*, 945–948.
Kutscher, L.M., and Shaham, S. (2017). Non-apoptotic cell death in animal development. Cell Death Differ.
Laser, H., Conforti, L., Morreale, G., Mack, T.G.M., Heyer, M., Haley, J.E., Wishart, T.M., Beirowski, B., Walker, S.A., Haase, G., et al. (2006). The slow Wallerian degeneration protein, WldS, binds directly to VCP/p97 and partially redistributes it within the nucleus. Mol Biol Cell *17*, 1075–1084.
Lau, C., Dölle, C., Gossmann, T.I., Agledal, L., Niere, M., and Ziegler, M. (2010). Isoform-specific targeting and interaction domains in human nicotinamide mononucleotide adenylyltransferases. J Biol Chem *285*, 18868–18876.
Lauwers, E., and Verstreken, P. (2013). Chaperoning the synapse--NMNAT protects Bruchpilot from crashing. EMBO Rep *14*, 5–6.

Lázár, O. (1980). Long-term persistence, after eye-removal, of unmyelinated fibres in the frog visual pathway. Brain Res *199*, 219–224.
Lee, T., and Luo, L. (2001). Mosaic analysis with a repressible cell marker (MARCM) for Drosophila neural development. Trends Neurosci *24*, 251–254.
Lee, T., Winter, C., Marticke, S.S., Lee, A., and Luo, L. (2000). Essential roles of Drosophila RhoA in the regulation of neuroblast proliferation and dendritic but not axonal morphogenesis. Neuron *25*, 307–316.
LeMosy, E.K., and Hashimoto, C. (2000). The nudel protease of Drosophila is required for eggshell biogenesis in addition to embryonic patterning. Dev Biol *217*, 352–361.
Lin, C.-W., and Hsueh, Y.-P. (2014). Sarm1, a neuronal inflammatory regulator, controls social interaction, associative memory and cognitive flexibility in mice. Brain Behav Immun *37*, 142–151.
Lin, D.M., and Goodman, C.S. (1994). Ectopic and increased expression of Fasciclin II alters motoneuron growth cone guidance. Neuron *13*, 507–523.
Lin, Y., and Wen, L. (2013). Inflammatory response following diffuse axonal injury. Int J Med Sci *10*, 515–521.
Lin, C.-W., Liu, H.-Y., Chen, C.-Y., and Hsueh, Y.-P. (2014a). Neuronally-expressed Sarm1 regulates expression of inflammatory and antiviral cytokines in brains. Innate Immun *20*, 161–172.
Lin, C.-W., Chen, C.-Y., Cheng, S.-J., Hu, H.-T., and Hsueh, Y.-P. (2014b). Sarm1 deficiency impairs synaptic function and leads to behavioral deficits, which can be ameliorated by an mGluR allosteric modulator. Front Cell Neurosci *8*, 87.
Lin, H.-C., Wu, J.-T., Tan, B.C.-M., and Chien, C.-T. (2009). Cul4 and DDB1 regulate Orc2 localization, BrdU incorporation and Dup stability during gene amplification in Drosophila follicle cells. J Cell Sci *122*, 2393–2401.
Lindsten, T., Ross, A.J., King, A., Zong, W.X., Rathmell, J.C., Shiels, H.A., Ulrich, E., Waymire, K.G., Mahar, P., Frauwirth, K., et al. (2000). The combined functions of proapoptotic Bcl-2 family members bak and bax are essential for normal development of multiple tissues. Mol Cell *6*, 1389–1399.
Liu, C.-W., Li, X., Thompson, D., Wooding, K., Chang, T., Tang, Z., Yu, H., Thomas, P.J., and DeMartino, G.N. (2006). ATP binding and ATP hydrolysis play distinct roles in the function of 26S proteasome. Mol Cell *24*, 39–50.
Liu, H.-Y., Chen, C.-Y., and Hsueh, Y.-P. (2014). Innate immune responses regulate morphogenesis and degeneration: roles of Toll-like receptors and Sarm1 in neurons. Neurosci Bull *30*, 645–654.
Loreto, A., Di Stefano, M., Gering, M., and Conforti, L. (2015). Wallerian Degeneration Is Executed by an NMN-SARM1-Dependent Late Ca(2+) Influx but Only Modestly Influenced by Mitochondria. Cell Rep *13*, 2539–2552.
Lu, H., Burns, D., Garnier, P., Wei, G., Zhu, K., and Ying, W. (2007). P2X7 receptors mediate NADH transport across the plasma membranes of astrocytes. Biochem Biophys Res Commun *362*, 946–950.

Lunn, E.R., Perry, V.H., Brown, M.C., Rosen, H., and Gordon, S. (1989). Absence of Wallerian Degeneration does not Hinder Regeneration in Peripheral Nerve. Eur J Neurosci *1*, 27–33.
Ma, M., Ferguson, T.A., Schoch, K.M., Li, J., Qian, Y., Shofer, F.S., Saatman, K.E., and Neumar, R.W. (2013). Calpains mediate axonal cytoskeleton disintegration during Wallerian degeneration. Neurobiol Dis *56*, 34–46.
MacDonald, J.M., Beach, M.G., Porpiglia, E., Sheehan, A.E., Watts, R.J., and Freeman, M.R. (2006). The Drosophila cell corpse engulfment receptor Draper mediates glial clearance of severed axons. Neuron *50*, 869–881.
Mack, T.G., Reiner, M., Beirowski, B., Mi, W., Emanuelli, M., Wagner, D., Thomson, D., Gillingwater, T., Court, F., Conforti, L., et al. (2001). Wallerian degeneration of injured axons and synapses is delayed by a Ube4b/Nmnat chimeric gene. Nat Neurosci *4*, 1199–1206.
Mahr, A., and Aberle, H. (2006). The expression pattern of the Drosophila vesicular glutamate transporter: a marker protein for motoneurons and glutamatergic centers in the brain. Gene Expr Patterns *6*, 299–309.
Massoll, C., Mando, W., and Chintala, S.K. (2013). Excitotoxicity upregulates SARM1 protein expression and promotes Wallerian-like degeneration of retinal ganglion cells and their axons. Invest Ophthalmol Vis Sci *54*, 2771–2780.
Matsui, A., Tran, M., Yoshida, A.C., Kikuchi, S.S., U, M., Ogawa, M., and Shimogori, T. (2013). BTBD3 controls dendrite orientation toward active axons in mammalian neocortex. Science *342*, 1114–1118.
Matsumoto, D.E., and Scalia, F. (1981). Long-term survival of centrally projecting axons in the optic nerve of the frog following destruction of the retina. J Comp Neurol *202*, 135–155.
Mayer, P.R., Huang, N., Dewey, C.M., Dries, D.R., Zhang, H., and Yu, G. (2010). Expression, localization, and biochemical characterization of nicotinamide mononucleotide adenylyltransferase 2. J Biol Chem *285*, 40387–40396.
McNaught, K.S.P., Perl, D.P., Brownell, A.-L., and Olanow, C.W. (2004). Systemic exposure to proteasome inhibitors causes a progressive model of Parkinson's disease. Ann Neurol *56*, 149–162.
Melnick, A., Ahmad, K.F., Arai, S., Polinger, A., Ball, H., Borden, K.L., Carlile, G.W., Prive, G.G., and Licht, J.D. (2000). In-depth mutational analysis of the promyelocytic leukemia zinc finger BTB/POZ domain reveals motifs and residues required for biological and transcriptional functions. Mol Cell Biol *20*, 6550–6567.
Melom, J.E., and Littleton, J.T. (2013). Mutation of a NCKX eliminates glial microdomain calcium oscillations and enhances seizure susceptibility. J Neurosci *33*, 1169–1178.
Meng, L., Mohan, R., Kwok, B.H., Elofsson, M., Sin, N., and Crews, C.M. (1999). Epoxomicin, a potent and selective proteasome inhibitor, exhibits in vivo antiinflammatory activity. Proc Natl Acad Sci U S A *96*, 10403–10408.

Metaxakis, A., Oehler, S., Klinakis, A., and Savakis, C. (2005). Minos as a genetic and genomic tool in Drosophila melanogaster. Genetics *171*, 571–581.
Meyer zu Horste, G., Miesbach, T.A., Muller, J.I., Fledrich, R., Stassart, R.M., Kieseier, B.C., Coleman, M.P., and Sereda, M.W. (2011). The Wlds transgene reduces axon loss in a Charcot-Marie-Tooth disease 1A rat model and nicotinamide delays post-traumatic axonal degeneration. Neurobiol Dis *42*, 1–8.
Milde, S., and Coleman, M.P. (2014). Identification of palmitoyltransferase and thioesterase enzymes that control the subcellular localization of axon survival factor nicotinamide mononucleotide adenylyltransferase 2 (NMNAT2). J Biol Chem *289*, 32858–32870.
Milde, S., Gilley, J., and Coleman, M.P. (2013). Subcellular localization determines the stability and axon protective capacity of axon survival factor Nmnat2. PLoS Biol *11*, e1001539.
Miller, B.R., Press, C., Daniels, R.W., Sasaki, Y., Milbrandt, J., and DiAntonio, A. (2009). A dual leucine kinase-dependent axon self-destruction program promotes Wallerian degeneration. Nat Neurosci *12*, 387–389.
Mistry, H., Wilson, B.A., Roberts, I.J.H., O'Kane, C.J., and Skeath, J.B. (2004). Cullin-3 regulates pattern formation, external sensory organ development and cell survival during Drosophila development. Mech Dev *121*, 1495–1507.
Morii, H., Shiraishi-Yamaguchi, Y., and Mori, N. (2006). SCG10, a microtubule destabilizing factor, stimulates the neurite outgrowth by modulating microtubule dynamics in rat hippocampal primary cultured neurons. J Neurobiol *66*, 1101–1114.
Mukherjee, P., Woods, T.A., Moore, R.A., and Peterson, K.E. (2013). Activation of the innate signaling molecule MAVS by bunyavirus infection upregulates the adaptor protein SARM1, leading to neuronal death. Immunity *38*, 705–716.
Murata, H., Sakaguchi, M., Kataoka, K., and Huh, N.-H. (2013). SARM1 and TRAF6 bind to and stabilize PINK1 on depolarized mitochondria. Mol Biol Cell *24*, 2772–2784.
Murray, M., and Edwards, M.A. (1982). A quantitative study of the reinnervation of the goldfish optic tectum following optic nerve crush. J Comp Neurol *209*, 363–373.
Muthukumar, A.K., Stork, T., and Freeman, M.R. (2014). Activity-dependent regulation of astrocyte GAT levels during synaptogenesis. Nat Neurosci *17*, 1340–1350.
Nern, A., Pfeiffer, B.D., and Rubin, G.M. (2015). Optimized tools for multicolor stochastic labeling reveal diverse stereotyped cell arrangements in the fly visual system. Proc Natl Acad Sci U S A *112*, E2967–76.
Neukomm, L.J., Burdett, T.C., Gonzalez, M.A., Züchner, S., and Freeman, M.R. (2014). Rapid in vivo forward genetic approach for identifying axon death genes in Drosophila. Proc Natl Acad Sci U S A *111*, 9965–9970.
Newsome, T.P., Asling, B., and Dickson, B.J. (2000). Analysis of Drosophila photoreceptor axon guidance in eye-specific mosaics. Development *127*, 851–860.

Noureddine, M.A., Donaldson, T.D., Thacker, S.A., and Duronio, R.J. (2002). Drosophila Roc1a encodes a RING-H2 protein with a unique function in processing the Hh signal transducer Ci by the SCF E3 ubiquitin ligase. Dev Cell *2*, 757–770.
O'Donnell, K.C., Vargas, M.E., and Sagasti, A. (2013). WldS and PGC-1α regulate mitochondrial transport and oxidation state after axonal injury. J Neurosci *33*, 14778–14790.
O'Neill, L.A.J., and Bowie, A.G. (2007). The family of five: TIR-domain-containing adaptors in Toll-like receptor signalling. Nat Rev Immunol *7*, 353–364.
Osterloh, J.M., Yang, J., Rooney, T.M., Fox, A.N., Adalbert, R., Powell, E.H., Sheehan, A.E., Avery, M.A., Hackett, R., Logan, M.A., et al. (2012). dSarm/Sarm1 is required for activation of an injury-induced axon death pathway. Science *337*, 481–484.
Ou, C.-Y., Lin, Y.-F., Chen, Y.-J., and Chien, C.-T. (2002). Distinct protein degradation mechanisms mediated by Cul1 and Cul3 controlling Ci stability in Drosophila eye development. Genes Dev *16*, 2403–2414.
Panneerselvam, P., Singh, L.P., Selvarajan, V., Chng, W.J., Ng, S.B., Tan, N.S., Ho, B., Chen, J., and Ding, J.L. (2013). T-cell death following immune activation is mediated by mitochondria-localized SARM. Cell Death Differ *20*, 478–489.
Parks, A.L., Cook, K.R., Belvin, M., Dompe, N.A., Fawcett, R., Huppert, K., Tan, L.R., Winter, C.G., Bogart, K.P., Deal, J.E., et al. (2004). Systematic generation of high-resolution deletion coverage of the Drosophila melanogaster genome. Nat Genet *36*, 288–292.
Perge, J.A., Niven, J.E., Mugnaini, E., Balasubramanian, V., and Sterling, P. (2012). Why do axons differ in caliber? J Neurosci *32*, 626–638.
Peth, A., Nathan, J.A., and Goldberg, A.L. (2013). The ATP costs and time required to degrade ubiquitinated proteins by the 26 S proteasome. J Biol Chem *288*, 29215–29222.
Pintard, L., Willems, A., and Peter, M. (2004). Cullin-based ubiquitin ligases: Cul3-BTB complexes join the family. EMBO J *23*, 1681–1687.
Polilov, A.A. (2012). The smallest insects evolve anucleate neurons. Arthropod Struct Dev *41*, 29–34.
Powell, J.R., and Dion, K. (2015). Effects of codon usage on gene expression: empirical studies on Drosophila. J Mol Evol *80*, 219–226.
Prelich, G. (2012). Gene overexpression: uses, mechanisms, and interpretation. Genetics *190*, 841–854.
Rallis, A., Moore, C., and Ng, J. (2010). Signal strength and signal duration define two distinct aspects of JNK-regulated axon stability. Dev Biol *339*, 65–77.
Rallis, A., Lu, B., and Ng, J. (2013). Molecular chaperones protect against JNK- and Nmnat-regulated axon degeneration in Drosophila. J Cell Sci *126*, 838–849.
Ratajczak, J., Joffraud, M., Trammell, S.A.J., Ras, R., Canela, N., Boutant, M., Kulkarni, S.S., Rodrigues, M., Redpath, P., Migaud, M.E., et al. (2016). NRK1 controls nicotinamide mononucleotide and nicotinamide riboside metabolism in mammalian cells. Nat Commun *7*, 13103.

Ren, J., Wen, L., Gao, X., Jin, C., Xue, Y., and Yao, X. (2008). CSS-Palm 2.0: an updated software for palmitoylation sites prediction. Protein Eng Des Sel *21*, 639–644.
Rongvaux, A., Andris, F., Van Gool, F., and Leo, O. (2003). Reconstructing eukaryotic NAD metabolism. Bioessays *25*, 683–690.
Rooney, T.M., and Freeman, M.R. (2014). Drosophila models of neuronal injury. ILAR J *54*, 291–295.
Roy, S., Hsiung, F., and Kornberg, T.B. (2011). Specificity of Drosophila cytonemes for distinct signaling pathways. Science *332*, 354–358.
Sasaki, Y., and Milbrandt, J. (2010). Axonal degeneration is blocked by nicotinamide mononucleotide adenylyltransferase (Nmnat) protein transduction into transected axons. J Biol Chem *285*, 41211–41215.
Sasaki, Y., Araki, T., and Milbrandt, J. (2006). Stimulation of nicotinamide adenine dinucleotide biosynthetic pathways delays axonal degeneration after axotomy. J Neurosci *26*, 8484–8491.
Sasaki, Y., Nakagawa, T., Mao, X., DiAntonio, A., and Milbrandt, J. (2016). NMNAT1 inhibits axon degeneration via blockade of SARM1-mediated NAD(+) depletion. Elife *5*.
Schlaepfer, W.W. (1974). Calcium-induced degeneration of axoplasm in isolated segments of rat peripheral nerve. Brain Res *69*, 203–215.
Schlaepfer, W.W. (1977). Structural alterations of peripheral nerve induced by the calcium ionophore A23187. Brain Res *136*, 1–9.
Schlaepfer, W.W., and Bunge, R.P. (1973). Effects of calcium ion concentration on the degeneration of amputated axons in tissue culture. J Cell Biol *59*, 456–470.
Schlaepfer, W.W., and Hasler, M.B. (1979). Characterization of the calcium-induced disruption of neurofilaments in rat peripheral nerve. Brain Res *168*, 299–309.
Schonrock, N., Humphreys, D.T., Preiss, T., and Götz, J. (2012). Target gene repression mediated by miRNAs miR-181c and miR-9 both of which are down-regulated by amyloid-β. J Mol Neurosci *46*, 324–335.
Schuldiner, O., Berdnik, D., Levy, J.M., Wu, J.S., Luginbuhl, D., Gontang, A.C., and Luo, L. (2008). piggyBac-based mosaic screen identifies a postmitotic function for cohesin in regulating developmental axon pruning. Dev Cell *14*, 227–238.
Schweiger, M., Hennig, K., Lerner, F., Niere, M., Hirsch-Kauffmann, M., Specht, T., Weise, C., Oei, S.L., and Ziegler, M. (2001). Characterization of recombinant human nicotinamide mononucleotide adenylyl transferase (NMNAT), a nuclear enzyme essential for NAD synthesis. FEBS Lett *492*, 95–100.
Schweisguth, F. (1999). Dominant-negative mutation in the beta2 and beta6 proteasome subunit genes affect alternative cell fate decisions in the Drosophila sense organ lineage. Proc Natl Acad Sci U S A *96*, 11382–11386.
Schwiebert, E.M., Liang, L., Cheng, N.-L., Williams, C.R., Olteanu, D., Welty, E.A., and Zsembery, A. (2005). Extracellular zinc and ATP-gated P2X receptor calcium entry channels: New zinc receptors as physiological sensors and therapeutic targets. Purinergic Signal *1*, 299–310.

Sebo, Z.L., Lee, H.B., Peng, Y., and Guo, Y. (2014). A simplified and efficient germline-specific CRISPR/Cas9 system for Drosophila genomic engineering. Fly (Austin) *8*, 52–57.
Shapira, S., Bakhrat, A., Bitan, A., and Abdu, U. (2011). The Drosophila javelin gene encodes a novel actin-associated protein required for actin assembly in the bristle. Mol Cell Biol *31*, 4582–4592.
Shin, J.E., and DiAntonio, A. (2011). Highwire regulates guidance of sister axons in the Drosophila mushroom body. J Neurosci *31*, 17689–17700.
Shin, J.E., Miller, B.R., Babetto, E., Cho, Y., Sasaki, Y., Qayum, S., Russler, E.V., Cavalli, V., Milbrandt, J., and DiAntonio, A. (2012a). SCG10 is a JNK target in the axonal degeneration pathway. Proc Natl Acad Sci U S A *109*, E3696–705.
Shin, J.E., Cho, Y., Beirowski, B., Milbrandt, J., Cavalli, V., and DiAntonio, A. (2012b). Dual leucine zipper kinase is required for retrograde injury signaling and axonal regeneration. Neuron *74*, 1015–1022.
Shivers, R., Kooistra, T., Chu, S., Pagano, D., and Kim, D. (2009). Tissue-Specific Activities of SARM-ASK1-MKK3 Signaling Coordinate Immunity and Behavior to Pathogenic and Nutritional Bacteria in C. elegans. Cell Host Microbe.
Sieburth, D., Ch'ng, Q., Dybbs, M., Tavazoie, M., Kennedy, S., Wang, D., Dupuy, D., Rual, J.-F., Hill, D.E., Vidal, M., et al. (2005). Systematic analysis of genes required for synapse structure and function. Nature *436*, 510–517.
Simon, D.J., Weimer, R.M., McLaughlin, T., Kallop, D., Stanger, K., Yang, J., O'Leary, D.D.M., Hannoush, R.N., and Tessier-Lavigne, M. (2012). A caspase cascade regulating developmental axon degeneration. J Neurosci *32*, 17540–17553.
Sluss, H.K., Han, Z., Barrett, T., Goberdhan, D.C., Wilson, C., Davis, R.J., and Ip, Y.T. (1996). A JNK signal transduction pathway that mediates morphogenesis and an immune response in Drosophila. Genes Dev *10*, 2745–2758.
Smith, D.H. (2009). Stretch growth of integrated axon tracts: extremes and exploitations. Prog Neurobiol *89*, 231–239.
Soltysik-Espanola, M., Rogers, R.A., Jiang, S., Kim, T.A., Gaedigk, R., White, R.A., Avraham, H., and Avraham, S. (1999). Characterization of Mayven, a novel actin-binding protein predominantly expressed in brain. Mol Biol Cell *10*, 2361–2375.
Spradling, A.C., Stern, D., Beaton, A., Rhem, E.J., Laverty, T., Mozden, N., Misra, S., and Rubin, G.M. (1999). The Berkeley Drosophila Genome Project gene disruption project: Single P-element insertions mutating 25% of vital Drosophila genes. Genetics *153*, 135–177.
Srivastava, S. (2016). Emerging therapeutic roles for NAD(+) metabolism in mitochondrial and age-related disorders. Clinical and Translational Medicine *5*, 25.
St Johnston, D. (2002). The art and design of genetic screens: Drosophila melanogaster. Nat Rev Genet *3*, 176–188.
Di Stefano, M., Nascimento-Ferreira, I., Orsomando, G., Mori, V., Gilley, J., Brown, R., Janeckova, L., Vargas, M.E., Worrell, L.A., Loreto, A., et al. (2015). A rise in NAD

precursor nicotinamide mononucleotide (NMN) after injury promotes axon degeneration. Cell Death Differ *22*, 731–742.
Stein, L.R., and Imai, S. (2012). The dynamic regulation of NAD metabolism in mitochondria. Trends Endocrinol Metab *23*, 420–428.
Stino, A.M., and Smith, A.G. (2017). Peripheral neuropathy in prediabetes and the metabolic syndrome. Journal of Diabetes Investigation.
Stogios, P.J., and Privé, G.G. (2004). The BACK domain in BTB-kelch proteins. Trends Biochem Sci *29*, 634–637.
Stogios, P.J., Downs, G.S., Jauhal, J.J.S., Nandra, S.K., and Privé, G.G. (2005). Sequence and structural analysis of BTB domain proteins. Genome Biol *6*, R82.
Stork, T., Sheehan, A., Tasdemir-Yilmaz, O.E., and Freeman, M.R. (2014). Neuron-glia interactions through the Heartless FGF receptor signaling pathway mediate morphogenesis of Drosophila astrocytes. Neuron *83*, 388–403.
Summers, D.W., DiAntonio, A., and Milbrandt, J. (2014). Mitochondrial dysfunction induces Sarm1-dependent cell death in sensory neurons. J Neurosci *34*, 9338–9350.
Summers, D.W., Gibson, D.A., DiAntonio, A., and Milbrandt, J. (2016). SARM1-specific motifs in the TIR domain enable NAD+ loss and regulate injury-induced SARM1 activation. Proc Natl Acad Sci U S A *113*, E6271–E6280.
T'Jampens, D., Devriendt, L., De Corte, V., Vandekerckhove, J., and Gettemans, J. (2002). Selected BTB/POZ-kelch proteins bind ATP. FEBS Lett *516*, 20–26.
Tasdemir-Yilmaz, O.E., and Freeman, M.R. (2014). Astrocytes engage unique molecular programs to engulf pruned neuronal debris from distinct subsets of neurons. Genes Dev *28*, 20–33.
Tazuke, S.I., Schulz, C., Gilboa, L., Fogarty, M., Mahowald, A.P., Guichet, A., Ephrussi, A., Wood, C.G., Lehmann, R., and Fuller, M.T. (2002). A germline-specific gap junction protein required for survival of differentiating early germ cells. Development *129*, 2529–2539.
Thibault, S.T., Singer, M.A., Miyazaki, W.Y., Milash, B., Dompe, N.A., Singh, C.M., Buchholz, R., Demsky, M., Fawcett, R., Francis-Lang, H.L., et al. (2004). A complementary transposon tool kit for Drosophila melanogaster using P and piggyBac. Nat Genet *36*, 283–287.
Vargas, M.E., Yamagishi, Y., Tessier-Lavigne, M., and Sagasti, A. (2015). Live Imaging of Calcium Dynamics during Axon Degeneration Reveals Two Functionally Distinct Phases of Calcium Influx. J Neurosci *35*, 15026–15038.
Velentzas, P.D., Velentzas, A.D., Pantazi, A.D., Mpakou, V.E., Zervas, C.G., Papassideri, I.S., and Stravopodis, D.J. (2013). Proteasome, but not autophagy, disruption results in severe eye and wing dysmorphia: a subunit- and regulator-dependent process in Drosophila. PLoS ONE *8*, e80530.
Vernon, A.C., Johansson, S.M., and Modo, M.M. (2010). Non-invasive evaluation of nigrostriatal neuropathology in a proteasome inhibitor rodent model of Parkinson's disease. BMC Neurosci *11*, 1.

Vial, J.D. (1958). The Early Changes in the Axoplasm during Wallerian Degeneration. J Cell Biol *4*, 551–556.
Wakatsuki, S., Saitoh, F., and Araki, T. (2011). ZNRF1 promotes Wallerian degeneration by degrading AKT to induce GSK3B-dependent CRMP2 phosphorylation. Nat Cell Biol *13*, 1415–1423.
Walker, L.J., Summers, D.W., Sasaki, Y., Brace, E.J., Milbrandt, J., and DiAntonio, A. (2017). MAPK signaling promotes axonal degeneration by speeding the turnover of the axonal maintenance factor NMNAT2. Elife *6*.
Waller, A. (1850). Experiments on the section of the glossopharyngeal and hypoglossal nerves of the frog, and observations of the alterations produced thereby in the structure of their primitive fibres. Philosophical Transactions of the Royal Society of London *140*, 423–429.
Wan, H.I., DiAntonio, A., Fetter, R.D., Bergstrom, K., Strauss, R., and Goodman, C.S. (2000). Highwire regulates synaptic growth in Drosophila. Neuron *26*, 313–329.
Wang, G., Han, T., Nijhawan, D., Theodoropoulos, P., Naidoo, J., Yadavalli, S., Mirzaei, H., Pieper, A.A., Ready, J.M., and McKnight, S.L. (2014). P7C3 neuroprotective chemicals function by activating the rate-limiting enzyme in NAD salvage. Cell *158*, 1324–1334.
Wang, J., Zhai, Q., Chen, Y., Lin, E., Gu, W., McBurney, M.W., and He, Z. (2005). A local mechanism mediates NAD-dependent protection of axon degeneration. J Cell Biol *170*, 349–355.
Wang, M.S., Davis, A.A., Culver, D.G., and Glass, J.D. (2002). WldS mice are resistant to paclitaxel (taxol) neuropathy. Ann Neurol *52*, 442–447.
Wang, X., Kim, J.H., Bazzi, M., Robinson, S., Collins, C.A., and Ye, B. (2013). Bimodal control of dendritic and axonal growth by the dual leucine zipper kinase pathway. PLoS Biol *11*, e1001572.
Wilbrey, A.L., Haley, J.E., Wishart, T.M., Conforti, L., Morreale, G., Beirowski, B., Babetto, E., Adalbert, R., Gillingwater, T.H., Smith, T., et al. (2008). VCP binding influences intracellular distribution of the slow Wallerian degeneration protein, Wld(S). Mol Cell Neurosci *38*, 325–340.
Wishart, T.M., Rooney, T.M., Lamont, D.J., Wright, A.K., Morton, A.J., Jackson, M., Freeman, M.R., and Gillingwater, T.H. (2012). Combining comparative proteomics and molecular genetics uncovers regulators of synaptic and axonal stability and degeneration in vivo. PLoS Genet *8*, e1002936.
Wong, J.J.L., Li, S., Lim, E.K.H., Wang, Y., Wang, C., Zhang, H., Kirilly, D., Wu, C., Liou, Y.-C., Wang, H., et al. (2013). A Cullin1-based SCF E3 ubiquitin ligase targets the InR/PI3K/TOR pathway to regulate neuronal pruning. PLoS Biol *11*, e1001657.
Wu, J.S., and Luo, L. (2006). A protocol for dissecting Drosophila melanogaster brains for live imaging or immunostaining. Nat Protoc *1*, 2110–2115.

Wu, C., Wairkar, Y.P., Collins, C.A., and DiAntonio, A. (2005). Highwire function at the Drosophila neuromuscular junction: spatial, structural, and temporal requirements. J Neurosci *25*, 9557–9566.
Wu, C., Daniels, R.W., and DiAntonio, A. (2007). DFsn collaborates with Highwire to down-regulate the Wallenda/DLK kinase and restrain synaptic terminal growth. Neural Dev *2*, 16.
Xiong, X., and Collins, C.A. (2012). A conditioning lesion protects axons from degeneration via the Wallenda/DLK MAP kinase signaling cascade. J Neurosci *32*, 610–615.
Xiong, X., Wang, X., Ewanek, R., Bhat, P., Diantonio, A., and Collins, C.A. (2010). Protein turnover of the Wallenda/DLK kinase regulates a retrograde response to axonal injury. J Cell Biol *191*, 211–223.
Xiong, X., Hao, Y., Sun, K., Li, J., Li, X., Mishra, B., Soppina, P., Wu, C., Hume, R.I., and Collins, C.A. (2012). The Highwire ubiquitin ligase promotes axonal degeneration by tuning levels of Nmnat protein. PLoS Biol *10*, e1001440.
Xu, T., and Rubin, G.M. (1993). Analysis of genetic mosaics in developing and adult Drosophila tissues. Development *117*, 1223–1237.
Xu, D., Li, Y., Arcaro, M., Lackey, M., and Bergmann, A. (2005). The CARD-carrying caspase Dronc is essential for most, but not all, developmental cell death in Drosophila. Development *132*, 2125–2134.
Xu, L., Yang, L., Hashimoto, K., Anderson, M., Kohlhagen, G., Pommier, Y., and D'Arpa, P. (2002). Characterization of BTBD1 and BTBD2, two similar BTB-domain-containing Kelch-like proteins that interact with Topoisomerase I. BMC Genomics *3*, 1.
Xu, L., Yang, L., Moitra, P.K., Hashimoto, K., Rallabhandi, P., Kaul, S., Meroni, G., Jensen, J.P., Weissman, A.M., and D'Arpa, P. (2003). BTBD1 and BTBD2 colocalize to cytoplasmic bodies with the RBCC/tripartite motif protein, TRIM5δ. Exp Cell Res *288*, 84–93.
Yamagishi, Y., and Tessier-Lavigne, M. (2016). An Atypical SCF-like Ubiquitin Ligase Complex Promotes Wallerian Degeneration through Regulation of Axonal Nmnat2. Cell Rep *17*, 774–782.
Yamamoto, S., Jaiswal, M., Charng, W.-L., Gambin, T., Karaca, E., Mirzaa, G., Wiszniewski, W., Sandoval, H., Haelterman, N.A., Xiong, B., et al. (2014). A drosophila genetic resource of mutants to study mechanisms underlying human genetic diseases. Cell *159*, 200–214.
Yan, D., Wu, Z., Chisholm, A.D., and Jin, Y. (2009). The DLK-1 kinase promotes mRNA stability and local translation in C. elegans synapses and axon regeneration. Cell *138*, 1005–1018.
Yang, H., Yang, T., Baur, J.A., Perez, E., Matsui, T., Carmona, J.J., Lamming, D.W., Souza-Pinto, N.C., Bohr, V.A., Rosenzweig, A., et al. (2007). Nutrient-sensitive mitochondrial NAD+ levels dictate cell survival. Cell *130*, 1095–1107.

Yang, J., Weimer, R.M., Kallop, D., Olsen, O., Wu, Z., Renier, N., Uryu, K., and Tessier-Lavigne, M. (2013). Regulation of axon degeneration after injury and in development by the endogenous calpain inhibitor calpastatin. Neuron *80*, 1175–1189.
Yang, J., Wu, Z., Renier, N., Simon, D.J., Uryu, K., Park, D.S., Greer, P.A., Tournier, C., Davis, R.J., and Tessier-Lavigne, M. (2015). Pathological axonal death through a MAPK cascade that triggers a local energy deficit. Cell *160*, 161–176.
Yin, T.C., Voorhees, J.R., Genova, R.M., Davis, K.C., Madison, A.M., Britt, J.K., Cintrón-Pérez, C.J., McDaniel, L., Harper, M.M., and Pieper, A.A. (2016). Acute Axonal Degeneration Drives Development of Cognitive, Motor, and Visual Deficits after Blast-Mediated Traumatic Brain Injury in Mice. eNeuro *3*.
Ylikallio, E., Pöyhönen, R., Zimon, M., De Vriendt, E., Hilander, T., Paetau, A., Jordanova, A., Lönnqvist, T., and Tyynismaa, H. (2013). Deficiency of the E3 ubiquitin ligase TRIM2 in early-onset axonal neuropathy. Hum Mol Genet *22*, 2975–2983.
Zang, S., Ali, Y.O., Ruan, K., and Zhai, R.G. (2013). Nicotinamide mononucleotide adenylyltransferase maintains active zone structure by stabilizing Bruchpilot. EMBO Rep *14*, 87–94.
Zhai, Q., Wang, J., Kim, A., Liu, Q., Watts, R., Hoopfer, E., Mitchison, T., Luo, L., and He, Z. (2003). Involvement of the ubiquitin-proteasome system in the early stages of wallerian degeneration. Neuron *39*, 217–225.
Zhai, R.G., Cao, Y., Hiesinger, P.R., Zhou, Y., Mehta, S.Q., Schulze, K.L., Verstreken, P., and Bellen, H.J. (2006). Drosophila NMNAT maintains neural integrity independent of its NAD synthesis activity. PLoS Biol *4*, e416.
Zhang, Y., Chen, K., Sloan, S.A., Bennett, M.L., Scholze, A.R., O'Keeffe, S., Phatnani, H.P., Guarnieri, P., Caneda, C., Ruderisch, N., et al. (2014). An RNA-sequencing transcriptome and splicing database of glia, neurons, and vascular cells of the cerebral cortex. J Neurosci *34*, 11929–11947.
Zhang, Z., Fujiki, M., Guth, L., and Steward, O. (1996). Genetic influences on cellular reactions to spinal cord injury: a wound-healing response present in normal mice is impaired in mice carrying a mutation (WldS) that causes delayed Wallerian degeneration. J Comp Neurol *371*, 485–495.
Zhu, W., and Oxford, G.S. (2011). Differential gene expression of neonatal and adult DRG neurons correlates with the differential sensitization of TRPV1 responses to nerve growth factor. Neurosci Lett *500*, 192–196.
Zhu, S., Perez, R., Pan, M., and Lee, T. (2005). Requirement of Cul3 for axonal arborization and dendritic elaboration in Drosophila mushroom body neurons. J Neurosci *25*, 4189–4197.
Zhuang, M., Calabrese, M.F., Liu, J., Waddell, M.B., Nourse, A., Hammel, M., Miller, D.J., Walden, H., Duda, D.M., Seyedin, S.N., et al. (2009). Structures of SPOP-substrate complexes: insights into molecular architectures of BTB-Cul3 ubiquitin ligases. Mol Cell *36*, 39–50.